VAPOR TRANSFER BY FORCED CONVECTION FROM A SMOOTH, PLANE BOUNDARY

By
J. E. Cermak and P. N. Lin

Department of Civil Engineering

Colorado Agricultural and Mechanical College
Fort Collins, Colorado
January-1955

CER No. 55JEC1 *Report No. 9*

Civil Engineering Department
Colorado A & M College
Fort Collins, Colorado

VAPOR TRANSFER BY FORCED CONVECTION FROM A SMOOTH, PLANE BOUNDARY

by

J. E. Cermak and P. N. Lin
Assistant Professors

Prepared for the
Office of Naval Research
Navy Department
Washington, D. C.

Under ONR Contract No. N9onr 82401
NR 063-071/1-19-49

January, 1955 CER No. 55JEC1 Report No. 9

ACKNOWLEDGMENTS

Grateful acknowledgment is made to the Mechanics Branch of the Office of Naval Research for sponsorship of the research reported herein. To Dr. Maurice L. Albertson, Head of Fluid Mechanics Research, under whose leadership the project was conceived and carried out, the writers are especially indebted. The literature reviews and theoretical analyses made by Dr. C. S. Yih under this project were most helpful in conducting the research.

Acknowledgment is also due the various staff members, graduate students and shop personnel who contributed in one way or another to the construction of the wind tunnel and experimental apparatus, and the collection and interpolation of the data. The authors are especially grateful to Duane F. Nelson, graduate assistant, for his work in preparing Chapter IV and his assistance in the collection and analysis of the data used in the present report; to W. Wiley McFarland for his assistance during the construction and early testing phase of the project; to Fred W. Browning, Assistant Engineer, who operated the wind tunnel, and to P. G. Hubbard, Research Engineer of the Iowa Institute of Hydraulic Research, for constructing the hot-wire anemometer.

Acknowledgment is also made to Dr. Dean F. Peterson, Head of the Department of Civil Engineering, for his support and assistance and to T. H. Evans, Dean of Engineering, under whose administrative supervision the work was conducted.

TABLE OF CONTENTS

LIST OF FIGURES

Chapter I

INTRODUCTION

The processes by which physical entities such as momentum, heat, and mass are transferred spatially are of universal interest in the scientific world. Evaporation, a single example of mass transport, is important to such individuals as the meteorologist; the oceanographer; the radar, chemical, irrigation, or air-conditioning engineer; the agronomist; and the physiologist alike.

Usually, means by which the transfer of physical quantities, such as momentum, heat, and mass occur are classified as molecular diffusion, free or gravitational convection, forced convection, conduction, and radiation. Depending upon the nature of a particular situation, transfer by any one mode may predominate, or several modes may be effective simultaneously.

In the research reported herein, investigation was limited to the particular case of evaporation from a smooth, plane boundary in which forced convection by fluid flow parallel to the boundary was the main cause of transport. This particular phenomenon is of much practical importance, particularly when the convective medium is in a turbulent state. Major objectives of the study were to determine (1) the forms for dimensionless parameters best relating the important variables involved, (2) the effect of dry approach length upon evaporation rates, and (3) the effect of lateral diffusion. Data collected are compared with results obtained using the mass transfer theory of Sutton (1)*. Use of an analogy between momentum transfer and mass transfer as given by Reynolds and modified by Kármán (2:55) also furnishes an equation (3:6) which is compared with the data.

The research described in this report is part of a systematic study of momentum, heat, and mass transfer which has been sponsored by the Office of Naval Research since 1949. Under the program, a low-velocity wind tunnel was first constructed for the experimental work. During this phase of the program and following its completion, an extensive review of literature together with some original contributions has resulted in a series of eight reports under the authorship of Dr. C. S. Yih. Further experimental data (not included in this report) are now being collected to determine the effect of the shape of the plane boundary upon the evaporation rate. Shapes under

* The first number is the entry number in the list of references. The number following the colon is the page number.

consideration are ellipses, rectangles, and equilateral triangles. Following the shape study, an investigation of roughness effects is planned.

List of Symbols

		dimensions
c_p	specific heat of air at constant pressure	$L^2/T^{2}{}^\circ F$
f_o	mean relative humidity of ambient air during a test run	
g	gravitational acceleration	L/T^2
h	$(C_i - C)/(C_i - C_o)$	
Δi	difference between total hot-wire current and base current	
k	Kármán constant	
ℓ	mixing length	L
m	exponent	
n	exponent	
p_o	barometric pressure	M/LT^2
q	heat transfer for unit area and unit time	M/T^3
t	time	T
t_o	initial time	T
Δt	time of evaporation run	T
u	local instantaneous velocity in the direction of x	L/T
u'	fluctuation of local instantaneous velocity from the mean in the direction of u	L/T
v	local instantaneous velocity in the horizontal direction perpendicular to u	L/T
v'	fluctuation of local instantaneous velocity from the mean in the direction of v	L/T
w	local instantaneous velocity in the vertical direction	L/T

w'	fluctuation of local instantaneous velocity from the mean in the direction of w	L/T
x	distance downstream from the beginning of evaporation boundary	L
x'	distance downstream from the leading edge of boundary	L
y	distance measured cross-wind from the center of evaporation surface	L
z	distance measured vertically from the surface of evaporation boundary	L
z_1	reference elevation	L
A	constant	
C	water vapor concentration	M/L^2T^2
C_f	drag coefficient -- $\dfrac{D_{x'}}{x' \rho U_o^2/2}$	
C_H	heat transfer coefficient -- $\dfrac{q}{\rho U_o c_p \Delta T}$	
C_i	saturation water vapor concentration at temperature T_m	M/L^2T^2
C_o	water vapor concentration of ambient air	M/L^2T^2
ΔC	$C_i - C_o$	M/L^2T^2
$D_{x'}$	drag force for boundary of unit width and length x'	M/T^2
E	evaporation weight per unit area and unit time	M/LT^3
K_h	exchange coefficient of heat in a vertical	L^2/T
K_m	exchange coefficient of momentum in a vertical	L^2/T
K_v	exchange coefficient of vapor in a vertical	L^2/T
K_x	exchange coefficient of vapor in the x-direction	L^2/T
K_y	exchange coefficient of vapor in the y-direction	L^2/T

K_z	exchange coefficient of vapor in the z-direction	L^2/T
L	length of evaporation boundary	L
N	evaporation coefficient -- $\frac{Ex}{\Delta C \, \nu_e}$	
Pr	Prandtl number	
P_a	water vapor pressure of ambient air	M/LT^2
P_w	water vapor pressure of saturated air at temperature T_m	M/LT^2
Ri	Richardson number -- $\left(\frac{T_o - T_m}{T_o}\right) \frac{gx}{U_o^2}$	
Ri_*	Richardson number -- $\left(\frac{T_o - T_m}{T_o}\right) \frac{gx}{U_*'^2}$	
$R_{x'}$	Reynolds number -- $\frac{U_o x'}{\nu}$	
R_*'	Reynolds number -- $\frac{U_*' x}{\nu_e}$	
$R(\xi)$	correlation coefficient for w'	
T_{db}	dry bulb temperature	
T_m	mean temperature of evaporation surface over a length x	
T_o	mean temperature of ambient air	
T_p	temporal mean temperature for individual plate during run	
T_{wb}	wet bulb temperature	
ΔT	$T_p - T_o$	
U	x-component of the velocity of mean motion	L/T
U_o	ambient velocity of the mean motion	L/T
U_*'	mean apparent shear velocity at the downstream end of the surface under consideration	L/T
U_*	mean shear velocity at the downstream end of the surface under consideration	L/T
W	weight of water evaporated from an individual plate during one test -- also mean velocity in the z-direction	ML/T^2 L/T

ΣW	total weight of water evaporated from a group of plates	ML/T^2
δ	thickness of momentum boundary layer	L
δ_1	thickness of a vapor or thermal boundary layer	L
θ	momentum thickness -- $\int_0^\infty \frac{U}{U_o}\left(1 - \frac{U}{U_o}\right) dz$	L
κ	thermal conductivity of air	
μ	dynamic viscosity of air	M/LT
ν	kinematic viscosity of air (molecular diffusivity coefficient for momentum transfer in air)	L^2/T
ν_e	molecular diffusivity coefficient for water vapor into air	L^2/T
ξ	time	T
π	3.14159--	
ρ_m	average density of air on the surface under consideration	M/L^3
ρ_o	density of ambient air	M/L^3
σ	Prandtl number -- ν/ν_e	
τ	shearing stress in a horizontal plane in the direction of x	M/LT^2
τ_o	shearing stress on the horizontal boundary in the direction of x	M/LT^2
Γ	Gamma function	

Test Coding

In order to describe adequately each test, a four-group designation separated by dashes is used. The meaning of each group is as follows:

GROUP	MEANING	SYMBOL
First	Number of test	1, 2, 3, - - -
Second	Turbulence promoter (tape) in	I
	Turbulence promoter (tape) out	O
Third	Buffer strips wet	W
	Buffer strips dry	D
Fourth	Number of upstream main plates dry	(0), (5), (6), (9)

A test having the designation 6 - I - W - (9) means that it was test number 6, the turbulence promoter (tape) was in place, the buffer plates were wet, and that the first 9 main plates were dry.

Chapter II

REVIEW OF LITERATURE

Available publications concerning evaporation from a plane surface may be divided into two groups. The first group consists of experimental studies, and the second group, theoretical analyses. Selected papers from both groups will be reviewed briefly with some comments.

Experimental Studies

In 1935, Powell and Griffiths (20) reported experiments performed in a wind tunnel 54 x 54 cm in cross-section. Evaporation from both plane and cylindrical surfaces was studied. The plane surface consisted of a tightly-stretched linen sheet with water fed to its underside. It was 18.2 cm crosswind and 24.3 cm long. The entire surface was maintained at a uniform temperature by electric strip heaters. Ambient velocities were measured with a rotating vane anemometer, whereas the deflection of a fine quartz fiber was calibrated and used in obtaining velocity profiles. Thermocouples and a thermocouple psychrometer were used respectively to determine the temperature at the evaporation surface and relative humidity of the air stream. The total amount of evaporation was determined by the difference between the amount of water fed to the evaporation element and the amount of water collected as excess, and also by the additional amount of electrical energy required to maintain the wet surface at a given temperature. For a range of velocity from 100 cm/sec to 300 cm/sec, and for a surface not less than 20 cm in width, Griffiths and Powell concluded that the rate of evaporation from a plane surface of width b and length x could be represented by

$$E = 2.12 \times 10^{-7}\, x^{0.77}\, b(P_w - P_a)(1 + 0.121\, U_o^{0.85}) .$$

Units in this formula were not specified. Apparently vapor pressure is in mm of Hg; length, in cm; velocity, in cm/sec; and E, in gm/cm^2-sec. They also reported a series of tests with rectangular surfaces 23 cm in length and 2, 4, 8, and 17 cm successively in width. According to their analysis of data, they arrived at a relationship for the variation of E with the width of the surface b, namely,

$$E \propto b^{\beta}$$

where β is equal to 0.80, 0.94, and 0.96, when the ambient velocity is equal to 60, 185, and 260 cm/sec, respectively. The present writers consider the equation and the relationship presented by Powell and Griffiths as contradictory to each other.

In 1940, Powell (21) stated that by plotting the data previously reported in terms of $Ex/(P_w - P_a)$ and U_ox all the data followed a single curve. A more detailed study of the effect of ridges as well as a study of evaporation from discs and rectangular surfaces placed at different angles with respect to the air stream were also reported. From observations of the wet-bulb temperatures of thermometers covered with free water layer, wet linen, wet filter paper, and water retained by gelatin, Powell showed that the vapor pressure at the surface of wet linen and similar materials did not differ appreciably from that at the surface of free water.

As the maximum wind velocity of the tunnel used by Powell and Griffiths was about 300 cm/sec, and the maximum length of their plane surface was 24.3 cm, the maximum Reynolds number in their study was relatively small, less than 10^5. According to Fig. 9 (20:182), the boundary layer over the plane surface appears to have been in transition.

Wade (29), in 1942 conducted a series of tests with water, acetone, benzene, ethyl-acetate, toluene, trichlorethylene, and carbon tetrachloride. The wind tunnel was 12 cm wide by 6 cm high, and the evaporation surface was 8.9 cm square. For ambient velocities up to about 400 cm/sec, Wade proposed the formula

$$E = 10^{-7}M^{0.71}\left\{\left[9.8 \log_{10}^{-1}(-0.011\, U_o)\right](P_e - P_d)^{1.25} + 1.57\, U_o^{0.85}(P_e - P_d)\right\}$$

where E = rate of transportation in gm/sec from a surface 8.9 cm square,

M = molecular weight,

U_o= ambient velocity in cm/sec,

P_e= vapor pressure of the liquid at the temperature of the evaporation surface in mm of Hg,

and P_d= partial vapor pressure of the liquid in the ambient air stream in mm Hg.

As in the study by Powell and Griffiths, Wade's tests were relatively limited in range and scope, and no effort was made to control the dynamic characteristic of flow.

Pasquill (17) in 1943 conducted elaborate experiments with water, aniline, methyl salicylate, and bromobenzene in a wind tunnel test section 2.5 ft square by 4 ft long, using three plane surfaces: circular, 24 cm in diameter; square, 19 by 19 cm; and rectangular, 20 cm crosswind by 10 cm downwind. Two series of velocity profiles were obtained. From these observations $1/m$ in $U = U_o(z/\delta)^{1/m}$ was found to be 0.135 and 0.123; i.e., $m \cong 7$. This was taken to indicate that the flow was turbulent. It was not stated, however, where these observations were made. All experiments were made using the circular surface, except for the series of tests using bromobenzene as the liquid. In the latter series, all three surfaces were used. It was shown that the data obtained with bromobenzene could be represented by Sutton's theory with an error less than 20%. In Pasquill's experiments, the total amount of evaporation was determined by weighing, velocity in a profile was measured by a pitot tube 0.3 cm in diameter, and temperature at a wet surface was measured by a surface thermometer of Negretti and Zambra type, which was essentially a conventional thermometer with a thin metal disk attached to the bulb.

An extensive experimental study of evaporation from a plane boundary was carried out by Albertson in 1948 (1,2). In this study, both laminar and turbulent regimes were investigated separately in a range of ambient velocity from 1 to 25 ft/sec, the length of evaporation boundary x was varied from 1/2 in. to 4 ft, and the length x' was varied from 1 to 5 ft. As the equipment of the present study is styled after that of Albertson, the details of his equipment will be omitted here. Albertson first proposed the use of N and R_{*} and found that, according to his evaporation data obtained with both laminar and turbulent boundary layer flows, N depended solely on R_{*}. This finding has been substantiated in the present study except for the fact that local shear velocity used in the present study is the value at the end of various lengths of evaporation boundary instead of that at the beginning of the evaporation boundary as used by Albertson.

In 1950, Maisel and Sherwood (12) published some results of their study on the evaporation of liquids from flat surfaces, cylinders, and spheres into a gas stream. In the study with plane surface, lengths of both the evaporation surface and the dry approach were variable. The evaporation surface was formed by covering fire bricks in pans with fine weave rayon cloth. There were three units of wet surfaces, each being 12.7 cm crosswind, and 5.1 cm long. The dry approach was in lengths of 13.0, 26.1, 52.1, and 102.2 cm. Air temperatures were kept between 40°C and 60°C, and the ambient velocity varied from 100 to 500 cm/sec. When a parameter containing an evaporation term was plotted against $R_{x'}$, the data obtained with the plane surface were found by Maisel and Sherwood to lie well above those of Powell and Griffiths, Wade, Pasquill, and others, and were "badly scattered". This was attributed by Maisel and Sherwood to the possible effect of the dry approach. It should be noted that for a given dry approach length and size of evaporation surface, the transition from laminar to turbulent flows still depends on the free stream turbulence, leading edge geometry, and other factors. Therefore, in the opinion of the present authors, even for a given length of dry approach, $R_{x'}$ is not an adequate parameter.

Maisel and Sherwood (13) also investigated the effect of intensity of turbulence on evaporation from spheres and cylinders. In each instance, they found a marked increase in the mass exchange coefficient as the intensity of turbulence exceeded about 4%.

Theories of Two-dimensional Evaporation

Laminar Flow

A theory for evaporation in laminar flow can be obtained by adapting the work of Pohlhausen (19) on heat transfer to mass transfer. Pohlhausen considered the transfer of heat and momentum to be governed by differential equations of the same form and thereby deduced and solved general equations for heat transfer in laminar flow from the Navier-Stokes equations by analogy. As all experiments performed in the present study are for boundary layer flow either in transition or in turbulent regime, this report does not cover the treatment of Pohlhausen.

Turbulent Flow

The theories of two-dimensional evaporation by turbulent exchange are based on the following assumptions:

(1) Exchange coefficient for momentum transport is the same as that for vapor transport.

(2) Pressure gradient is negligible along the boundary, which implies that the shear stress is constant in a profile.

Sutton's theory of turbulent exchange--Sutton's theory (27) may be regarded as an application of the theory of diffusion by continuous movement proposed by Taylor in 1920 (28). Starting with the definition of correlation for vertical motion at two instants, one can write

$$\int_0^{t_o} \overline{w'^2}\, R(\xi)\, d\xi = \int_0^{t_o} \overline{w'(t) w'(t+\xi)}\, d\xi$$

$$= \overline{w'(t) \int_0^{t_o} w'(t+\xi)\, d\xi} \quad .$$

Since the vertical distance traveled by a particle in an interval t_o is

$$\ell = \int_0^{t_o} w'(t+\xi)\, d\xi \ ,$$

it follows that

$$\int_0^{t_o} \overline{w'^2} R(\xi)\, d\xi = \overline{w'(t) \int_0^{t_o} w'(t+\xi)\, d\xi} = \overline{w'\ell} \quad .$$

For steady turbulent flow, $\overline{w'^2}$ does not vary with time, so that

$$\overline{w'\ell} = \overline{w'^2}\int_0^{t_o} R(\xi)d\xi \quad . \tag{1}$$

This was taken by Sutton as the expression for the momentum exchange coefficient. To obtain an expression for $R(\xi)$, Sutton reasoned that, for motion near a smooth surface, the correlation between the fluctuating velocities at successive instants of time depended on the time interval between the velocity fluctuations ξ, the viscosity μ characterizing the process of energy dissipation, and the energy of turbulence as measured by $\rho\overline{w'^2}$. From the dimensional view point, an expression contaning the foregoing quantities is

$$R(\xi) = \left(\frac{\nu}{\nu + \overline{w'^2}\,\xi}\right)^n , \tag{2}$$

which satisfies the conditions:

$$R(0) = 1$$

and

$$R(\infty) \rightarrow 0 \ .$$

Substituting from Eq. 2 in Eq. 1 and integrating, one has

$$\overline{w'\ell} \cong \frac{\nu^n}{1-n}\left(\overline{w'^2}\, t_o\right)^{1-n} .$$

According to Hesselberg and Bjordkal (8), w' is of normal distribution for which

$$\overline{w'^2} = \frac{\pi}{2}\,\overline{|w'|}^2 \quad .$$

Following Prandtl, one may write $\overline{|w'|} = \ell\left|\frac{dU}{dz}\right|$. Since t_o is approximately equal to $\frac{\ell}{\overline{|w'|}}$ and hence equal to $\left|\frac{dU}{dz}\right|^{-1}$,

$$\overline{w'^2}t_o = \frac{\pi}{2}\,\ell^2\left|\frac{dU}{dz}\right| \ .$$

Using an expression for ℓ proposed by Kármán (10), one has

$$\ell = k\,\frac{dU}{dz}\left(\frac{d^2U}{dz^2}\right)^{-1} ,$$

and

$$K_m(z) = \overline{w'\ell} = \frac{\left(\frac{\pi K^2}{2}\right)^{1-n}}{1-n}\,\nu^n\left(\left|\frac{dU}{dz}\right|^3\left|\frac{d^2U}{dz^2}\right|^{-2}\right)^{1-n} .$$

Thus by means of Sutton's theory, the exchange coefficient $\overline{w'\ell}$ may be computed when the velocity distribution is known.

Schmidt and Ertel (5) have found that

$$K_m(z)\frac{dU}{dz} = \text{const.}$$

Using this condition, Sutton obtained

$$K_m(z) = \frac{\left(\frac{\pi k^2}{2}\right)^{1-n}(2-n)^{1-n}(n)^{1-n}}{(1-n)(2n-2)^{2(1-n)}}\ \nu^n U_o{}^{1-n} z^{2\left(\frac{1-n}{2-n}\right)} z_1{}^{\frac{-n(1-n)}{2-n}} . \quad (3$$

If $U \propto z^m$, then in Eq. 3,

$$m = n/(2-n) .$$

The expression for K_m may be used to derive an expression for U_*/U_o. Noting that $\tau = \rho K_m \frac{\partial U}{\partial z}$, one has

$$\frac{U_*}{U_o} = F_2(n,k)\left(\frac{U_o x'}{\nu}\right)^{\frac{-n}{2(n+1)}} , \qquad (4)$$

where $$F_2(n,k) = \left[\frac{0.243^{1-n} n^2 2^{n-2}(n+1)^{-n}(n+2)^{-n}}{(1-n)^{3-2n}}\right]^{\frac{1}{2(1+n)}} . \qquad (5)$$

Sutton's solution of evaporation--Having Eq. 3, the following equation for two-dimensional exchange can be solved by assuming $K_v = K_m$,

$$U\frac{\partial C}{\partial x} = \frac{\partial}{\partial z}\left(K_v \frac{\partial C}{\partial z}\right) . \qquad (6)$$

Sutton made the transformations,

$$\phi = \frac{C - C_o}{C_i - C_o} , \qquad \xi = \frac{x}{L} , \text{ and } \qquad \zeta = \left(\frac{U_o}{aL}\right)^{\frac{1}{2}} z^{m+\frac{1}{2}} ,$$

and obtained

$$\frac{\partial\phi}{\partial\xi} = \frac{\partial^2\phi}{\partial\zeta^2} + \frac{1}{(2m+1)\zeta}\frac{\partial\phi}{\partial\zeta} \qquad (7)$$

with the boundary conditions

$$\lim_{\zeta\to 0} \phi(\xi,\zeta) = 1 \qquad (0 \le \xi \le 1),$$

$$\lim_{\zeta\to 0} \phi(\xi,\zeta) = 0 \qquad (0 \le \xi \le 1),$$

and $$\lim_{\xi\to 0} \phi(\xi,\zeta) = 0 \qquad (0 < \zeta).$$

Assuming further that $\phi = \zeta^p \psi(\xi, \zeta)$,

where $$p = \frac{n}{2+n} = \frac{m}{2m+1} ,$$

Sutton obtained $$\frac{\partial \psi}{\partial \xi} = \frac{\partial^2 \psi}{\partial \zeta^2} + \frac{1}{\zeta}\frac{\partial \psi}{\partial \zeta} - \frac{p^2}{\zeta^2}\psi ,$$

of which a solution is $$\frac{C}{\xi} K_p \left(\frac{\alpha \zeta}{\xi}\right) \exp\left(- \frac{\zeta^2 + 4\alpha^2}{4\xi}\right) ,$$

K_p being the modified Bessel function of the second kind, and α and C being arbitrary constants. Choosing C as a suitable function of α, one arrives at the expression

$$\frac{C - C_o}{C_i - C_o} = \phi(\xi, \zeta)$$

$$= \frac{2\tan p\pi}{\pi} \zeta^p \int_o^\infty \frac{(2\alpha)^{1-p}}{\xi} K_p \left(\frac{\alpha\zeta}{\xi}\right) \exp\left(- \frac{\zeta^2 + 4\alpha^2}{4\xi}\right) d\alpha$$

$$= 1 - \frac{1}{\pi} \sin\frac{2\pi}{2+n} \Gamma\left(\frac{2}{2+n}\right) \Gamma\left[\frac{U_1^{\,n} z^{\frac{2+n}{2-n}}}{\left(\frac{2+n}{2-n}\right)^2 a\, x\, z_1^{\frac{n}{2-n}}} , \frac{n}{2+n}\right] , \qquad (8)$$

where $$a = \frac{[0.243(2 - n)n]^{1-n} \, \nu_e^{\,n} \, z_1^{\frac{n^2-n}{2-n}}}{(1 - n)(2 - 2n)^{2 - 2n}} .$$

The total rate of vapor transport for unit width from a surface of a length x is then given by

$$Ex = \int_o^\infty (C - C_o) U dz = (C_i - C_o) \int_o^\infty \phi(1, \zeta) U dz$$

$$= \Delta C \int_o^\infty \phi(1, \zeta) U dz .$$

Sutton, however, wrote

$$Ex = \int_o^L \left| \lim_{z \to o} K_z \frac{\partial C}{\partial z} \right| dx , \qquad (9)$$

and obtained the following:

$$\frac{E}{\nu \Delta C} = F_1(n,k) \left(\frac{U_* x}{\nu}\right)^{\frac{2}{2+n}} , \tag{10}$$

where $$F_1(n,k) = (2+n)^{\frac{4}{2+n}} \frac{1}{2\pi} \sin\frac{2\pi}{2+n} \Gamma\left(\frac{2}{2+n}\right) \left(\frac{\pi k^2}{2}\right)^{(1-n)/(2+n)}$$

$$n^{-n/(n+2)} (1-n)^{-1/(2+n)} (2n-2)^{-2(1-n)/(2+n)} . \tag{11}$$

As discussed in Chapter III, Eq. 11 appears to be numerically in error.

Pasquill's modification of Sutton's theory--In his paper of 1943, Pasquill (17) suggested that, for vapor transport, ν in Sutton's expression for K_v should be replaced by ν_e , the diffusivity of vapor in air. This amounts to writing

$$\frac{E}{\nu_e \Delta C} = F_1(n,k)\left(\frac{U_* x}{\nu_e}\right)^{\frac{2}{2+n}} . \tag{12}$$

The data obtained by Pasquill (17) lie between the curves representing Eqs. 10 and 12, a fact seemingly indicating that the use of ν_e is not necessarily superior to the use of ν . As will be explained in Chapter IV of this report, however, ν_e should be used.

Köhler's solution of evaporation--Based on Sutton's theory of turbulent exchange, Köhler (11) also obtained a solution of Eq. 6. In terms of ϕ , Eq. 6 may be written as

$$U \frac{\partial \phi}{\partial x} = \frac{\partial}{\partial z}\left(K_v \frac{\partial \phi}{\partial z}\right) . \tag{13}$$

Setting $K_v(z) = \dfrac{dz}{d\zeta_1}$,

one has $$\frac{\partial^2 \phi}{\partial \zeta^2} = K_v(\zeta_1)\, U(\zeta_1) \frac{\partial \phi}{\partial x} . \tag{14}$$

From Sutton's expression for K_m , it can be readily found that

$$A(\zeta_1)U(\zeta_1) = \frac{(\pi k^2/2)^{\frac{2(1-n)}{n}}\, n^{\frac{4-3n}{n}}\, \nu^2\, U_o^{\frac{2-n}{n}}}{(2-n)(1-n)^{2/n}\,(2n-2)^{4(1-n)/n}\, z_1}\, \zeta_1^{\frac{2-n}{n}}$$

$$= \frac{(\pi k^2/2)^{q-3} (q-1)^{q-1} \nu^2 U_o^{q-2}}{(q-2)(q-3)^{3q-7} z_1} \zeta_1^{q-2} = \sigma \zeta_1^{q-2} ,$$

where $n = 2/(q-1)$.

Thus Eq. 13 is reduced to

$$\frac{\partial^2 \phi}{\partial \zeta_1^2} = \sigma \zeta_1^{q-2} \frac{\partial \phi}{\partial x} , \tag{15}$$

with boundary conditions

$$\lim_{\zeta \to 0} \phi(x, \zeta_1) = 1 \quad (0 \leq x \leq L) ,$$

$$\lim_{\zeta \to \infty} \phi(x, \zeta_1) = 0 \quad (0 \leq x \leq L) ,$$

and $$\lim_{x \to 0} \phi(x, \zeta_1) = 0 \quad (0 < \zeta) .$$

The solution satisfying Eq. 14 and the boundary conditions has been obtained by Köhler as

$$\frac{C - C_o}{C_i - C_o} = \phi = 1 - \frac{1}{\Gamma\left(\frac{1}{q}\right)} \Gamma\left(\frac{1}{q}, \frac{\sigma \zeta_1^{q}}{q^2 x}\right) , \tag{16}$$

which is the same as Yih's solution obtained by a different method as reviewed below.

<u>Yih's solution of evaporation</u>--In 1952, Yih (31) presented an elegant solution of Eq. 6, using a procedure similar to that first used by Blasius and later by Goldstein (6) and Mangler(14) in their analyses of boundary layer problems. Because of the requirement of dimensional homogeneity, the effective number of variables may be reduced by forming appropriate dimensionless groups. Yih let

$$h = \frac{C_i - C}{C_i - C_o} ,$$

and

$$\eta = z \left(\frac{U_o z_1^{1-2m}}{K_v x}\right)^{\frac{1}{1+2m}} ,$$

and showed that, in order to satisfy the boundary conditions, one has

$$h = f(\eta) . \tag{17}$$

Substituting from Eq. 16 in Eq. 6, one is led to

$$- \frac{\eta^{1+m}}{1+2m} \frac{dh}{d\eta} = \eta^{1-m} \frac{d^2h}{d\eta^2} + (1 - m) \eta^{-m} \frac{dh}{d\eta} , \tag{18}$$

the boundary conditions being

$$\lim_{\eta \to 0} h = 0 ,$$

and $$\lim_{\eta \to \infty} h = 1 .$$

Eq. 17 may be easily solved to obtain

$$h = \frac{C_i - C}{C_i - C_o} = \Gamma\left[\frac{m}{1+2m}, \frac{\eta^{1+2m}}{(1+2m)^2}\right]\left[\Gamma\left(\frac{m}{1+2m}\right)\right]^{-1}. \quad (19)$$

Yih, however, did not specify whether ν or ν_e should be used in the evaluation of K_v .

Cermak's equation--In 1939, Kármân (30) derived an equation for heat transfer

$$\frac{1}{C_H} = \frac{2}{C_f} + 5\left(\frac{2}{C_f}\right)^{\frac{1}{2}} \left\{\sigma - 1 + \ln\left[1 + \frac{5}{6}(\sigma - 1)\right]\right\} ,$$

where C_f and C_H are defined respectively by

$$\tau = C_f \frac{\rho U_o^2}{2} ,$$

and $$q = C_H \rho c_p U_o \Delta T ,$$

c_p being the specific heat and T the temperature.

In 1952, Cermak (4) adapted this equation to vapor transport by writing instead of C_H ,

$$C_e = \frac{E}{\rho g U_o \Delta C} .$$

Assuming a 1/7-power relationship of velocity distribution, he finally obtained the following equation for the range of $10^3 \leq R_* \leq 10^5$:

$$N^{-1} = \frac{6.23 R_*^{-8/9}}{\left(\frac{x'}{x}\right)^{4/45}} - \frac{3.77 R_*^{-1}}{\left(\frac{x'}{x}\right)^{1/10}} . \quad (20)$$

Chapter III

THEORETICAL CONSIDERATIONS

Evaporation as studied herein is essentially a phenomenon of turbulent exchange. As the characteristics of turbulence in the flow determines the relative importance of viscous and inertial terms in the equation of motion, and the regime of boundary layer flow in turn determines the condition of turbulence, a mathematical solution for the problem of evaporation from a two-dimensional plane smooth boundary must be different for different regimes of flow. Sutton (27) proposed a theory of turbulence and presented a mathematical solution for the case of a fully-turbulent boundary layer (see Chapter II), making the assumption that the exchange coefficients for vapor and momentum are equal. There are indications, however, that the exchange coefficients for vapor and momentum may be assumed to be equal only under neutral and unstable conditions (18).

Under the so-called stable conditions, in which the density of air decreases with elevation, the assumption of equal exchange coefficients for vapor and momentum becomes questionable (18). A theory of evaporation for the last case still awaits future investigation.

In the case of a boundary layer in transition, the flow over the surface is neither laminar nor fully-turbulent. Under this condition, even in the absence of a density gradient, there is the additional complication that molecular diffusion might, under certain circumstances, become as important as turbulent exchange through the movement of eddies. A theory for this case has yet to be developed.

Although mathematical solutions are not available for all cases of flow, dimensional analysis may be applied to group significant variables, thereby establishing, in a sense, a law of similarity for evaporation from a two-dimensional plane smooth surface. Such a law of similarity will be developed in this chapter and will then be used as a guide to present the experimental data in a significant and concise manner. For the case of two-dimensional turbulent exchange in a fully-developed turbulent boundary layer, existing mathematical solutions will be discussed.

Dimensional Analysis

According to a priori reasoning, evaporation from a saturated surface may be influenced by the following set of conditions:

(1) Physical properties and dynamic and vapor characteristics of the ambient gas stream,

(2) characteristics of the evaporation surface, including temperature, shape, and size of the surface, and

(3) properties of the evaporating liquid.

Experiments conducted under the same set of conditions just stated will produce identical results, which is another way of stating that the set of conditions mentioned above will uniquely determine the distribution of vapor and velocity in the flow and hence the rate of evaporation from the surface. Consequently, for a given regime of boundary layer flow, one may write for the mean rate of evaporation from a plane smooth surface of a length x downwind and of infinite width crosswind (see Fig. 1),

$$E = f_1(U_o,\ C_o,\ C_i,\ \rho_o,\ \rho_m,\ x,\ x',\ \nu_e,\ g) \ . \tag{21}$$

As the velocity distribution is also uniquely determined under the given set of conditions, the velocity gradient may be expressed in terms of significant variables as follows:

$$\frac{dU}{dz} = f_2(U_o,\ C_o,\ C_i,\ \rho_o,\ \rho_m,\ x,\ x',\ \nu_e,\ g,\ z) \ .$$

Now for fully turbulent flow, it is substantially established (21) that

$$\sqrt{\frac{\tau}{\rho}} = kz\,\frac{dU}{dz} \ ,$$

where k is the Kármán constant and may be regarded as constant over the entire profile. In the presence of a density gradient corresponding to an inversion condition, Sheppard (26) has found that the greater the inversion the smaller k becomes, but it may still be regarded as a constant with respect to z.

In flow of negligible longitudinal pressure gradient, the shearing stress is generally regarded as constant in a vertical. Therefore, since

$$\frac{1}{k}\sqrt{\frac{\tau_o}{\rho}} = z\,\frac{dU}{dz} \ ,$$

the quantity $z\,\frac{dU}{dz}$ likewise may be regarded as a constant in a vertical, and, noting that $\nu_e/\nu = 0.6$, one may write

$$z\,\frac{dU}{dz} = f_3(U_o,\ \rho_m,\ x,\ x',\ \rho_o,\ \nu_e,\ g) \ .$$

In the present study, the "apparent shear velocity" is denoted by U_*' and defined as the quantity $0.38\ z\,(dU/dz)$. Obviously

$$U_*' \propto z\,\frac{dU}{dz} \ .$$

Therefore $$U_*' = f_4(U_o,\ x,\ x',\ \rho_m,\ \rho_o,\ \nu_e,\ g) \ ,$$

whence, $$U_o = f_5(U_*',\ \rho_m,\ x,\ x',\ \rho_o,\ \nu_e,\ g) \ .$$

Eq. 21 then becomes

$$E = f_6(U_*', C_o, \rho_m, C_i, x, x', \rho_o, \nu_e, g) .$$

But actually E varies directly with $\Delta C = C_i - C_o$; therefore,

$$E = f_7(U_*', \Delta C, \rho_m, x, x', \rho_o, \nu_e, g) .$$

Choosing ρ_o, x, ΔC, and ν_e as the repeating variables, one may obtain

$$\frac{Ex}{\nu_e \Delta C} = f_8\left(\frac{U_*' x}{\nu_e}, \frac{\rho_o - \rho_m}{\rho_o}, \frac{gx}{U_*'^2}, \frac{x}{x'}\right) .$$

The third dimensionless group in the function f_8 is a form of the Froude number expressing the effects of gravity. In a flow without a free surface, it is difficult to visualize that the Froude number is a relevant parameter, unless there is a vertical density gradient. On the basis of this reasoning, one may agree that the two parameters $(\rho_o - \rho_m)/\rho_o$ and $gx/U_*'^2$ are conjugated and should be combined to form a single parameter. A reasonable combination is

$$\frac{\rho_o - \rho_m}{\rho_o} \cdot \frac{gx}{U_*'^2} ,$$

which is a form of the Richardson number in terms of the bulk characteristics of the flow. The Richardson number is usually written (9) as

$$\frac{g}{T} \frac{\partial T}{\partial z} \Big| \left(\frac{\partial U}{\partial z}\right)^2 \quad \text{or} \quad \frac{g}{\rho} \frac{\partial \rho}{\partial z} \Big| \left(\frac{\partial U}{\partial z}\right)^2 ,$$

the former form being the more commonly used among meteorologists. Following the practice of the meorologists, two forms of the Richardson number are adopted in the present study, namely,

$$Ri_* = \left(\frac{T_o - T_m}{T_o}\right) \frac{gx}{U_*'^2} \quad \text{and} \quad Ri = \left(\frac{T_o - T_m}{T_o}\right) \frac{gx}{U_o^2} .$$

The function f_8 is therefore reduced to the special form,

$$\frac{Ex}{\nu_e \Delta C} = f_9\left[\frac{U_*' x}{\nu_e}, \frac{(T_o - T_m)gx}{T_o U_*'^2}, \frac{x}{x'}\right] ; \qquad (22)$$

i. e.,

$$N = f_9(R_*', Ri_*, x/x') .$$

It should be pointed out that a form of the Richardson number is used herein merely as a parameter indicating the rôle played by gravitational forces when a vertical gradient of density exists. The question of whether or not a critical Richardson number for turbulent flow exists (17) is not considered in this report.

Returning to the function f_4 , if U_o , ρ_o , and x are chosen as the repeating variables, one may obtain

$$\frac{U_*}{U_o} = f_{10}\left(\frac{\rho_o - \rho_m}{\rho_o} , \frac{gx}{U_o^2} , \frac{U_o x'}{\nu_e} , \frac{x}{x'}\right) .$$

Again since the Froude number would be an irrelevant parameter in a flow without a free surface, unless a vertical gradient of density exists; the first and second dimensionless groups in f_{10} are combined to form a Richardson number

$$\frac{U_*}{U_o} = f_{11}\left[\frac{U_o x'}{\nu} , \frac{(T_o - T_m)gx}{T_o U_o^2} , \frac{x}{x'}\right]$$

$$= f_{11}\left(R_{x'} , Ri , \frac{x}{x'}\right) . \qquad (23)$$

Experimental data will first be used to determine f_{11} . With this information, R_* may be computed, and the form of f_9 may then be studied.

The Case of a Fully-developed Turbulent Boundary Layer

In what follows, sveral topics will be considered. The derivation and solution of the equation of two-dimensional, turbulent exchange will first be examined. Then the methods of computing the total rate of evaporation will be discussed in detail. Following this, an expression for the vertical distribution of temperature will be derived by analogy.

The general equation of turbulent exchange

Let an infinitesimal element in turbulent flow be considered. The flow entering the element through the face dydz on the left is Udydz , as shown in the figure. With this flow, there is an influx

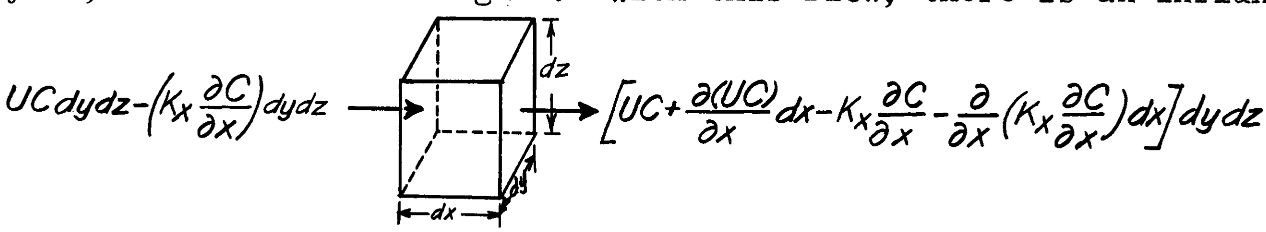

of vapor given by UCdydz . If a positive vapor gradient exists witl respect to x , then since an effect of turbulence is a tendency to equalize transferable properties of the flow, there will be a flow cf vapor in the direction of negative x , given by $-K_x\frac{\partial C}{\partial x}dydz$, K_x here being the exchange coefficient for vapor in the x-direction. Thus the resultant flow of vapor entering the element through the face dydz is

$$\left(UC - K_x\frac{\partial C}{\partial x}\right)dydz .$$

Through the face dydz to the right of the element, vapor is being transported out by the mean flow at a rate of

$$\left[UC + \frac{\partial (UC)}{\partial x} dx\right] dydz \ .$$

If again a positive vapor gradient exists with respect to x, then due to turbulent mixing, vapor will be transferred back into the element at a rate of

$$\left[-K_x \frac{\partial C}{\partial x} - \frac{\partial}{\partial x}\left(K_x \frac{\partial C}{\partial x}\right) dx\right] dydz \ .$$

The resultant rate at which vapor is being transported through the face dydz to the right of the element is therefore

$$\left[UC + \frac{\partial (UC)}{\partial x} dx - K_x\frac{\partial C}{\partial x} - \frac{\partial}{\partial x}\left(K_x\frac{\partial C}{\partial x}\right) dx\right] dydz \ .$$

Consequently, the net rate at which vapor is taken from the element by flow in the x-direction is given by

$$\left[UC + \frac{\partial (UC)}{\partial x}dx - K_x\frac{\partial C}{\partial x} - \frac{\partial}{\partial x}\left(K_x\frac{\partial C}{\partial x}\right)dx\right]dydz - \left[UC - K_x\frac{\partial (UC)}{\partial x}dx\right]dydz$$

$$= \left[\frac{\partial (UC)}{\partial x} - \frac{\partial}{\partial x}\left(K_x\frac{\partial C}{\partial x}\right)\right] dxdydz \ .$$

In a similar manner, it can be shown that the net rates at which vapor is taken from the element by flow in the remaining two directions are respectively

$$\left[\frac{\partial (VC)}{\partial y} - \frac{\partial}{\partial y}\left(K_y\frac{\partial C}{\partial y}\right)\right] dxdydz \ ,$$

and $$\left[\frac{\partial (WC)}{\partial z} - \frac{\partial}{\partial z}\left(K_z\frac{\partial C}{\partial z}\right)\right] dxdydz \ .$$

Therefore, the element is losing vapor at a resultant rate of

$$\left[\frac{\partial (UC)}{\partial x} - \frac{\partial}{\partial x}\left(K_x\frac{\partial C}{\partial x}\right) + \frac{\partial (VC)}{\partial y} - \frac{\partial}{\partial y}\left(K_y\frac{\partial C}{\partial y}\right) + \frac{\partial (WC)}{\partial z} - \frac{\partial}{\partial z}\left(K_z\frac{\partial C}{\partial z}\right)\right] dxdydz \ ,$$

which must be equal to the rate at which the vapor content of the element is decreasing. This leads to the general equation of exchange

$$\frac{\partial (UC)}{\partial x} + \frac{\partial (VC)}{\partial y} + \frac{\partial (WC)}{\partial z}$$

$$- \frac{\partial}{\partial x}\left(K_x\frac{\partial C}{\partial x}\right) - \frac{\partial}{\partial y}\left(K_y\frac{\partial C}{\partial y}\right) - \frac{\partial}{\partial z}\left(K_z\frac{\partial C}{\partial z}\right) = - \frac{\partial C}{\partial t} \ .$$

For flow at low velocities, air may be considered as incompressible, so that

$$\frac{\partial U}{\partial x} + \frac{\partial V}{\partial y} + \frac{\partial W}{\partial z} = 0 \ ,$$

and the equation of exchange becomes

$$\frac{\partial}{\partial x}\left(K_x\frac{\partial C}{\partial x}\right)+\frac{\partial}{\partial y}\left(K_y\frac{\partial C}{\partial y}\right)+\frac{\partial}{\partial z}\left(K_z\frac{\partial C}{\partial z}\right)=\frac{DC}{Dt} \qquad (24)$$

where $\frac{D}{Dt}$ stands for $U\frac{\partial}{\partial x}+V\frac{\partial}{\partial y}+W\frac{\partial}{\partial z}+\frac{\partial}{\partial t}$

Eq. 24 is the general equation of turbulent exchange for incompressible flow.

The equation for turbulent exchange in two-dimensional flow

For the case of two-dimensional flow, turbulent exchange is considered to be predominantly in the vertical direction and $V = W = 0$. As a result, the left side of Eq. 24 is reduced to $\frac{\partial}{\partial z}\left(K_z\frac{\partial C}{\partial z}\right)$, and the right hand side to $U\frac{\partial C}{\partial x}$ for the steady state. Finally, then, the equation of diffusion for the case of steady, two-dimensional, turbulent flow is

$$\frac{\partial}{\partial z}\left(K_v\frac{\partial C}{\partial z}\right)=U\frac{\partial C}{\partial x}\,. \qquad (6)$$

Solution of Eq. 6

As previously summarized in Chapter II, Sutton proposed a theory of turbulent exchange, which enabled him to derive an expression for K_z as a function of z and certain physical constants. By using this expression of K_z and assuming a power form of velocity distribution, Eq. 6 becomes a linear equation of the parabolic type. Sutton, Yih, and Köhler each proposed a method for the solution of the resultant equation. These methods have been reviewed in Chapter II. In this connection, a slight mathematical error in Sutton's solution has been noted. A step in Sutton's solution is to set

$$\zeta=\left(\frac{U_o{}^n}{aL}\right)^{\frac{1}{2}} z^{m+\frac{1}{2}}\,.$$

In order to arrive at Eq. 7, however, the right-hand side of the last expression for ζ should have contained the factor $\frac{2}{(2m+1)}$.

Total rate of evaporation

In Yih's solution of Eq. 6, the total rate of evaporation is not calculated. Both Sutton (27) and Köhler (11) have derived expressions for the total rate of evaporation by writing

$$Ex=\int_o^L\left|\lim_{z\to o} K_z\frac{\partial C}{\partial z}\right|dx\,, \qquad (9)$$

where C is given by the solution of Eq. 6 for two-dimensional turbulent exchange of vapor. The expression $K_z \frac{\partial C}{\partial z}$ represents the rate at which vapor is being transported vertically through a unit area, only when the flow is fully turbulent. As the boundary is approached, i. e., as $z \rightarrow 0$, the flow is no longer fully turbulent, in the sense that vapor transport by molecular diffusion is now of the same order as vapor transport by turbulent exchange. Therefore, strictly speaking, one should write

$$Ex = \int_0^L \left| \lim_{z \to 0} (\lambda + K_z) \frac{\partial C}{\partial z} \right| dx = \int_0^L \lim_{z \to 0} \left| \lambda \frac{\partial C}{\partial z} \right| dx \, , \quad (25)$$

where λ is a physical constant characterizing the molecular diffusion, and has been set equal to both ν and ν_e. If C, given by the solution of Eq. 6 is to apply over the entire range of turbulent and laminar layers, then in order to satisfy Eq. 25, one must have

$$\lim_{z \to 0} \frac{\partial C}{\partial z} \neq 0 \, ,$$

and $$\lim_{z \to 0} K_z \rightarrow 0 \, .$$

Intended for turbulent flow, none of the solutions by Sutton, Yih, and Köhler satisfies these two conditions. That the integral $\int_0^L \left(\lim_{z \to 0} K_z \frac{\partial C}{\partial z} \right) dx$ has a non-zero value should therefore be considered as a mathematical incident without physical significance. Also that the theoretical total rate of evaporation computed by Eq. 9 comes close to experimental data (17) is a matter of coincidence rather than the result of strict reasoning.

On the other hand, one may find the total rate of evaporation by writing

$$Ex = \int_0^\infty \left[U(C - C_o) \right]_{\text{at } x} dz \quad (26)$$

In Eq. 26, C is again given by the solution of Eq. 6, so that some error is involved in evaluating the part of the integral for the laminar sublayer. This part of the integral in question, however, is a small portion of the entire integral owing to the small relative thickness of the zone where viscous effects are appreciable and also owing to the fact that U rapidly approaches zero as the solid boundary is approached. As any error in a small portion of a quantity cannot cause appreciable error in the entire quantity itself, Eq. 26 is the more reliable way of evaluating the total rate of evaporation. Because of the difficulty involved in the integration of incomplete Gamma functions, graphical integration is used to evaluate the integral in Eq. 26.

In the atmosphere, where the momentum boundary layer may be much thicker than the vapor boundary layer, the infinite upper limit of integration in Eq. 26 is justifiable. In wind tunnel studies, the vapor boundary layer may be thicker than the momentum boundary layer, It is then more reasonable to write

$$Ex = \int_0^{\delta} U(C - C_o)dz + U_o \int_{\delta}^{\infty} (C - C_o)dz \ , \tag{27}$$

because the velocity distribution outside of the boundary layer is uniform. Two curves relating N and R_* have been computed by means of Eq. 27 (see Figs. 26 to 30), according as ν or ν_e is used in the evaluation of K_z .

Temperature profile

In a wind tunnel, where large-scale mixing like that in the atmosphere does not exist, the temperature of the fluid is a conservative entity, and is therefore transferable, so that one may write for the turbulent exchange of heat in steady, two-dimensional flow,

$$U\frac{\partial T}{\partial x} = \frac{\partial}{\partial z}\left(K_h\frac{\partial T}{\partial z}\right) \ , \tag{28}$$

which is analogous to Eq. 6. The boundary conditions to be satisfied are as follows:

(a) $T = T_o$ at $z = \infty$,
(b) $T = T_m$ at $z = 0$, and
(c) $T = T_o$ at $x = 0$ for $z > 0$.

Obviously then, by analogy, the solution of Eq. 28 is

$$\frac{T_m - T}{T_m - T_o} = \Gamma\left[\frac{m}{1+2m} \, , \, \frac{\eta_1^{\,1+2m}}{(1+2m)^2}\right]\left[\Gamma\left(\frac{m}{1+2m}\right)\right]^{-1} \ , \tag{29}$$

where $$\eta_1 = \left(\frac{U_o \, \delta^{\,1-2m}}{K_h \ x}\right)^{\frac{1}{1+2m}} z \ .$$

K_h may be evaluated by means of Eq. 3. It is probably better to replace ν in Eq. 3 by the thermal diffusivity of air, as suggested by Pasquill (17).

Theoretical temperature profile is of interest in the present study in that the dry bulb temperature measurements are considered more reliable than measurements involving wet bulb temperatures. If the theoretical temperature profile should fall close to the measured one, the fundamental principles and assumptions involved in the theoretical analysis could be regarded as sound. The inference is then that the theoretical vapor profile could be regarded as substantially correct, even if the theoretical vapor profile should not come close to the measured profile everywhere in the zone of turbulent flow. In the wind tunnel, relative humidity is determined by wet and dry bulb thermocouples. For measurements made at relatively low velocities, wet bulb temperature readings may be in error because of the heat lost in the water occasionally dripping from the wet bulb.

Summary

In this chapter, significant dimensionless groups, on which N and U_*'/U_0 depend, are first developed, introducing two forms of the Richardson number in terms of bulk characteristics of the flow. Then, for the case of fully-developed, turbulent flow, the correct method of calculating the total rate of evaporation is discussed in detail. For the sake of checking Sutton's theory of turbulent exchange, an expression for the vertical distribution of temperature is finally presented.

Chapter IV

EQUIPMENT AND TEST PROCEDURE

The key equipment specifically designed for the present study consists of the procelain evaporation surface and the automatic water feed system. In what follows, all the equipment used as well as the testing procedure will be briefly described.

Wind Tunnel

The wind tunnel had a 6-ft square test section 28 ft in length. Although it was constructed to operate as a recirculating tunnel, air for this study was not recirculated because the amount of water evaporated would have continuously increased the relative humidity of the ambient air stream. A plan view of the tunnel is shown in Fig. 2.

The axial velocity distribution in a plane perpendicular to flow was measured at points on a grid of 6-in. squares. This velocity distribution in the test section, 1 ft upstream from the leading edge of the test boundary, was found to be very good -- not varying by more than 1% from the mean excepting in the thin boundary layer along the wall. Screens at the beginning of the transition created a uniform turbulence and reduced the overall turbulence intensity of the ambient air stream to about 0.7 % at a mean velocity of 8 ft/sec.

Air was drawn through the test section by a wooden aircraft propeller with a $2\frac{1}{2}$-ft radius. Power for the propeller was supplied by either a 92 HP gasoline engine or by a 180 HP diesel engine, depending upon power requirements. Fig. 3 shows the test section and a portion of the transition. Fig. 4 shows the air intake and exit, and the gasoline engine housing.

Experimental Boundary

The experimental boundary, as shown on Figs. 5 and 6 was mounted on two I-beams and two angle-irons, the evaporation surface being 13 in. above the floor of the tunnel. The evaporation surface was made of smooth porous porcelain about 1/8 " thick. Leveling of the surface was accomplished by the use of an engineer's level and a sensitive machinist's level.

The evaporation surface consisted of 15 central units, 4 in. wide, varying in length from $\frac{1}{2}$ in. to 12 in. These units were called "main plates". On both sides of the strip of main plates were strips of 12-in. x 12-in. "buffer plates". Buffer plates were used to eliminate the effect of lateral diffusion.

Cold rolled steel and "Lucite" were used to fabricate the nose piece as shown on Fig. 7.

A turbulence promoter, consisting of a piece of 5/16-in. wide surveyor's chain, was installed with its wide edge perpendicular to the main floor, 1 ft upstream from the leading edge, to help create a turbulent boundary layer over the entire evaporation surface.

A grid of 1 3/8-in. x 3/4-in. boards, projecting vertically above the downstream edge of the boundary, was used for the purpose of effecting symmetrical flow conditions in the neighborhood of the nose peice.

Evaporation Pans

The evaporation pans were constructed of aluminum plates and rods as shown on Fig. 7. For insurance against leakage the pans were covered with aluminum foil as shown on Figs. 8 and 9.

Automatic Water Feed and Measuring System

The automatic water feed and measuring system for main plates 1 - 5 is shown on Fig. 10. The two systems for main plates 6 -10 and 11 - 15 were identical with the system shown except for burette size. The burettes and evaporation pans were filled from the 1-gal. bottles before commencing a run. During a run, buffer plates were fed from the 1-gal. bottles, and main plates were fed from the burettes. Distilled water was used at all times.

The system was untouched during the run. Automatic feed was accomplished by setting the lower ends of the air tubes within the burettes and bottles at plate level. The areas of the ambient air tubes within the burettes were measured, and on the basis of these measurements, corrections were applied to the evaporation volumes as indicated by the graduated burette readings.

Velocity Measurements

The hot-wire anemometer was used almost exclusively for velocity measurements; however, the ambient air velocities for some of the runs with dry boundaries were checked with a pitot tube. Good agreement was obtained.

The hot-wire anemometer was made of 0.0003-in. tungsten wire, 1/8 in. long. A constant temperature circuit was used.

The hot-wire anemometer tips were calibrated before each run in a specially designed calibration tank. A typical calibration curve is shown in Fig. 11.

For setting the ambient velocity, a forward tunnel hot-wire anemometer was suspended from the tunnel ceiling about $1\frac{1}{2}$ ft upstream from the leading edge and about $1\frac{1}{2}$ ft below the ceiling. Fig. 12 shows this arrangement. Thermocouples, one dry bulb, and one wet bulb can be seen on each side of the anemometer tip.

For measuring mean velocity and turbulent intensity profiles, a traversing hot-wire anemometer was mounted on the mechanism shown on Figs. 13 and 14. Vertical movements of the anemometer tip could be controlled to 0.001 in. The anemometer tip was initially set with a feeler gage.

The vertical traversing mechanism was mounted on a tripod stand, having two legs resting on the boundary and one against the ceiling. The tripod stand could be moved so that velocity profiles could be taken at any point along the center line of the boundary.

Profiles at the front of the wetted boundary were not taken during evaporation runs, but rather directly before or directly after the evaporation runs so that no disturbance of the evaporation processes might occur.

Plate Temperature Measurements

A silver soldered copper constantan thermocouple, made from B & S No. 30 wire, was located at the center of each main plate at plate surface elevation for measuring T_p . The thermocouple circuit included a reference junction located inside of a thermos bottle which was filled with ice made from distilled water. A Leeds and Northrup precision potentiometer was used for taking e.m.f. measurements.

Relative Humidity Measurements

The relative humidity of the incoming air was measured with a sling psychrometer, located between duct turns (2) and (3), shown on Fig. 2. The psychrometer dry bulb temperature DB agreed very well with that given by the dry bulb thermocouple on the forward tunnel hot-wire anemometer mount. The wet bulb thermocouple located on the anemometer mount gave inconsistent temperature readings as compared to the sling psychrometer measurements.

Relative humidity profiles were taken at the rear of the wetted boundary during each evaporation run. Dry bulb and wet bulb thermocouples, located adjacent to the traverse hot-wire anemometer tip, were used for relative humidity measurements. In some runs this wet bulb thermocouple also gave inconsistent readings. The dry bulb temperature profiles are listed in Table 30.

Barometric Pressure Readings

A recording type barometer was used to determine barometric pressure. The reliability of the barometer was determined monthly by checking it against the barometer of the U.S. Weather Bureau Station at Colorado A & M College.

Typical Evaporation Run

A typical evaporation run proceeded in the following manner. Hot-wire anemometers for the forward tunnel and traverse positions were calibrated and then placed in their proper positions. The propeller was then started and the tunnel velocity was set at the ambient velocity desired. The evaporation plates were flooded and sponged to remove air pockets which tended to form under the plate surface. After evaporation had proceeded for about one hour, initial burette readings were taken and then all thermocouples read. Burette and thermocouple readings were generally taken at 30-minute intervals. At the approximate midpoints of these 30-minute intervals, sling psychrometer readings were taken. At some time during the run, velocity and temperature profiles data at the rear of the wetted boundary were taken. The velocity profile data at the front of the wetted boundary were usually taken directly before or directly after the evaporation run, so that the traversing mechanism would not disturb the air flow over the plates. Barometric pressure readings were taken as needed. After collecting the foregoing information the run was considered completed.

Chapter V

ANALYSIS AND DISCUSSION OF DATA

In the analysis of data, two major cases of boundary layer flow are considered, namely, the case of a fully-developed, turbulent boundary layer and the case of a boundary layer in transition. Data pertaining to each case will be analyzed separately and then compared with each other. Local shear velocity at the end of any length of the evaporation surface is always used in preparing the plot of N against R'_* .

Comparison of the data obtained herein with those of the previous workers other than Albertson has not been made, because most of the previous data do not include information regarding temperatures and velocity profiles. As stated in Chapter II, the present study substantiates the evaporation data obtained by Albertson.

The Kármán Constant and the Apparent Shear Velocity

Because the boundary drag is not measured directly in the tests, shear velocities must be computed from the velocity profiles. All of the velocity profiles are presented in Table 29. In the case of fully turbulent flow in the absence of density gradients, a convenient and frequently-used procedure is to apply the Kármán-Prandtl equations of velocity distribution. When the boundary layer is in transition from laminar to turbulent flow, this procedure cannot be applied. Resort is then made to the Kármán momentum equation for boundary layer flow, which applies equally well whether the flow is fully turbulent or not. When the former procedure is employed the shear velocity can be computed from the velocity gradient if the Kármán constant is known.

According to Nikuradse's experiments (15, 16) with water in pipes, this constant may be taken as 0.4 . But, according to Schulz-Grunow (25), who measured both boundary drag and velocity profiles in an air stream over a plane boundary, this constant is equal to 0.38 . The latter value is adopted for k for two reasons. Firstly, the boundary geometry in Schulz-Grunow's experiments is similar to that used in the present study. Secondly, Schulz-Grunow's experiments and the experiments conducted in the course of the present investigation cover approximately the same range of Reynolds number.

In the tests performed for the present study, the boundary and ambient stream temperatures often differed by more than ten degrees Fahrenheit, the boundary being cooler (compare the vlues of T_p and T_m in Tables 1 - 28). Sheppard (26) found that under the inversion conditions, in which density decreased with height above the ground, k decreased as the density gradient increased. The true value of k under different density gradients can be determined only when the boundary drag is measured, and therefore not without requiring rather extensive instrumentation. As k itself depends on various flow conditions, the difficulty of not knowing k may be overcome by adopting a new quantity "apparent shear velocity", which has already been defined in Chapter III. It is the shear velocity computed from a velocity profile as if k were not affected by the presence of a density gradient. If U_* is the true shear velocity, then $U_*' \propto U_*/k$. This may be shown by assuming a logarithmic form of velocity distribution, which gives

$$\frac{U}{U_*} = \frac{2.3}{k} \log \frac{zU_*}{\nu} + \text{const.}$$

$$= 5.94 \, \frac{0.38}{k} \log \frac{zU_*}{\nu} + \text{const.} \, ,$$

so that $$U_* = \frac{k}{0.38} \, \frac{U_1 - U_2}{5.94 \log z_1/z_2} = \frac{k}{0.38} U_*' \, ,$$

i.e., $$U_*' = 0.38 \, \frac{U_*}{k} = \frac{U_1 - U_2}{5.94 \log z_1/z_2} \, .$$

It is obvious that U_*', being determined by velocities at two levels, is relatively easy to obtain in the field.

Regimes of Boundary Layer Flow

The present study is concerned mainly with two regimes of boundary layer flow. The boundary layer was either fully turbulent or in transition.

In order to ensure a fully turbulent boundary layer over the entire boundary, a steel tape, 5/16 in. wide, was placed in front of the nose piece to "stimulate" the flow (see Chapter IV). That the flow was turbulent was verified by observation of smoke injected in the flow, and by the "logarithmic" distribution of velocities in a vertical. The effectiveness of the tape as a turbulence promoter may be appreciated by inspecting Figs. 15 - 18[1]. Attention is especially called to Fig. 16 which shows a great increase in turbulence intensity for ambient speeds as low as 4 ft/sec at the upstream end of the evaporation surface.

[1] The "noise level" for many of the points in Figs. 16 - 18 exceeds the level of turbulence. Recent measurements with a low "noise level" instrument give a free-stream turbulence intensity of about 0.006. The value of Figs. 16 - 18 lies in giving the variation of turbulence intensity when the actual turbulence intensity exceeds the "noise level".

At the downstream end of the evaporation boundary, which is 11.3 ft long, the effect of the turbulence promoter is negligible, when the speeds are high, say 18 ft/sec and 32 ft/sec, (see Fig. 18). For velocities from 4 ft/sec to 8 ft/sec, the effect of the turbulence promoter is still considerable at the downstream end of the evaporation boundary.

When the tape is not present, flow along the boundary may include, in the order of occurrence, first a laminar boundary layer, then a region of transition, and finally a fully-turbulent boundary layer. The length of each zone of flow depends on the turbulence in the ambient stream, the surface condition of the boundary, the leading edge geometery, and even the density gradient over the boundary. Analysis based on the principle of momentum, of which details will be given later in this Chapter, shows that, in evaporation experiments conducted in the absence of a turbulence promoter, the boundary layer over the evaporation surface is essentially in the region of transition where the flow is neither laminar nor fully-turbulent. Smoke injected in the flow during the tests showed definitely that the transition zone was over the evaporation surface. The section, at which sudden expansion of the boundary layer took place, was observed to oscillate longtitudinally along the evaporation surface. Therefore, strictly speaking, the flow was unsteady. This unsteadiness of flow is largely responsible for the greater scatter usually found in all data pertaining to a boundary layer in transition.

Apparent Shear Velocity in a Turbulent Boundary Layer

The apparent shear velocity in a turbulent boundary layer is computed by fitting a straight line to a velocity profile plotted on "semi-logarithmic" paper, and then applying the Kármán-Prandtl equation of velocity distribution. In the region close to the boundary, viscous effects become important, and the flow is no longer fully-turbulent. On the "edge" of the boundary layer, there is a short transition from rotational flow in the boundary layer to the irrotational flow in the free stream. Since the Kármán-Prandtl equation is intended for fully-turbulent flow, points of velocity profile lying in the two regions just mentioned are expected to deviate from the Kármán-Prandtl equation of velocity distribution. Consequently in fitting a line to a velocity profile, more weight is given to the points in the intermediate section of the profile. With the apparent shear velocity thus computed, a dimensionless velocity profile is prepared, plotting U/U_* against zU_*/ν again on the semi-logarthmic paper. The slope of the intermediate section of such a profile should be the same for all runs.

Shear velocity in the absence of a density gradient

When water is not fed to the evaporation surface, no appreciable temperature gradient exists, and the apparent shear velocity becomes equal to the true shear velocity. In Fig. 19, shear velocities obtained under this condition are plotted against the Reynolds number $R_{x'}$. Although considerable scatter can be seen, the general trend is quite definite. This trend is indicated by a mean curve drawn by visual inspection.

For $R_{x'} \geq 4 \times 10^5$, the mean curve in Fig. 19 coincides with a curve given by the equation $\frac{U_*}{U_o} = \frac{0.172}{R_{x'}}$ derived on the basis of the 1/7-power relationship of velocity distribution. A study of the velocity profiles for points lying in this range of Reynolds number reveals that the exponent of the equation of velocity distribution has in general a value between 1/4 and 1/6, instead of 1/7. The good approximation rendered by the equation cited above is thus somewhat surprising.

As stated in Chapter II, Sutton's theory of turbulent exchange may be applied to derive an expression for U_*/U_o which may be written as

$$\frac{U_*}{U_o} = F_2(n,k)\left(\frac{U_o x'}{\nu}\right)^{-n/2(n+1)} , \tag{4}$$

where $$n = \frac{2m}{1 + m} ,$$

m being the exponent in the power relationship of velocity distribution. If velocity profiles corresponding to points in the neighborhood of the mean curve in Fig. 19 are used to determine m and hence n , then the mean curve can be closely reproduced by Eq. 4. It is thus seen that, subject to the experimental error involved, Sutton's theory of turbulence is valid over the entire range of the present study.

Apparent shear velocity in the presence of a density gradient

Under inversion conditions, there is a gradient of decreasing density with height because of the temperature's gradient increasing with height. Mixing in such a medium requires raising heavier fluid to a higher level and forcing lighter fluid downward. This process in itself entails work to be done on the fluid, in order to overcome the stabilizing density gradient. If the total rate of energy transmitted from the main flow to the eddies is constant, which is the case for flow over a solid boundary, then the power actually available for mixing will be decreased by the rate at which kinetic energy of the eddies is converted to work done in overcoming the stabilizing density gradient. Thus, the greater the stabilizing gradient, the less will be the power available for mixing.

In the case of momentum transfer, a decrease in the rate of turbulent mixing means a less uniform velocity distribution and hence a greater velocity gradient. If the equation

$$\frac{dU}{dy} = \frac{U_*}{ky}$$

is to hold, k must decrease. This is exactly what Sheppard (26) found from his experiments. The more important conclusion, however, is that the apparent shear velocity increases under inversion conditions because the apparent shear velocity, being proportional to $y\frac{dU}{dy}$, will increase whenever the velocity gradient increases. This expectation is verified by the data presented in Fig. 20, in which the ratio of apparent shear velocity to the corresponding shear velocity in the absence of a density gradient is plotted against the Richardson number $\frac{T_o - T_m}{T_o}\frac{gx}{U_o^2}$. It can be seen that the greater the Richardson number (i.e., the greater the influence of the stabilizing density gradient) the greater becomes the ratio $\frac{U_*'/U_o}{f_{12}(R_{x'})}$.

The data used in preparing Fig. 20 have a range of x'/x from 2.05 to 1.09. Since no systematic variation of $\frac{U_*'/U_o}{f_{12}(R_{x'})}$ with x'/x can be observed, the former parameter apparently depends only on Ri, i.e.,

$$\frac{U_*'/U_o}{f_{12}(R_{x'})} = f_{13}(Ri) .$$

Therefore,

$$U_*'/U_o = f_{12}(R_{x'})\, f_{13}(Ri) ,$$

which is the simplified form of f_{11} obtained in Chapter II.

Fig. 20 indicates that for values of Ri less than 0.4, density gradient in the flow has little effect on U_*'/U_o, which now depends only on $R_{x'}$ and is consequently equal to U_*/U_o. In other words, the apparent shear velocity is now equal to the actual shear velocity when $Ri \leq 0.4$. This is possible only if the Kármán constant is not affected. Therefore, one may also conclude from Fig. 20 that the Kármán constant changes little for $Ri \leq 0.4$.

Apparent Shear Velocity in the Case of a Boundary Layer in Transition

As stated before, when the turbulence promoter is removed, there will be a region of transition in the boundary layer in which the flow is neither laminar nor fully turbulent. In this region, the Kármán-Prandtl equation of velocity distribution over a smooth boundary, being deduced on the basis of fully turbulent flow, can no longer be applied. A method of computing the shear velocity in this case is to differentiate the momentum thickness with respect to x (or x'), assuming the ambient velocity to be constant along the boundary.

Calculation of shear velocity

By applying the principle of momentum to a unit width of the boundary, one can write the drag on the boundary over a length of x' as

$$D_{x'} = \int_0^\infty \rho U(U_o - U)dz ,$$

from which one obtains the so-called momentum thickness

$$\theta = \frac{D_{x'}}{\rho U_o^2} = \int_0^\infty \frac{U}{U_o}\left(1 - \frac{U}{U_o}\right) dz .$$

Since by definition the total drag coefficient is

$$D_{x'} = x' \ C_f \frac{\rho U_o^2}{2} ,$$

$$\frac{D_{x'}}{\rho U_o^2} = \frac{x' \ C_f}{2} .$$

Now $$\tau = \frac{dD_{x'}}{dx'} ,$$

so that $$\frac{d}{dx}\left(\frac{D_{x'}}{\rho U_o^2}\right) = \frac{U_*^2}{U_o^2} = \frac{d}{dx'}\left(\frac{x'C_f}{2}\right) ,$$

that is, $$\frac{U_*^2}{U_o^2} = \frac{1}{2} \frac{d}{dR_{x'}}(R_{x'}C_f) .$$

By plotting $\frac{U}{U_o}\left(1 - \frac{U}{U_o}\right)$ against z, the momentum thickness can be obtained by means of a planimeter as the area under the plot. The parameter C_f is then given by $2\theta/x'$. Knowing C_f, a plot of C_f against $R_{x'}$ can be prepared, and the value of U_*/U_o can be calculated by numerical differentiation of $R_{x'}C_f$ with respect to $R_{x'}$.

Fig. 21 shows C_f computed in this manner from data obtained with the boundary dry. It is significant that the transition starts as early as the beginning of the evaporation boundary, which is only 0.98 ft downwind from the leading edge of the solid boundary. It is also significant that the transition is less abrupt than indicated by a semi-empirical equatioh given by Prandtl (22)

$$C_f = 0.074 \ (R_{x'})^{-1/5} - \frac{A}{R_{x'}} ,$$

where A is a constant depending on the so-called "transitional Reynolds number", that is, the Reynolds number on the C_f against $R_{x'}$ plot where the transition curve departs from the Blasius curve for a laminar boundary layer.

In Fig. 22, data obtained with the boundary wet are plotted. Again it may be noted that in every case transition starts at the upwind edge of the evaporation boundary, and that transition is much more gradual than indicated by Prandtl's equation stated above. The corresponding curves for local shear velocity are obtained by differentiating $R_{x'}C_f$ with respect to $R_{x'}$, (see Fig. 23). It is of interest to compare Fig. 23 with Fig. 24, which shows the data of Burgers and Hegge Zijnen (3). From these figures it can be seen that the transition of shear velocity in both figures is far from being abrupt as often assumed. In the laminar range, the Burgers and Hegge Zijnen data lie slightly above the Blasius curve, Fig. 24. According to Hansen (15:10), this is due to the decreasing pressure gradient of flow in a tunnel. The same reasoning may be used to justify slight modification of the two curves of Fig. 22. But, as little numerical change will be involved, this refinement has not been made.

Effect of density gradient

Tests with the boundary layer in transition were made at speeds of ambient flow not less than 8 ft/sec (Tables 23 to 28). In the range of ambient speed from 8 to 32 ft/sec, and in the range of temperature gradients that may possibly be encountered in the wind tunnel at Fort Collins, the corresponding Richardson numbers are probably less than one. This can be seen from Fig. 20, where the second group of points from the right represents data obtained at the ambient speed of 8 ft/sec. For this last group of points, the Richardson number ranges from 0.5 to 1. For other ambient speeds greater than 8 ft/sec, the Richardson number would range from 0.04 to 0.2. Thus, for tests made at an ambient speed not less than 8 ft/sec, the Richardson number will not be greater than one.

Fig. 20 shows that, for Richardson numbers up to about one, the maximum effect of density gradient on the apparent shear velocity is about 8%. In view of the large scatter found even in the case of a fully turbulent boundary layer where the mean flow is quite steady (see Fig. 18), an error of 8% in the apparent shear velocity is actually not objectionable. For ambient speeds of 18 ft/sec and 32 ft/sec, Fig. 20 shows that density gradients have practically no effect on the apparent shear velocity.

If one is to isolate the density gradient effect for the case of the boundary layer in transition, one must be able to control the occurrence of transition, so that velocity profiles can be measured at identical ambient speeds with the transition of boundary layer flow occurring over identical parts of the boundary. Because the transition from laminar to turbulent flow may depend on the turbulence present in the ambient stream drawn from the atmosphere, and perhaps also on such disturbances as vibration of the air tunnel (neither of which can be controlled at present), it is not practicable to control the occurrence of the transition. Therefore, with the present equipment, the effect of density gradients on the apparent shear velocity cannot be studied when the boundary layer is in transition.

Fortunately, as discussed in the previous paragraph, the resultant error caused by neglecting the effect of density gradients will be small.

Evaporation in the Case of a Turbulent Boundary Layer

When water is fed to the buffer plates, the width of the evaporation surface is 28 in., with the main evaporation plates occupying a width of 4 in. in the center. Since the width of the main plates is relatively small, evaporation from these main plates with the buffer plates wet may be regarded as a two-dimensional case. Data for evaporation from the main plates have been collected with the buffer plates wet and dry respectively, so that some idea of the magnitude of lateral diffusion can be had by comparing the two sets of data.

Two-dimensional case

The evaporation data for the case of fully turbulent boundary layers obtained with buffers wet are presented in Figs. 26 to 30 in terms of $Ex/\nu_e \Delta C$ and $U_*^! x/\nu_e$, where $U_*^!$ is taken as the value of the apparent shear velocity at x.. In these figures, all the data obtained with a turbulence promoter placed in the tunnel and with the buffers wet are plotted. The ambient speeds range from 4 ft/sec to 48 ft/sec. The length of the dry approach, i.e., $(x' - x)$, changes from 0.98 ft to 6.27 ft. The temperature gradients are such that the Richardson number varies from 0.041 to 5.6. Despite all these variations, no discernible, systematic variation of N with any of the variables just mentioned can be observed in Fig. 30. The significance of this observation cannot be too strongly stressed, for one may then draw the important conclusion that the evaporation parameter N is primarily a function of $R_*^!$ only. It should be pointed out that this conclusion does not imply that the length of the dry approach and the Richardson number do not have any effect on N. Quite to the contrary, both the dry approach and the Richardson number can have important effects on N. The foregoing conclusion merely indicates that any effect of the dry approach and Ri on N may be accounted for by evaluating $U_*^!$ properly -- i.e., using Figs. 19 and 20. In other words, any influence of the dry approach and Ri on N is exercised through their influence on $U_*^!$. Once the correct value of $U_*^!$ at the end of the section of the boundary under consideration is evaluated, then N is determined uniquely by $R_*^!$. It is thus clear that within the range of the present experiments the expression deduced in Chapter II for N may be reduced to

$$\frac{Ex}{\nu_e \Delta C} = f_{14}\left(\frac{U_*^! x}{\nu_e}\right) .$$

Fig. 20 shows that for Ri up to 0.8, the apparent shear velocity is within 6% of the true shear velocity, i.e.,

$$\frac{U'_*}{U_o} \cong 1.06\ f_{12}(R_{x'}) = 1.06\ \frac{U_*}{U_o}\ .$$

As most runs have $Ri \leq 0.8$, the apparent shear velocity in most cases is approximately equal to the true shear velocity. Therefore, it is logical to compare the experimental data with theoretical expressions derived on the basis of zero density gradient. In each of Figs. 26 to 30, three curves representing various results of theoretical analysis are shown. All but Cermak's equation are based on Sutton's theory of turbulent exchange. It can be seen from these figures that the theory of Sutton as modified by Pasquill leads to a curve that follows the data reasonably well. When Pasquill's modification is not incorporated in Sutton's theory, the resultant curve is lower than the previous one. Both curves are calculated by means of Eq. 27, using the expressions of vapor distribution in a vertical obtained by Köhler and Yih, (see Chapter II).

Theoretical values of N given by Eqs. 10 and 11 are smaller than those predicted by the two curves just mentioned, the corresponding difference being in general on the order of 30% of the values given by Eqs. 10 and 11. As mentioned in Chapter III, there is no reason to expect the N-values computed by Eq. 9 to be identical to those computed by Eq. 27, because Eq. 9 is not theoretically sound. It will be recalled that Eqs. 10 and 11 are derived on the basis of Eq. 9 (see Chapter II). In a later part of the present chapter (see Vapor distribution in a vertical), it will be shown that vapor profiles computed according to any of Eqs. 8, 16, and 19 are identical; so that actually if Eq. 27 is applied, identical values of N will be obtained by using any one of Eqs. 8, 16, and 19 in the computations.

As mentioned in Chapter II, Pasquill (17) found that his data lay between the curves representing Eqs. 10 and 12, so that it was not certain whether ν_e should be used to evaluate K_v. Since the value of E given by Eq. 10 is lower than the correct value by about 30%, Pasquill's original plot, Fig. 31, should be modified. The modified plot, Fig. 32, shows definitely that the curve obtained by using ν_e in the computations is closer to the data than the other curve.

Figs. 26 to 30 also show that Cermak's equation follows the data very well, except for the lower region, where R'_* is less than 400.

Lateral diffusion

When water is not fed to the buffer plates on both sides of the main plates, the evaporation surface is only 4 in. wide crosswind and yet a maximum of 136 in. longitudinally. Since on each side of the main plates, there must exist a transition zone in which vapor concentration in each horizontal plane decreases from the concentration over the main plates to the concentration in the ambient streams, there exist on each side of the main plates horizontal vapor gradients in each level below the top of the vapor boundary layer. If horizontal velocity fluctuation exists in a crosswind direction, then mixing in this direction due to turbulence will transport vapor away from the main plates in the direction of the decreasing vapor gradient. This process is generally referred to as lateral diffusion of vapor. From what has been said so far, it should be obvious that lateral diffusion is a result of the combined effects of the lateral velocity fluctuations and the presence of the lateral vapor gradients.

An increase in the ambient wind velocity will result in an increase of both the lateral velocity fluctuations and the vapor concentration at a given point in the vapor boundary layer over the main plates. Consequently, both the lateral velocity fluctuations and the lateral vapor gradients will be increased by an increase in ambient speed. Therefore, one may conclude that lateral diffusion increases with the ambient speed.

For a given ambient speed and for a given elevation, points farther downwind from the leading edge of the main plates will have greater vapor concentrations and probably greater lateral velocity fluctuations, as a result of the growth of both the momentum and vapor boundary layers. Thus it can be seen that, other things being equal, an increase in x has the same effect as an increase in U_o. As an increase in U_o will result in an increase in U_* at a given point, it can also be seen that an increase in $U_* x/\nu_e$ may be due to an increase in either or both of U_o and x, and hence may result in an increase in lateral diffusion.

In view of the foregoing discussion, the fact that the deviation of no-buffer data from the curve for two-dimensional evaporation as R_* increases appears reasonable. (Compare Figs. 25 and 30, also see Fig. 34.)

Evaporation in the Case of a Boundary Layer in Transition

In Figs. 33 to 35 are represented all the evaporation data obtained without the turbulence promoter, using again the parameters N and R_*. The apparent shear velocity is obtained from the appropriate curve in Fig. 23 with the aid of Fig. 22.

Fig. 35 shows all evaporation data obtained with buffers wet, under both regimes of boundary layer flow. Open circles represent data collected in a fully turbulent boundary layer, whereas solid circles represent data collected in a boundary layer in transition. It is of great interest to note that in Fig. 35 no systematic deviation exists between the two sets of data. Hence the conclusion may be made that the regimes of boundary layer flow have no influence on N as long as U_* is properly evaluated. In other words, regimes of boundary layer flow can influence N only through its influence on U_*. Fig. 34 showing all data obtained with buffers dry lends further support to the conclusion just made. In Fig. 34, considerable scatter can be seen. This scatter, however, is not systematic.

Vapor Distribution in a Vertical

For the case of the fully-developed, turbulent boundary layer, solutions of Eq. 6 obtained by Sutton, Köhler, and Yih (see Chapter II) may be used to determine the vapor distribution in a vertical. In the present study, the Köhler-Yih solution is first used, with the exchange coefficient evaluated by the modified Sutton's theory of turbulent exchange. The modification of Sutton's theory as suggested by Pasquill consists in using the vapor diffusivity to evaluate the exchange coefficient for vapor (see Chapter II).

Two profiles of vapor distribution have thus been computed for runs 1-I-W-(0) and 8-I-W-(0), the ambient velocities in these runs being 48 ft/sec and 18 ft/sec respectively. Runs of higher ambient velocities have been chosen, because the thermocouple psychrometer is believed to yield more reliable results in flow of higher velocity (see Chapter II). In Fig. 36, the computed profiles are compared with the experimental data. The agreement between the data and the theoretical curves may be considered excellent, indicating that the modification of Sutton's theory as suggested by Pasquill is sound. In this connection, it should be pointed out that the values of C_o and C_i used in computing the theoretical curves are the local values, occurring at the place and during the period the vapor profile was measured. These values are tabulated below and are different from the mean values listed in the tables at the end of this report.

Run No.	U_o ft/sec	x = 11.3 ft	
		C_o	C_i lb/ft^3 x 10^6
1-I-W-(0)	48	276	386
8-I-W-(0)	18	432	739

The vapor profile for Run 8-I-W-(0) has also been computed by using Eq. 8 obtained by Sutton. The following table shows that the vapor profiles computed by using Eqs. 8 and 19 are identical.

z ftx10^3	C by Eq. 19 lb/ft^{3}x 10^3	C by Eq. 8 lb/ft^{3}x 10^3	z ftx10^3	C by Eq. 19 lb/ft^{3}x 10^3	C by Eq. 8 lb/ft^{3}x 10^3
1.2	0.621	0.620	140	0.461	0.459
2	0.609	0.609	180	0.452	0.451
4	0.591	0.590	220	0.447	0.446
8	0.569	0.569	240	0.444	0.443
12.3	0.555	0.555	300	0.439	0.438
30	0.522	0.520	350	0.437	0.436
40	0.511	0.510	400	0.435	0.435
60	0.494	0.493	450	0.435	0.434
80	0.482	0.481	500	0.433	0.433
123	0.465	0.464	600	0.433	0.432

Note: $\nu = \nu_e$
$C_i = 0.739$ lb/ft^{3}x10^3
$C_o = 0.432$ lb/ft^{3}x10^3

Temperature Distribution in a Vertical

As explained in Chapter III, an expression for temperature distribution in a vertical may be obtained for the case of the turbulent boundary layer by analogy. Following Pasquill's suggestion, thermal diffusivity will replace ν in Eq. 3 . The resultant exchange coefficient is then taken as K_h . As the vapor concentration in the experiments reported herein amounts to only a few per cent by weight of air, it is considered more logical to use the thermal diffusivity of air in the computations. The thermal diffusivity of water vapor in saturated air, however, is within 6% of the thermal diffusivity of air.

Figure 37 shows two profiles of temperature distribution. The experimental data are those of runs 1-I-W-(0) and 8-I-W-(0), and the theoretical curves are computed according to Eq. 29 obtained by analogy from the Köhler-Yih solution of Eq. 6. The value of K_h used in Eq. 28 is computed in the manner explained in the previous paragraph. The ambient and plate temperatures used in these computations are as follows:

Run No.	U_o ft/sec	x = 11.3 ft	
		T_o	T_i °F
1-I-W-(0)	48	45.8	38.5
8-I-W-(0)	18	69.1	56.9

These are the local values occurring at the time the temperature distribution was measured and are therefore different from the mean values given in the tables in the end of this report. The theoretical curves may be considered as excellent representations of the experimental data.

The fact that the theoretical distributions of vapor and temperature have been born out by experimental data lends further support to the conclusion that Sutton's theory of turbulent exchange should be modified in the manner suggested by Pasquill.

Thickness of Vapor and Thermal Boundary Layers

In view of the excellent agreement between the theoretical and experimental distributions of vapor and temperature, an expression for the thickness of vapor and thermal boundary layers may be obtained from the Köhler-Yih solution of Eq. 6 by applying the modified Sutton's theory of turbulent exchange. This expression is

$$\Gamma\left[\frac{m}{1+2m}, \frac{\eta^{1+2m}}{(1+2m)^2}\right] = \Gamma\left(\frac{m}{1+2m}\right), \tag{30}$$

where $$\eta = m\left[(Pr)^{\frac{-1}{1+m}}(1+2m)(1+3m)\right]^{\frac{-2m}{1+2m}}\left(\frac{U_o}{U_*}\right)^2\left(\frac{x'}{x}\right)^{\frac{1}{1+2m}}\frac{\delta_1}{x}. \tag{31}$$

In Eq. 31, δ_1 is the thickness of a vapor or thermal boundary layer, and Pr, the Prandtl number, is equal to 0.6 for vapor exchange and 0.74 for heat exchange. Thus, as soon as the vertical velocity distribution at a section, and the length of the approach $(x' - x)$ are known, the thickness of a vapor or thermal boundary layer can be computed by means of Eqs. 29 and 30.

Concluding Remarks

For the turbulent boundary layer, the data presented and discussed in this chapter are well represented by theoretical curves computed by a procedure of integration explained in Chapter II, the exchange coefficient for vapor being evaluated by Sutton's theory of turbulent exchange as modified by Pasquill. It is found that the solutions of the differential equation of two-dimensional evaporation obtained by Sutton, Köhler, and Yih all yield identical vapor profiles. However, it is only by integrating a vapor profile at the end of the evaporation boundary that one obtains theoretical values of N and R_* well representing the data. A formula Eq. 10 for the total rate of evaporation derived by Sutton by considering an integral extended over the evaporation surface gives values of N about 30% lower than the mean experimental values.

Although the present study is limited to R_* of about 10^5, the theoretical curves are by no means similarly limited, and may well be valid over a larger range.

Chapter VI

CONCLUSIONS

Within the scope of the present study, the following conclusions may be drawn:

1. The evaporation parameter N may be considered as uniquely determined by the Reynolds number R_* regardless of the regime of boundary layer flow (see Figs. 30 and 35). This conclusion implies that the length of the dry approach relative to the length of the evaporation surface, the Richardson number, and the regime of flow can influence N only insofar as U_* is influenced. In the tests carried out for the present study, the length of the dry approach varies from x/12 to x approximately, and Ri varies from about 0.04 to 5.6.

2. Sutton's theory of turbulent exchange as modified by Pasquill proves to be a sound basis for theoretical study of mass and heat transport by forced convection (see Chapter V).

3. With the aid of the modified Sutton's theory, vertical distribution of vapor in the region of fully-developed, turbulent flow can be accurately predicted by the solutions obtained by Sutton, Köhler, and Yih, i.e., by Eqs. 8 and 16 or 19 (see Chapter V and Fig. 36).

4. On the basis of the modified Sutton's theory of turbulent exchange, evaluation of the theoretical vapor flux through the vertical section at the end of an evaporation surface leads to a curve relating N and R_* that is a good representation of the experimental data (see Figs. 26 to 30).

5. An equation derived by Cermak on the basis of Reynolds analogy as well as the 1/7-power relationship of velocity distribution closely follows the data, when R_* exceeds about 400.

6. For the case of fully-developed, turbulent flow without large-scale mixing, an expression for the vertical distribution of temperature has been derived by analogy from the Köhler-Yih solution of evaporation. With K_h evaluated by the modified Sutton's theory, the resultant theoretical distribution of temperature in a vertical predicts accurately the experimental distribution (see Chapter V and Fig. 37).

7. For the case of the turbulent boundary layer,

$$\frac{U_*'}{U_o} = f_{12}(R_{x'})\, f_{13}(Ri) \ ,$$

where $f_{13}(Ri) = 1$ for $0 < Ri \leq 0.4$, and $f_{12}(R_{x'})$ can be expressed by an equation given by Sutton as follows:

$$0.243^{1-n}\left[\frac{n^2 2^{n-2}(n+1)^{-n}(n+2)^{-n}}{(1-n)^{3-2n}}\right]^{\frac{1}{2(1+n)}}\left(\frac{U_o x'}{\nu}\right)^{\frac{-n}{2(n+1)}} .$$

When $2\text{x}10^5 \leq R_{x'} \leq 2\text{x}10^6$, $f_{12}(R_{x'})$ is closely represented by the well-known formula $\dfrac{0.172}{R_{x'}{}^{0.10}}$ derived on the basis of 1/7-power relationship of velocity distribution (see Figs. 19 and 20).

8. The Kármán constant does not vary appreciably when Ri lies between zero and 0.4 (see <u>Apparent shear velocity and density gradient</u>, Chapter V).

9. The form of a vapor or thermal boundary layer in fully-developed, turbulent regime, is intrinsically defined by the following equation:

$$\Gamma\left[\frac{m}{1+2m} , \frac{\eta^{1+2m}}{(1+2m)^2}\right] = \Gamma\left(\frac{m}{1+2m}\right)$$

where

$$\eta = m\left[(Pr)^{\frac{-1}{1+m}}(1+2m)(1+3m)\right]^{\frac{-2m}{1+2m}}\left(\frac{U_o}{U_*}\right)^2\left(\frac{x'}{x}\right)^{\frac{1}{1+2m}}\frac{\delta_1}{x} .$$

In this equation, δ_1 is the thickness of the boundary layer at a distance x from the leading edge of the wetted or heated plate. The Prandtl number Pr is equal to 0.6 for vapor exchange, and 0.74 for heat exchange (see Chapter V).

10. When the Reynolds number R_*' is less than about 10^3, the effect of lateral diffusion is not appreciable. In the range of $R_*' > 10^3$, lateral diffusion tends to increase the rate of evaporation beyond the rate of two-dimensional evaporation, (compare Figs. 25 and 30, and also see Fig. 33).

BIBLIOGRAPHY

1. Albertson, M.L. Analysis of evaporation as a boundary layer phenomenon. Dissertation, State University of Iowa, 1948.

2. Albertson, M.L. Evaporation from a plane boundary. Heat Transfer and Fluid Mechanics Institute, held at Stanford University, p. 243-54, 1951.

3. Burgers and van der Hegge Zijnen. Proc. 1st International Congress for Applied Mechanics, Delft, p. 113-28, 1924.

4. Cermak, J.E. and Koloseus, H.J. Lake Hefner model studies--Final Report - Part I. Department of Civil Engineering, Colorado A and M College, Report No. 54JEC20, Nov. 1953.

5. Ertel, H. Beweis der Wilhelm Schmidtschen konjugierten potenz Formeln für Austausch und Windgeschwindigkeit in den bodennsken Luftschichten. Meteorologische Zeitschrift, 50:386, 1933.

6. Goldstein, S. A note on the boundary layer equations. Proc. Cambr. Phil. Soc., v. 35, 1939.

7. Hansen, M. Velocity distribution in the boundary layer of a submerged plate. NACA TM 585, Oct. 1930.

8. Hesselberg, T. and Bjordkal, E. Über das Verteilungsgesetz der Windruhe. Beitrage Phys. frei. Atmos., v. 15, 1929.

9. Hewson, E.W.(ed.) International symposium on atmospheric turbulence in the boundary layer. Geophysical research paper No. 19. Geophysics Research Directorate, Air Force Cambridge Research Center, Air Research and Development Command, p. 25-31, 1952.

10. Kármán, T. Mechanische Ähnlichkeit und Turbulenz. Nachrichten von der Gesellschaft der Wissenschaften zu Göttingen, Fachgruppe I, No. 5, p. 58-76, 1930.

11. Köhler, H. On evaporation from snow surfaces. Arkiv für Geofysik. Band 1, nr. 8, p. 11-185, 1950.

12. Maisel, D.S. and Sherwood, T.K. Evaporation of liquids into turbulent gas streams. Chemical Engineering Progress, p. 131-8, March 1950.

13. Maisel, D.S. and Sherwood, T.K. Effect of air turbulence on rate of evaporation of water. Chemical Engineering Progress, 46:172-5, April 1950.

14. Mangler, W. Die "ähnlichen" Lösungen der Prandtlschen Grenzsichtgleichungen. Zeitsch. ang. Math. und Mech., 23, 1943.

15. Nikuradse, J. Strömung in glatten Rohren. VDI - Forschungsheft 356, 1932.

16. Nikuradse, J. Strömungsgesetze in rauhen Rohren. VDI - Forschungsheft 361, 1933.

17. Pasquill, F. Evaporation from a plane, free-liquid surface into a turbulent air stream. Proc., Royal Society, Series A, 182:75-95, 1943.

18. Pasquill, F. Eddy diffusion of water vapor and heat near the ground. Proc., Royal Society, Series A, 198:116-40, 1949.

19. Pohlhausen, E. Der Wärmeaustauch zwischen festen Körpern und Flüssigkeiten mit kleiner Reibung und kleiner Wärmeleitung. Zeit. für ang. Math. und Mech. Heft 2, p. 115-21, 1921.

20. Powell, R.W. and Griffiths, E. The evaporation of water from plane and cylindrical surfaces. Trans., Inst. of Chemical Engineers, 13:175-98, 1935.

21. Powell, R. W. The evaporation of water from saturated surfaces. Engineering, v. 150, Oct. 4, 1940.

22. Prandtl, L. Ergebnisse der Aerodynamischen Versuchsanstalt zu Göttingen, 3:3-5, 1927; 4:27, 1932.

23. Prandtl, L. and Reichardt, H. Einfluss von Wärmeschichtung auf die Eigenschaften einer turbulenten Strömung. Deutsche Forschung, Heft 21, p. 110-21, 1934.

24. Rouse, H. Elementary fluid mechanics. New York, John Wiley, 1946. 366p.

25. Schultz-Grunow, F. New resistance formula for smooth plates. NACA TM 986, 1941.

26. Sheppard, P.A. The aerodynamic drag of earth's surface and the value of von Kármán's constant in the lower atmosphere. Proc., Royal Society (London), A188, p. 208-22, 1940.

27. Sutton, O.G. Wind structure and evaporation in a turbulent atmosphere. Proc., Royal Society (London), A40, p. 701-22, 1934.

28. Taylor, G.I. Diffusion by continuous movements. Proc., London Mathematical Society, Series 2, 20:196-211, 1922.

29. Wade, S.H. Evaporation of liquids in currents of air. Ind. Chemist, v. 18, No. 205, p. 55-8, 1942.

30. Yih, C.S. A comparative study of momentum transfer, heat transfer, and vapor transfer, Part II. Report No. 2 under ONR Contract No. N9 onr-82401, June 1951.

31. Yih, C.S. On a differential equation of atmospheric diffusion. Trans., AGU, v. 33, No. 1, 1952.

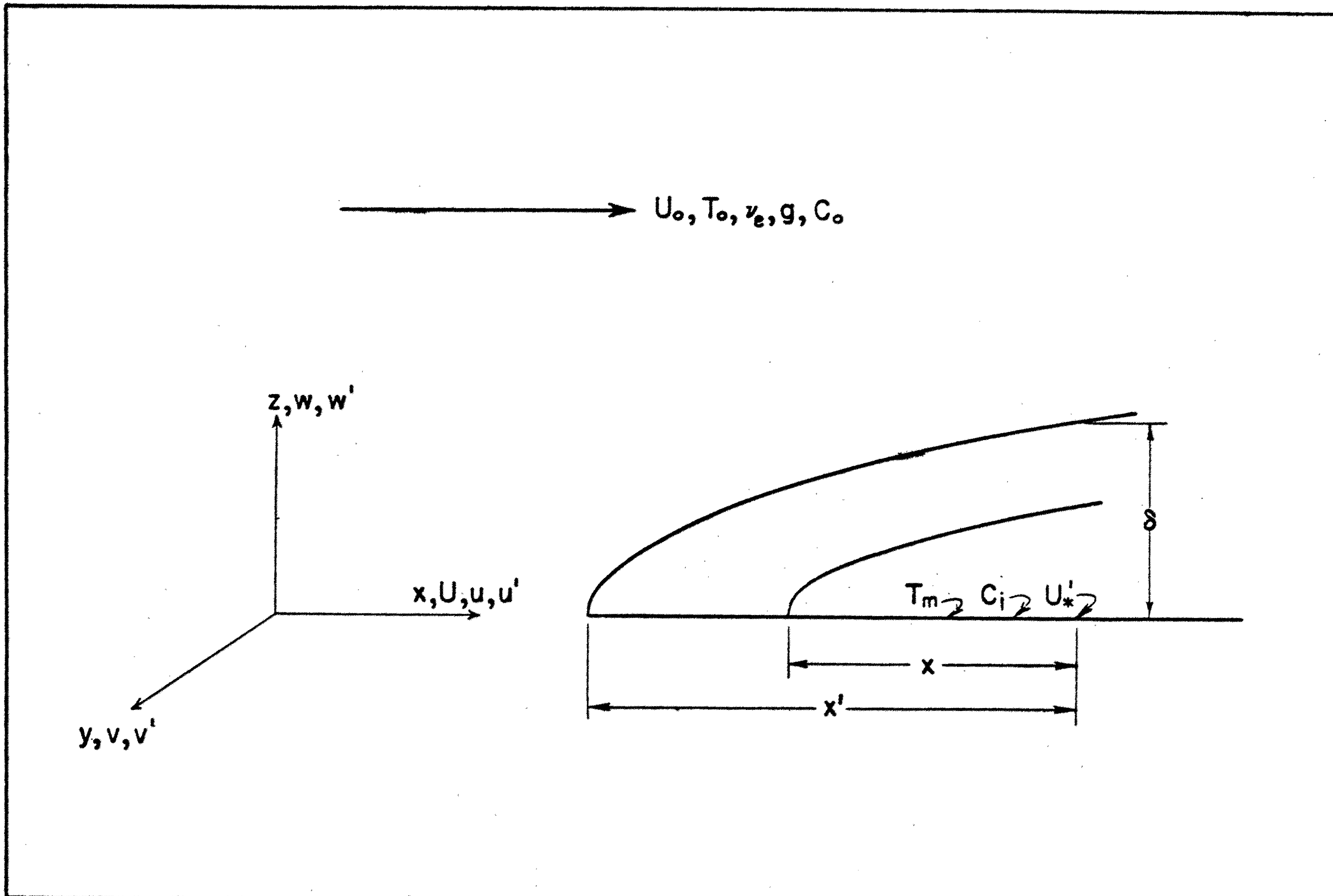

Fig. 1 Definition sketch.

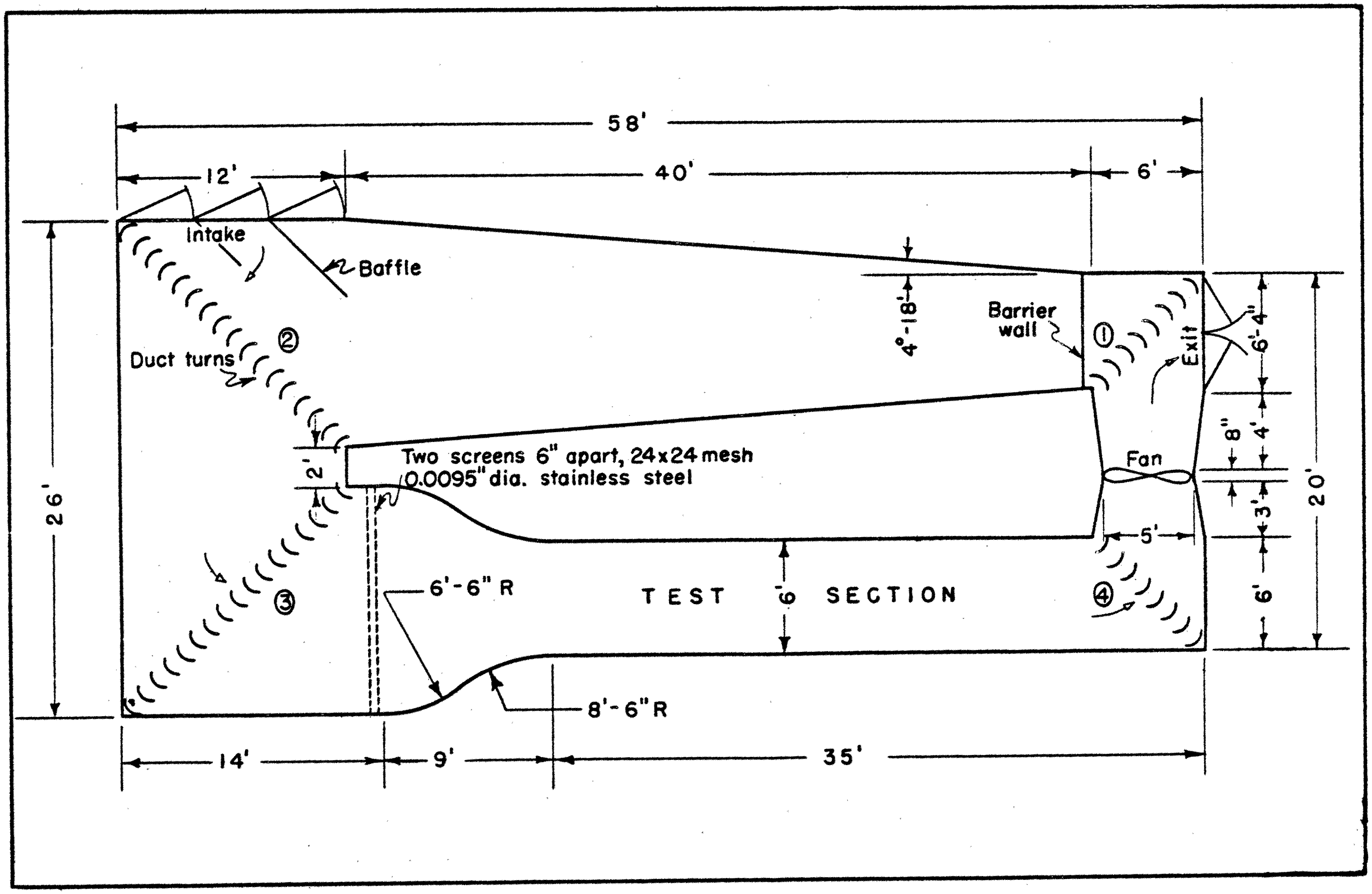

Fig. 2 Plan of wind tunnel.

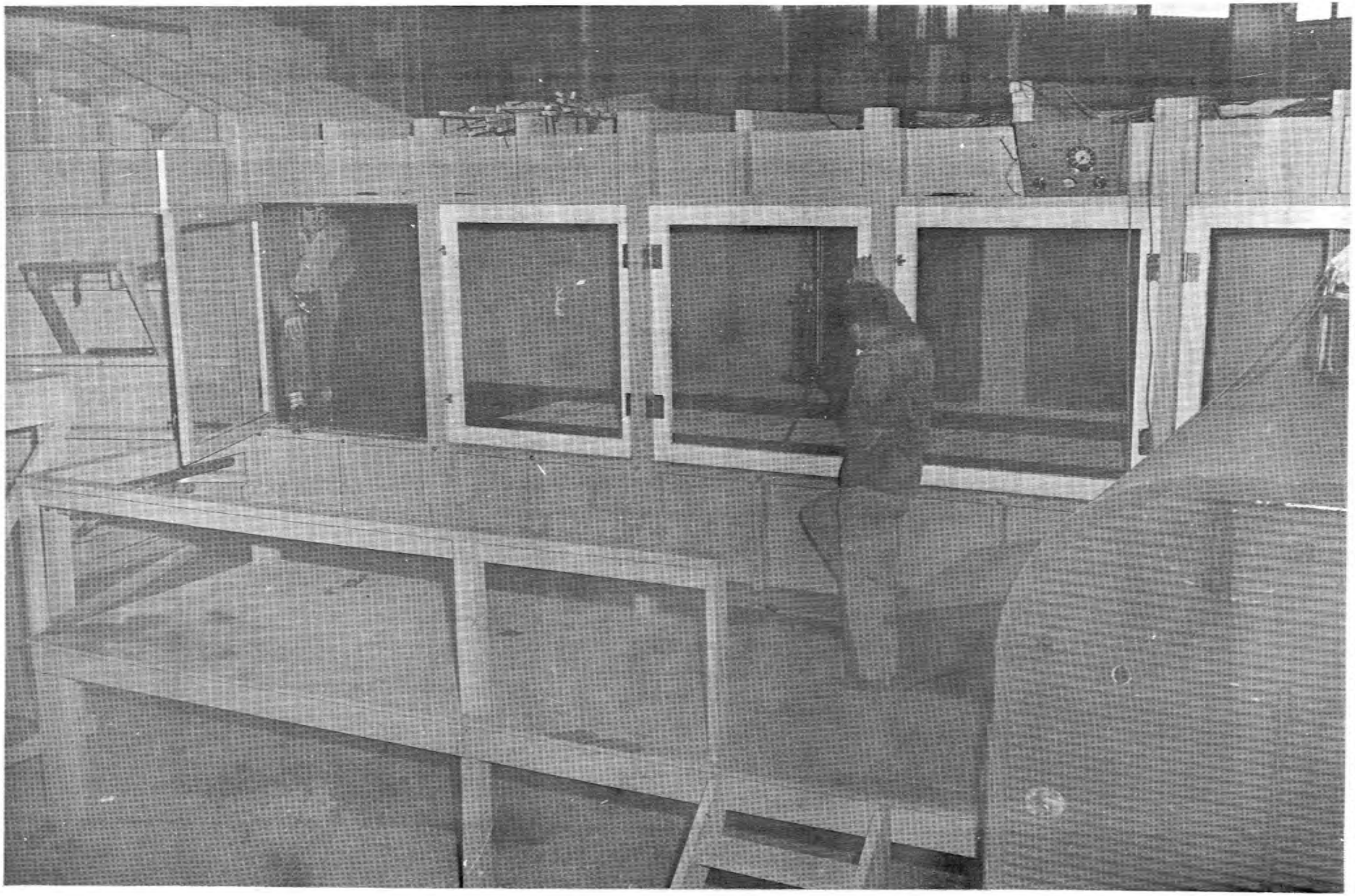

Fig. 3 View of test section of wind tunnel.

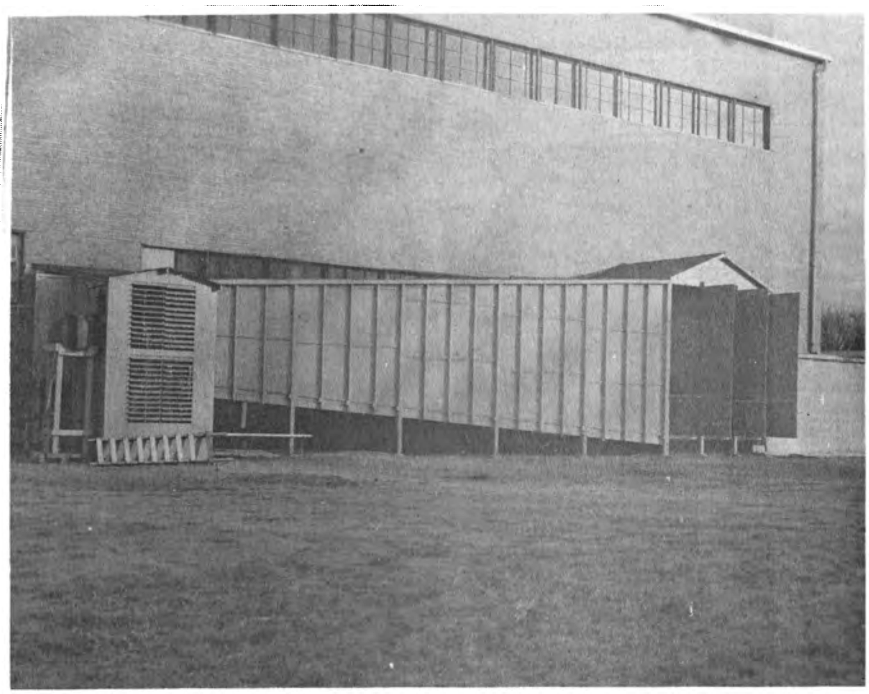

Fig. 4 View of outside portion of wind tunnel.

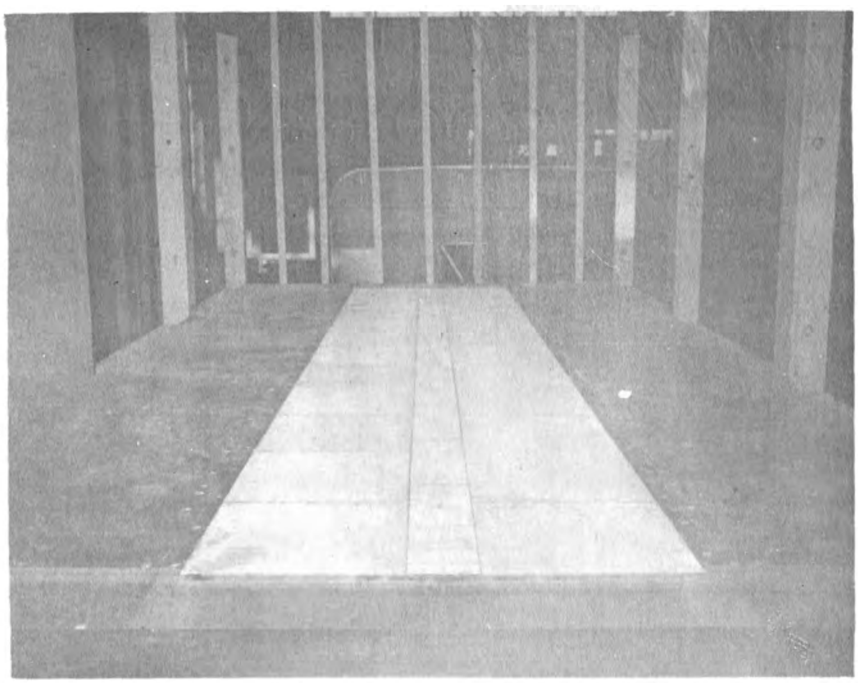

Fig. 5 View of experimental boundary inside the test section.

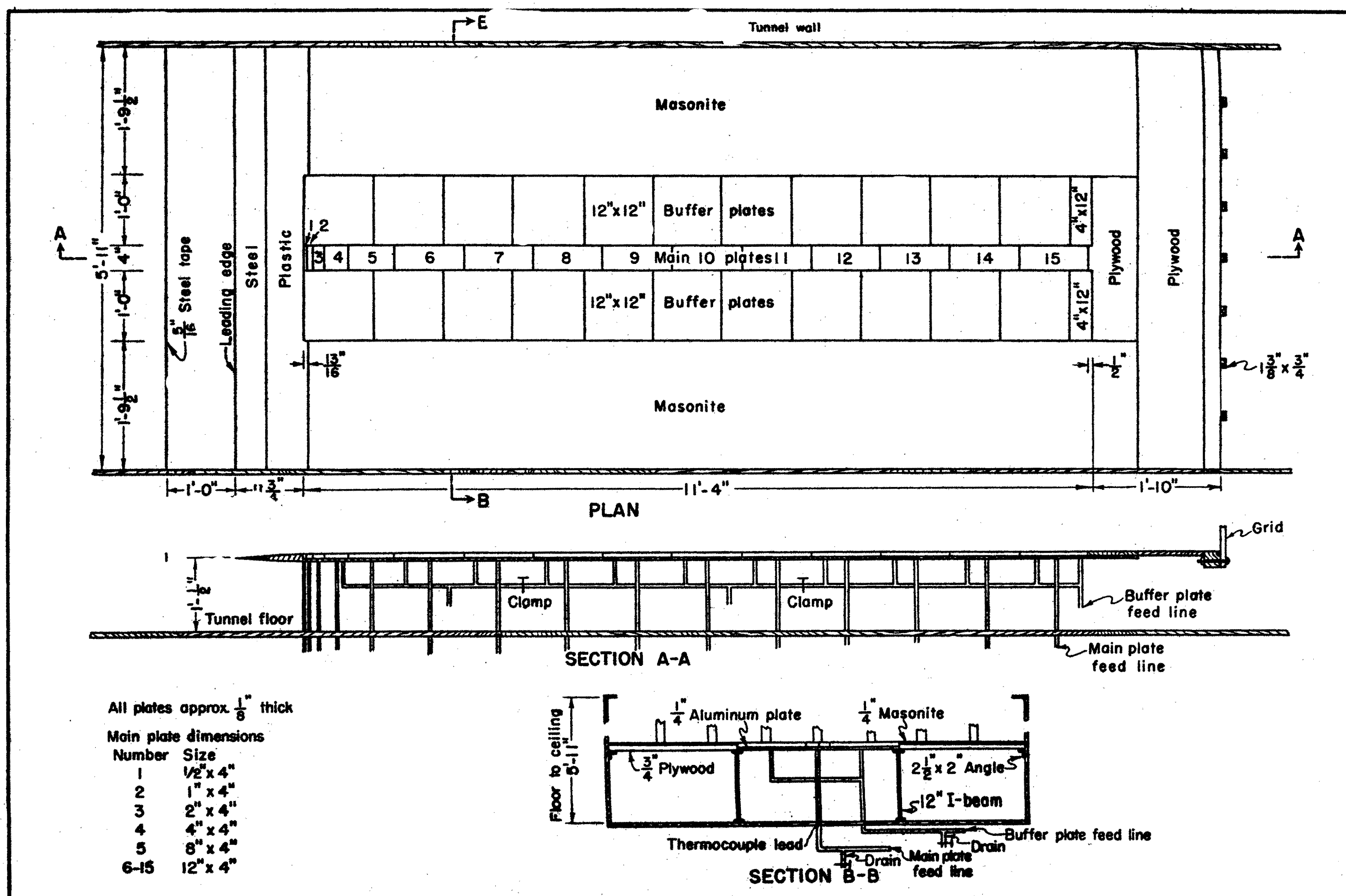

Fig. 6 Details of experimental boundary

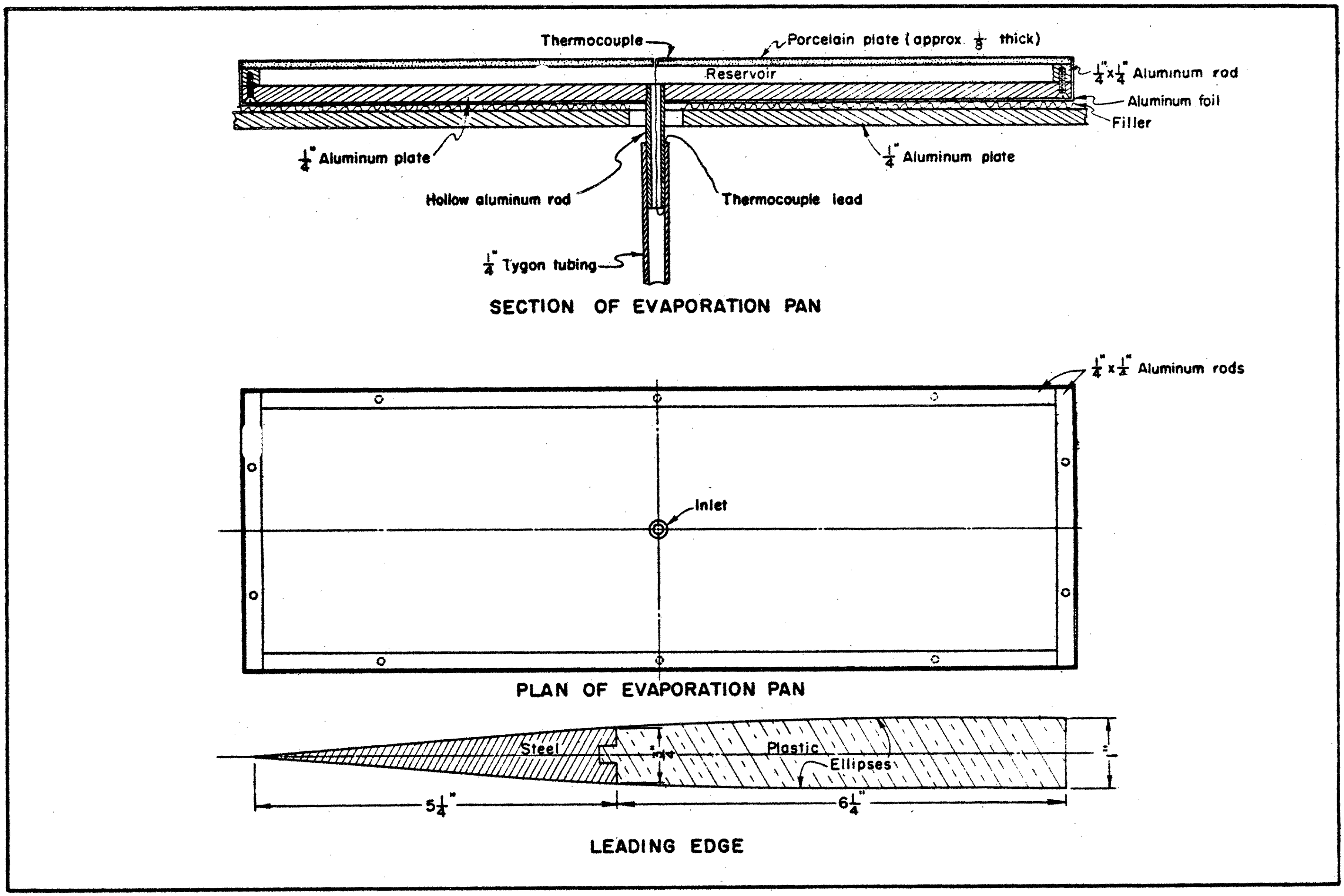

Fig. 7 Details of evaporation pan and nose piece

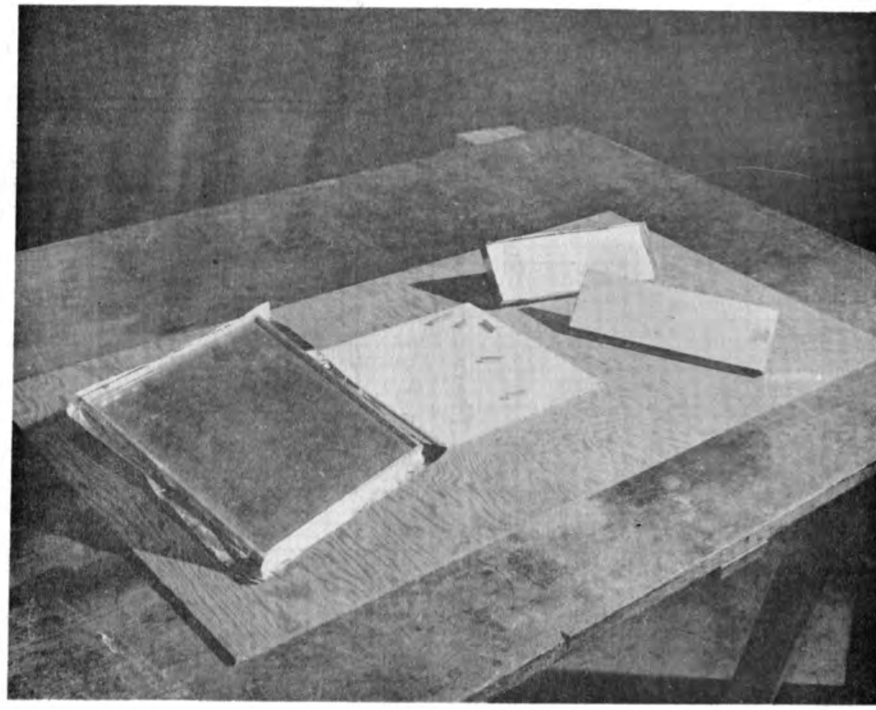

Fig. 8 Components of evaporation pans.

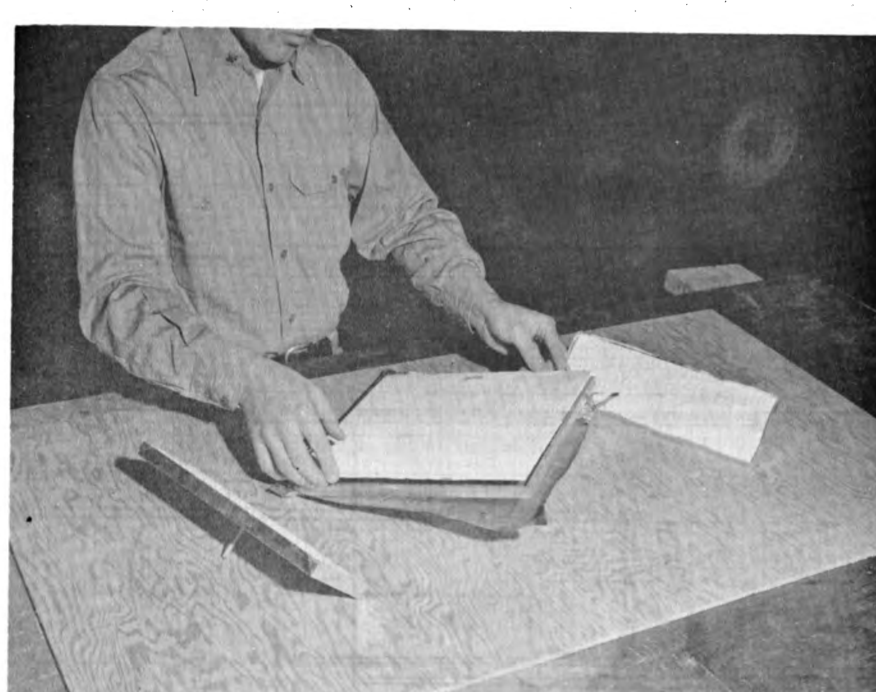

Fig. 9 Assembled evaporation pans.

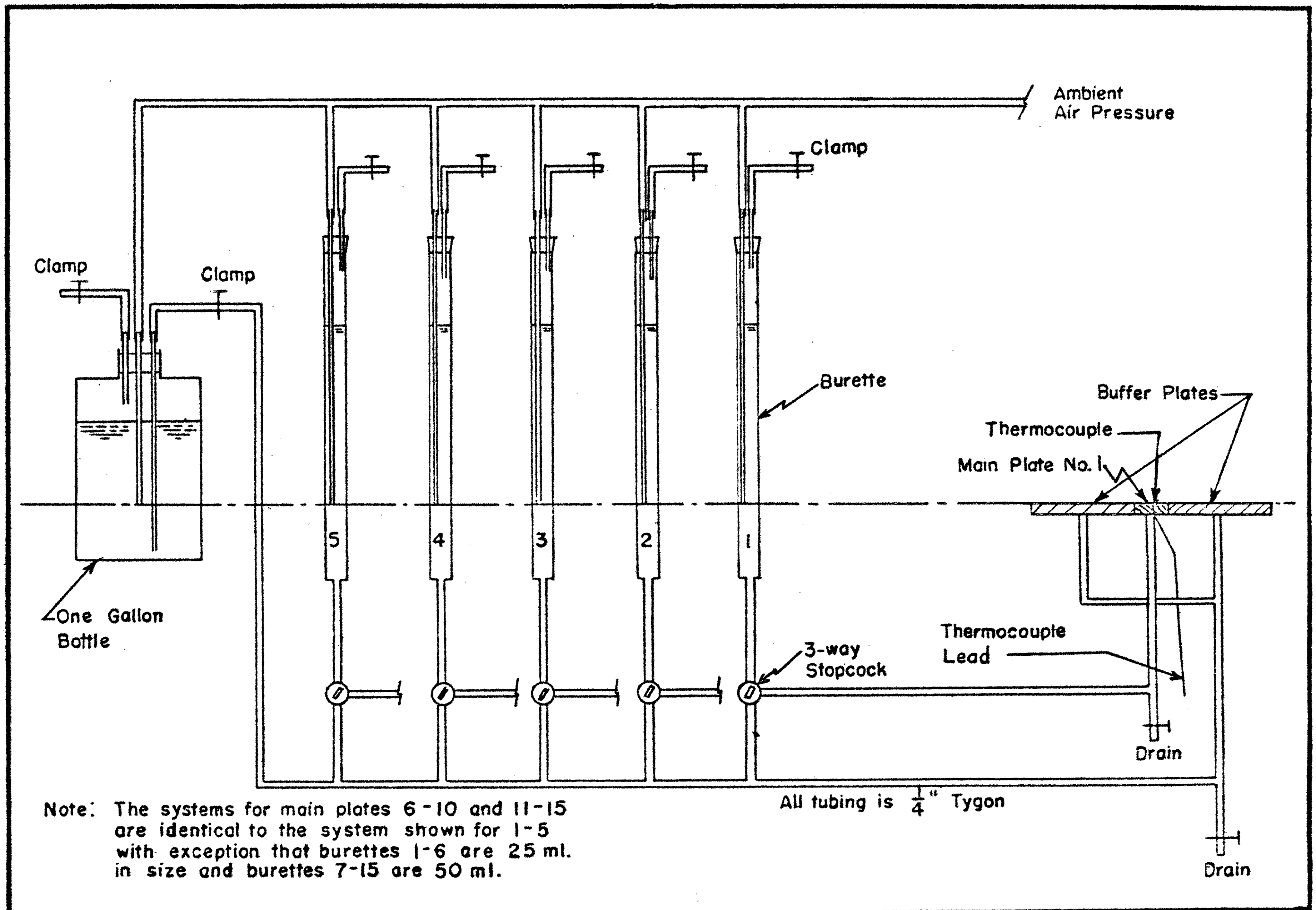

Fig. 10 Automatic water feed and measuring system

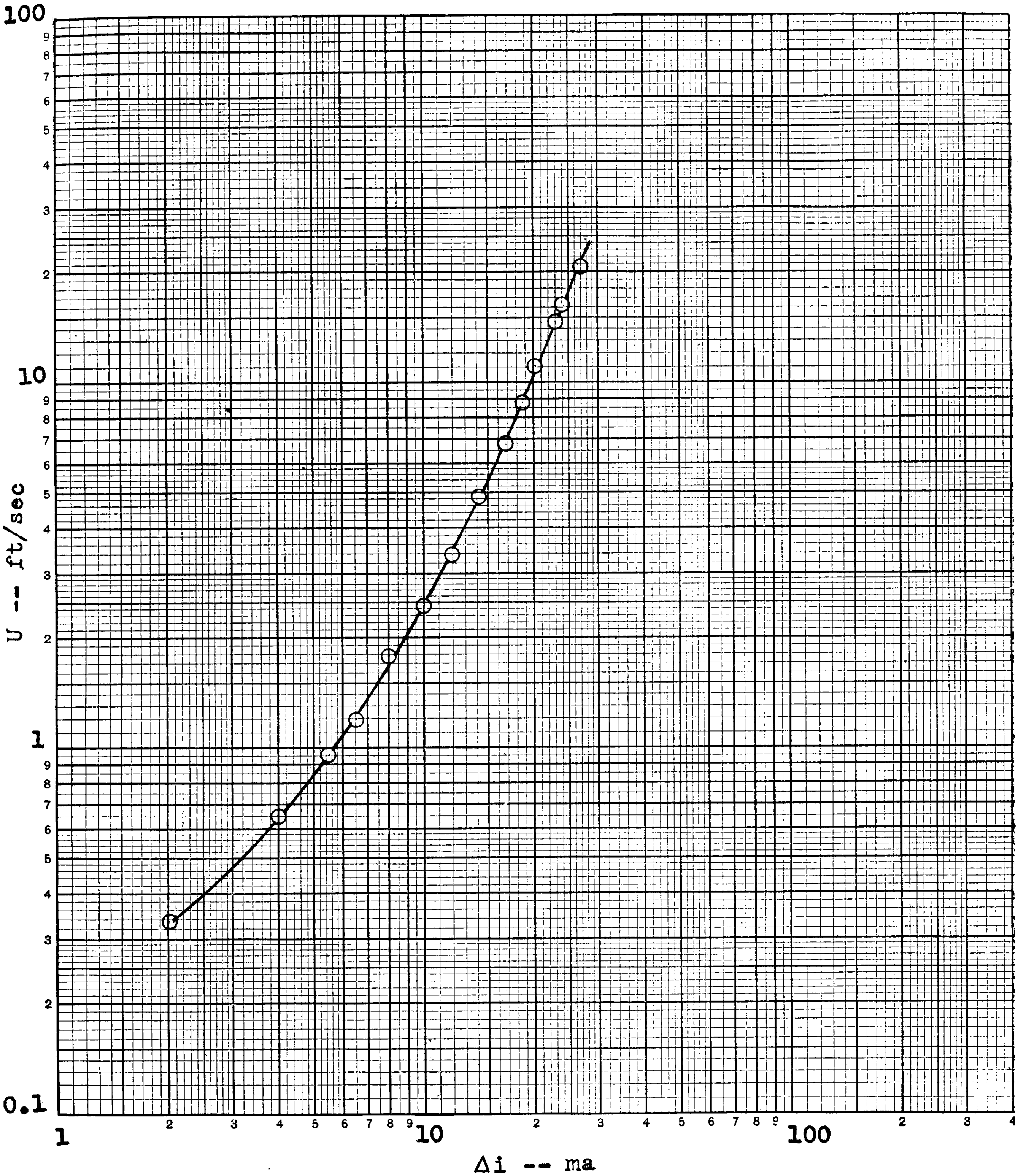

Fig. 11 Typical calibration curve for hot-wire anemometer.

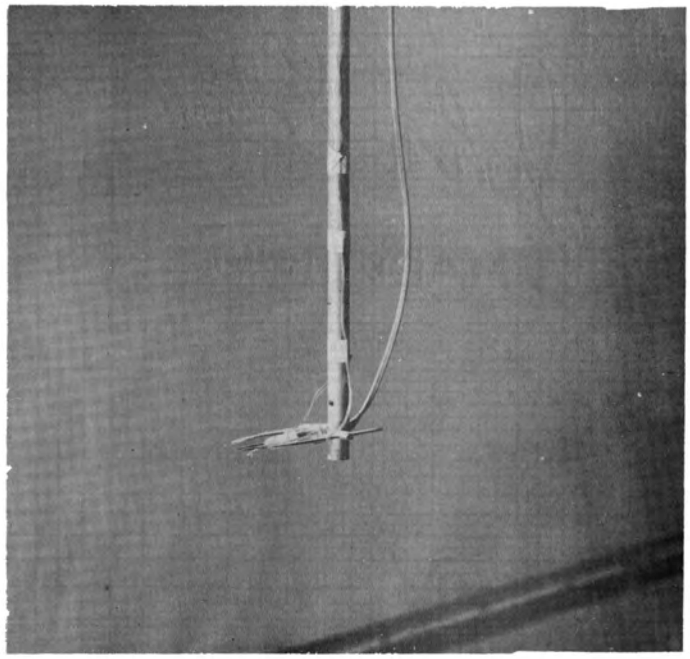

Fig. 12 View of forward measuring probe.

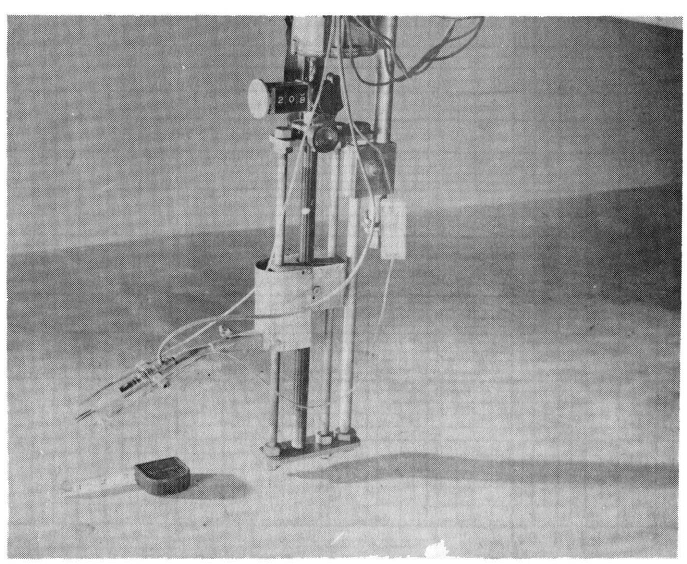

Fig. 13 View of vertical traversing mechanism.

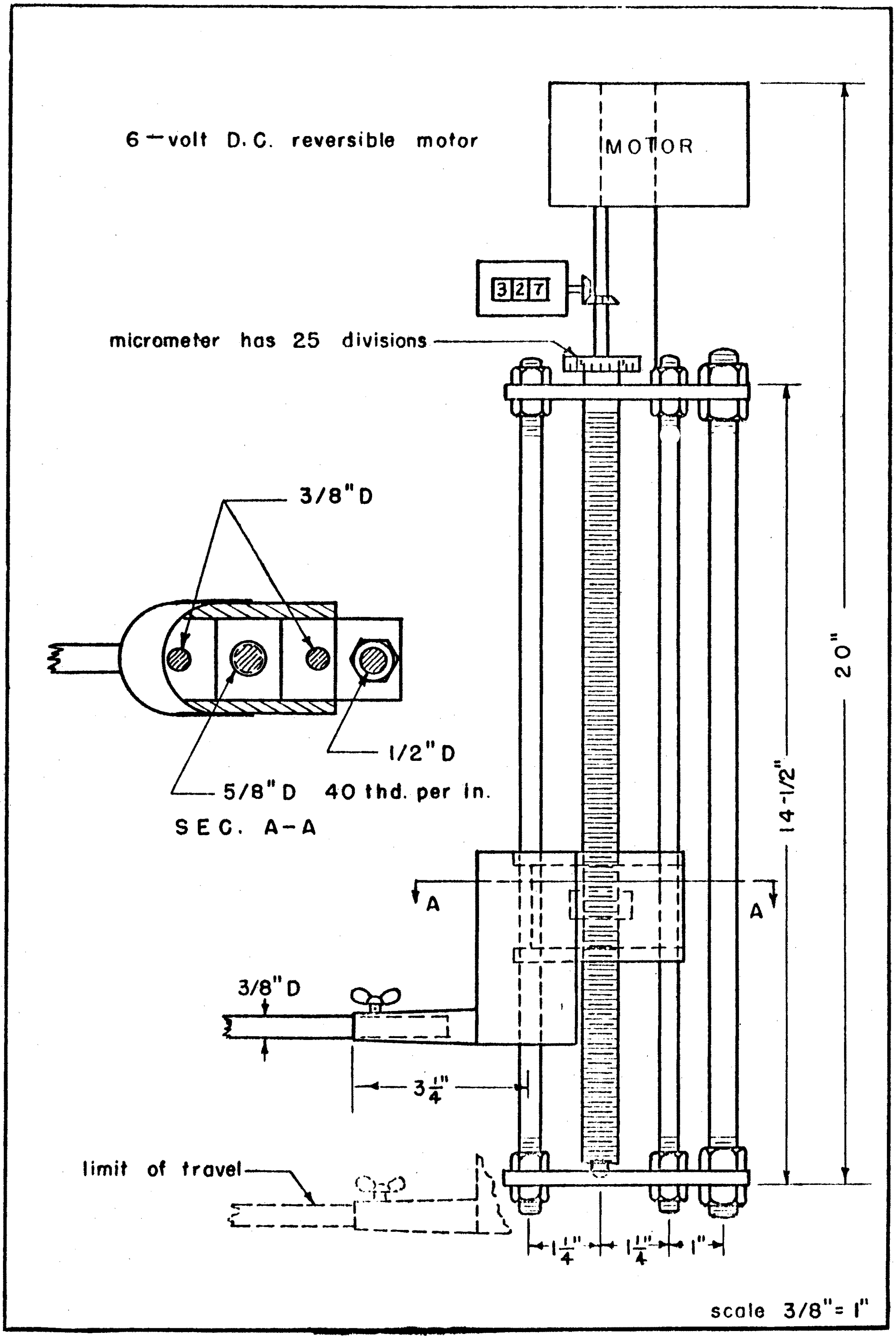

Fig. 14 Details of vertical traversing mechanism

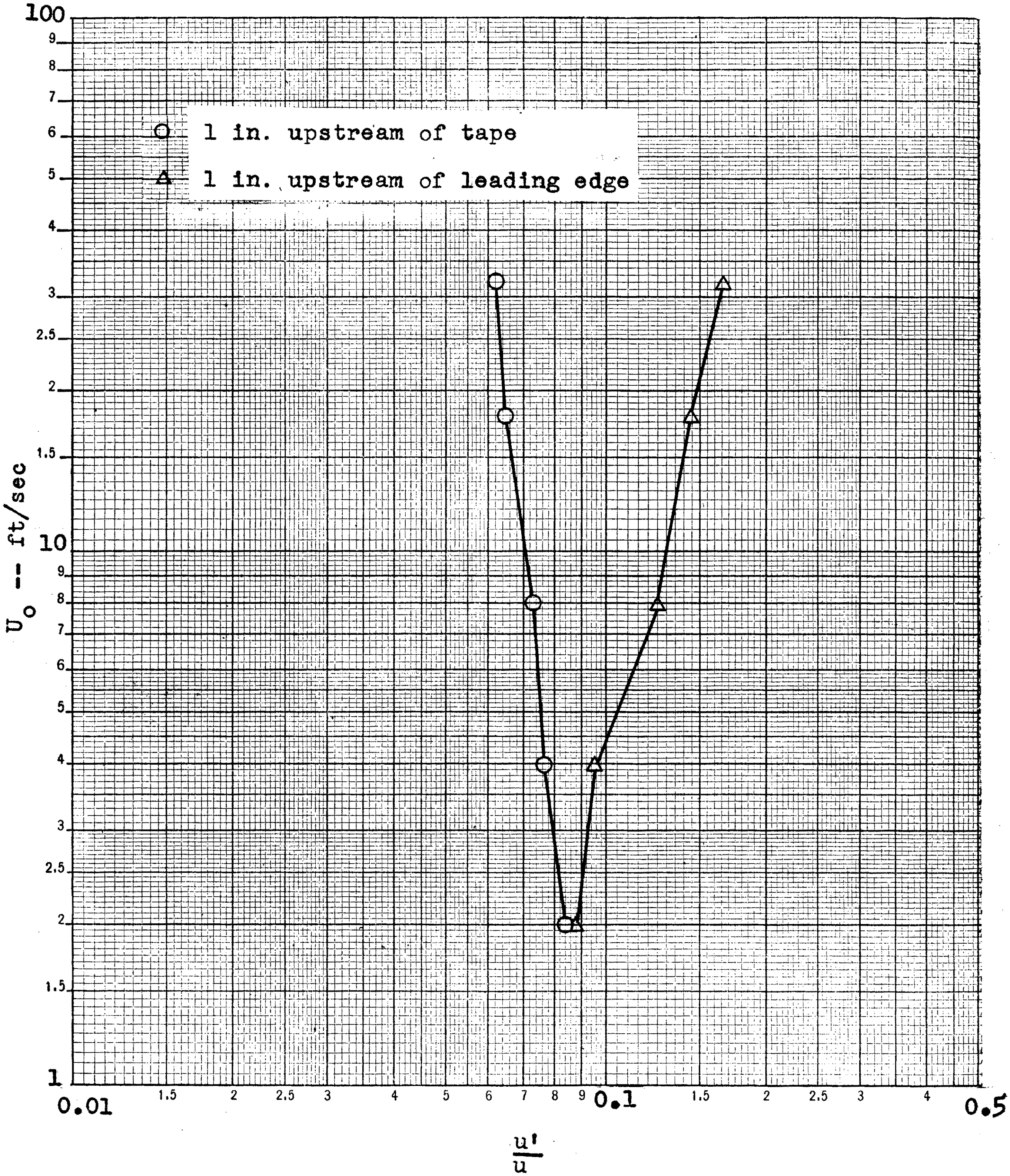

Fig. 15 Effect of turbulence promoter (tape) on turbulence intensity.

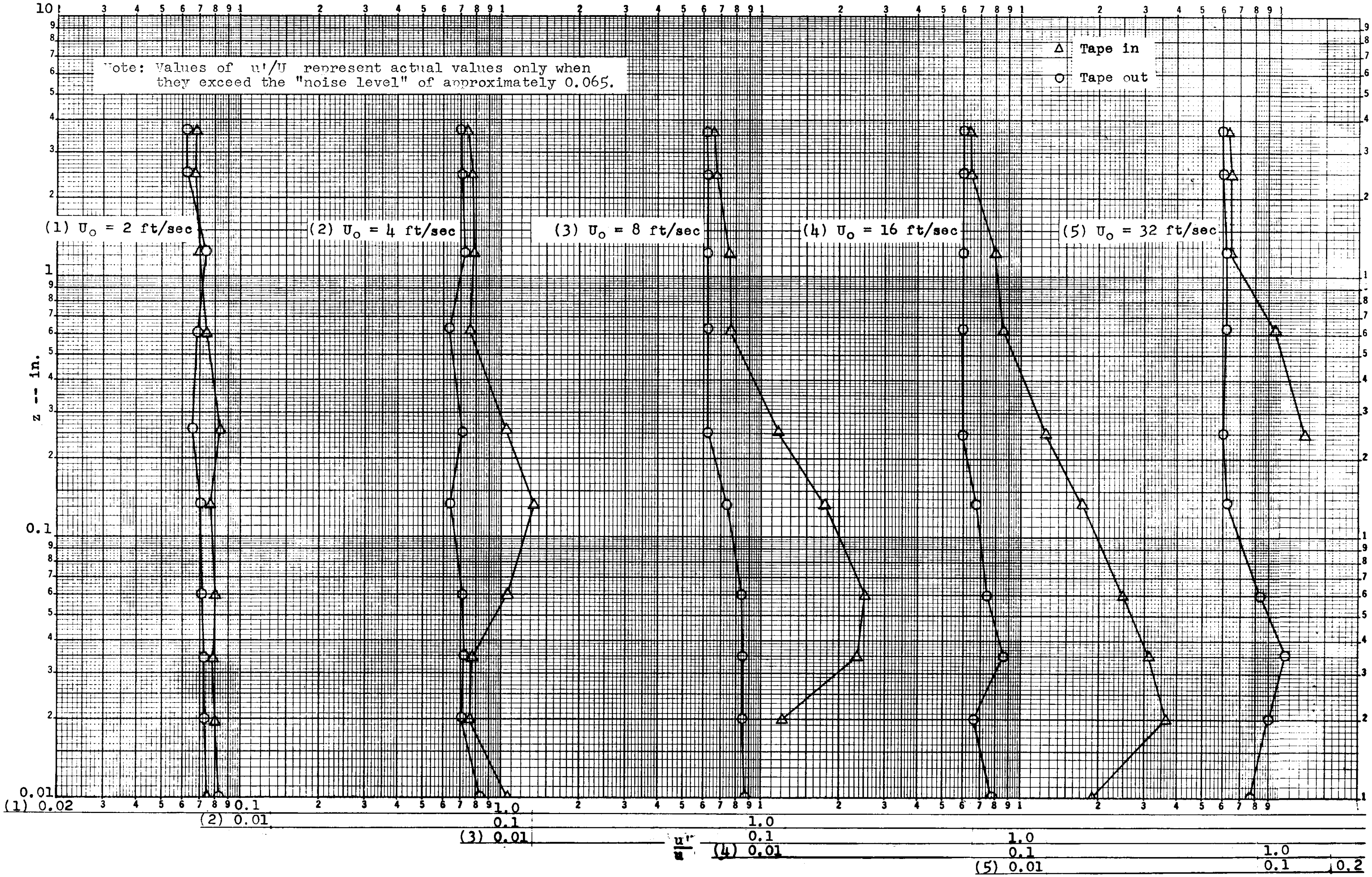

Fig. 16 Turbulence intensity profiles.
$x' = 0.96$ ft

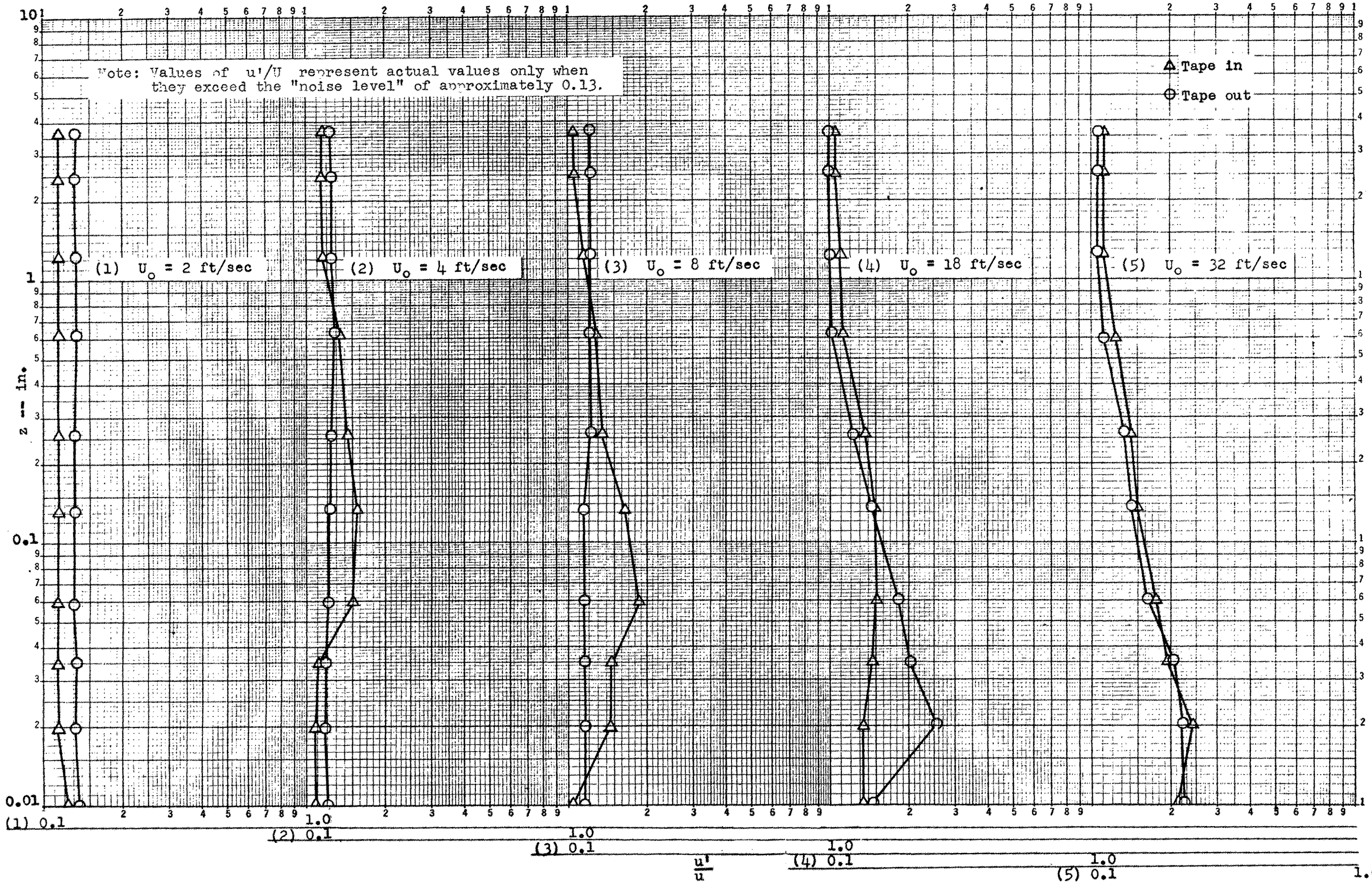

Fig. 17 Turbulence intensity profiles.
x' = 3.75 ft

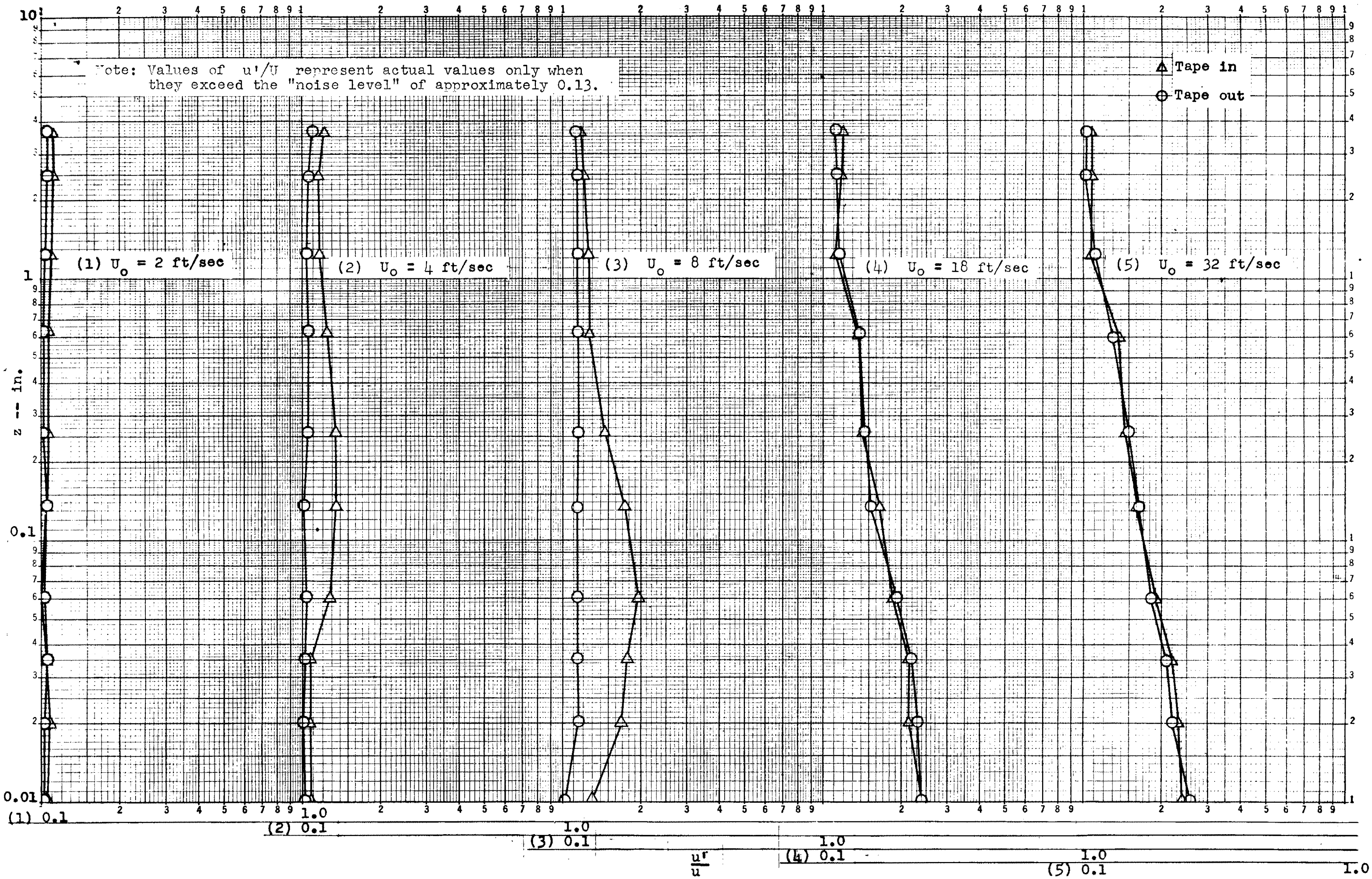

Fig. 18 Turbulence intensity profiles.
x' = 12.25 ft

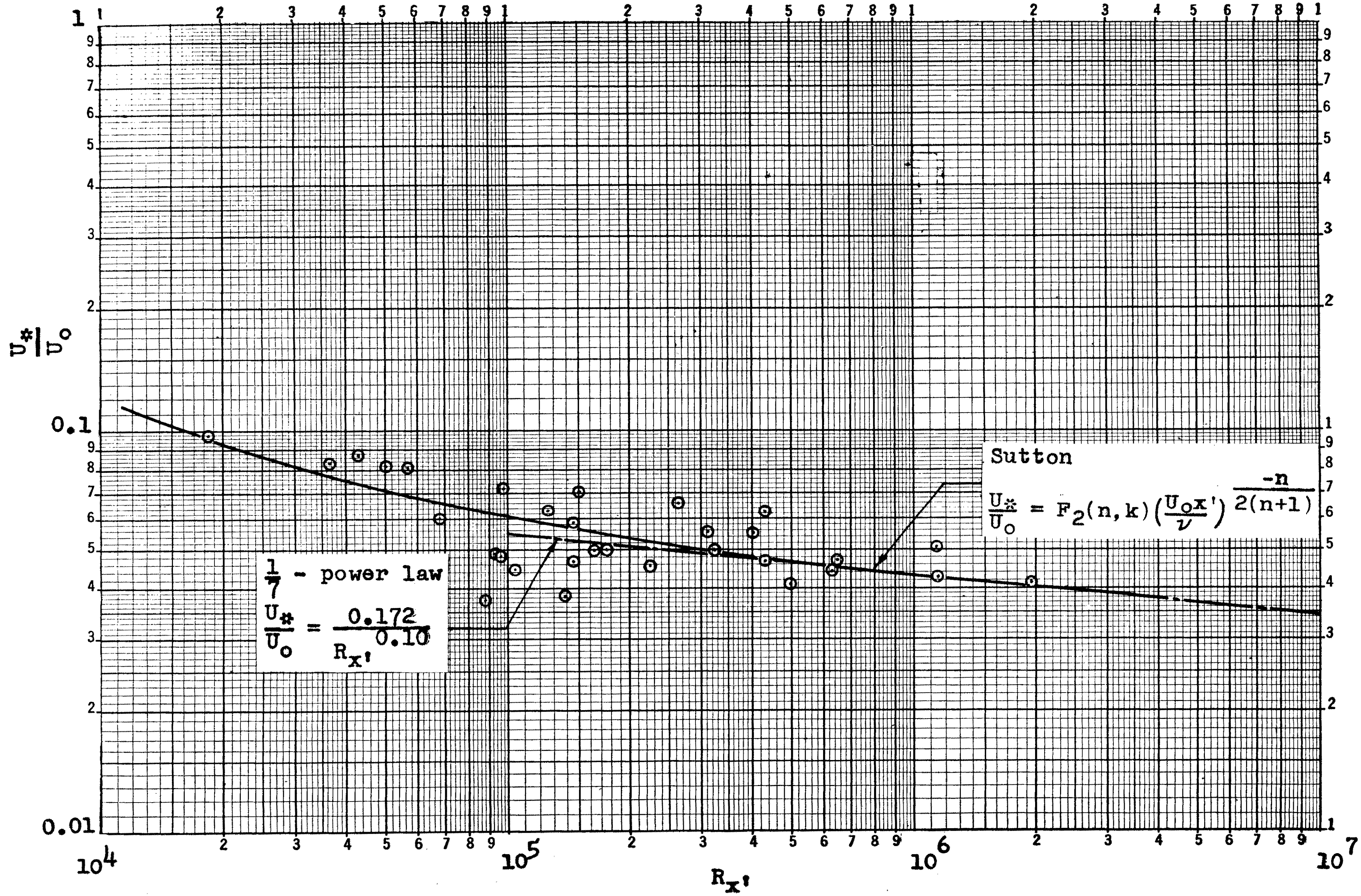

Fig. 19 Variation of U_*/U_o with R_*' for turbulent boundary layer free from density gradients.

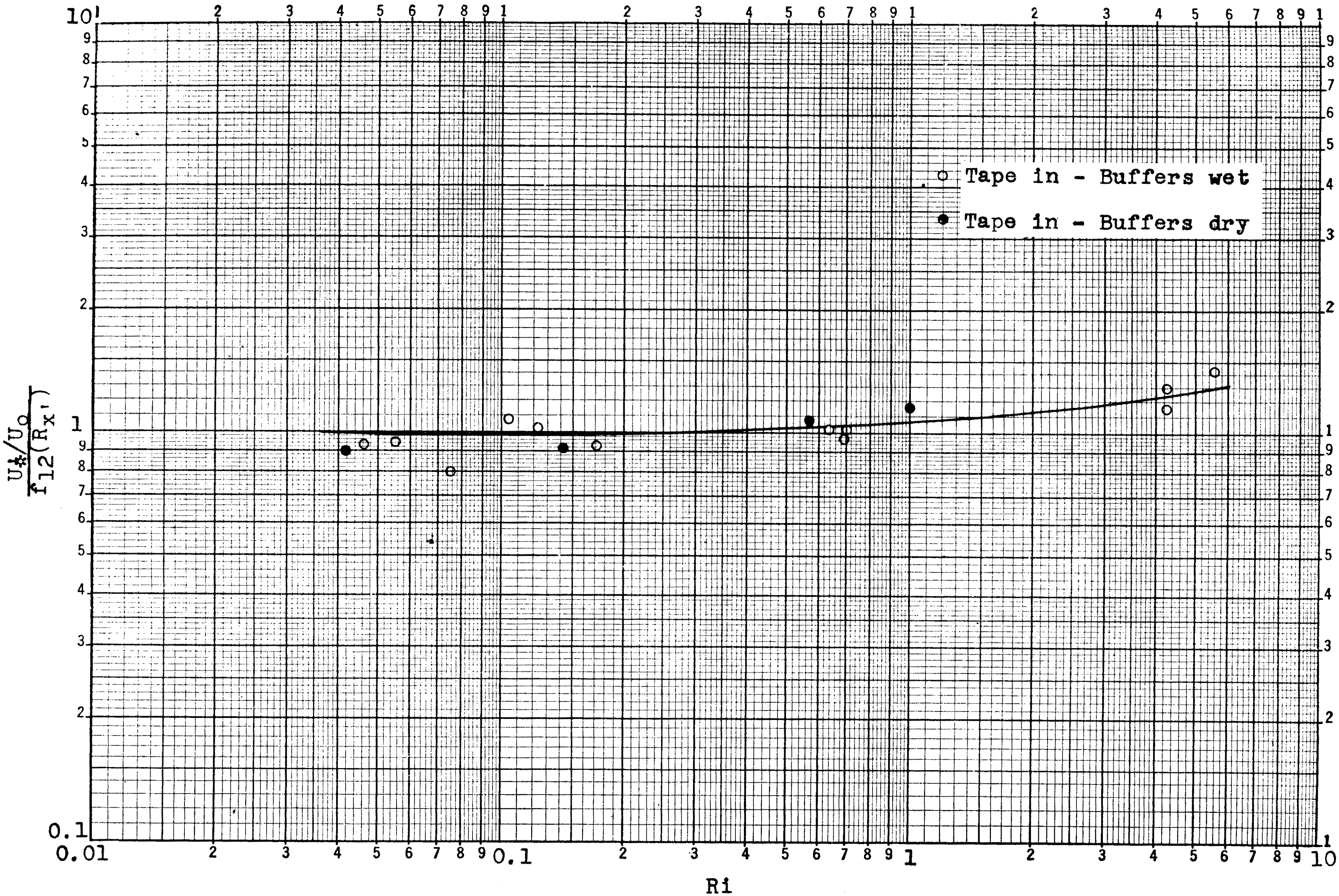

Fig. 20 Effect of temperature gradient on apparent shear velocity in turbulent boundary layer.

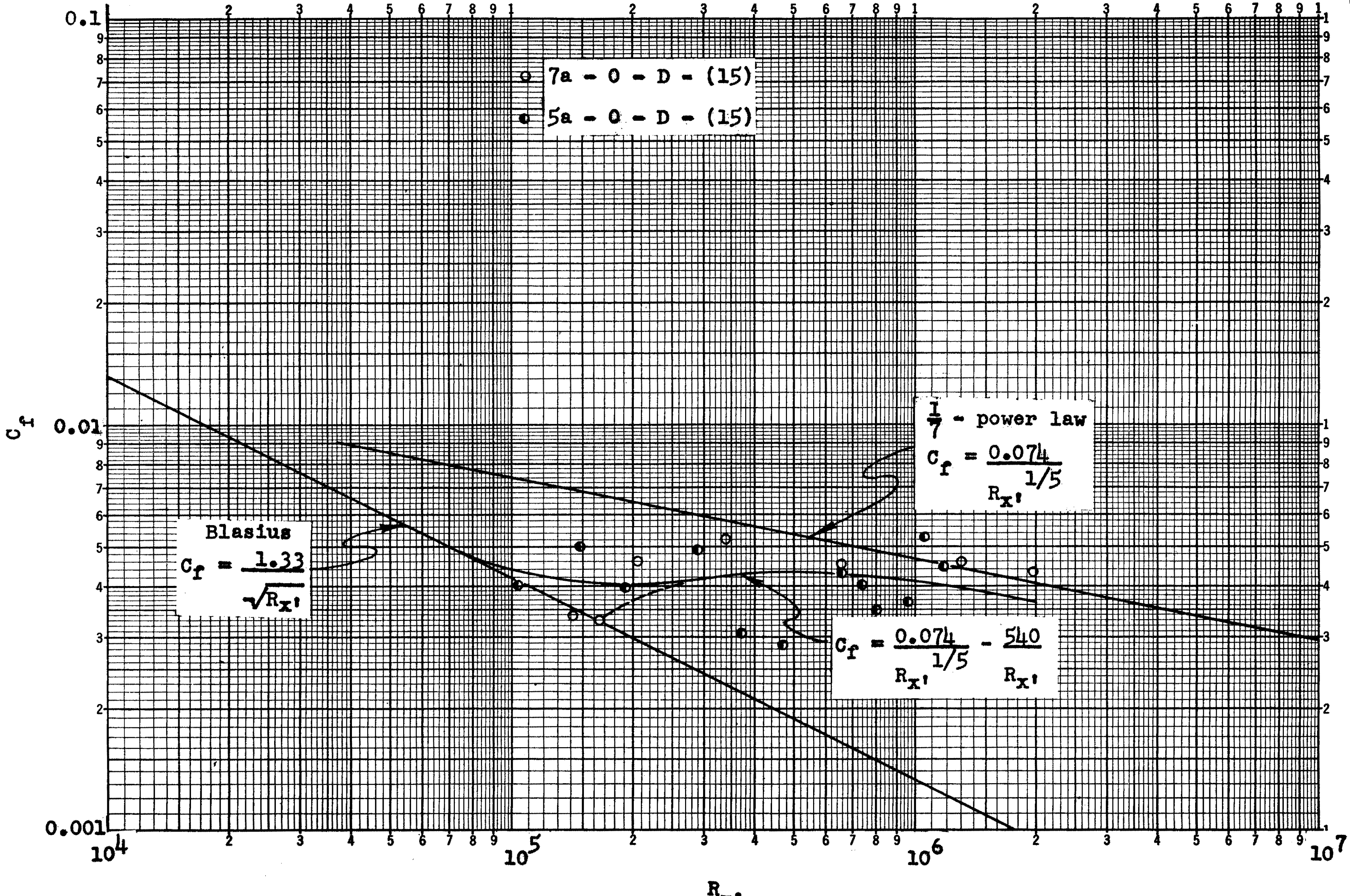

Fig. 21 Total drag coefficient for boundary layer in transition (boundary dry).

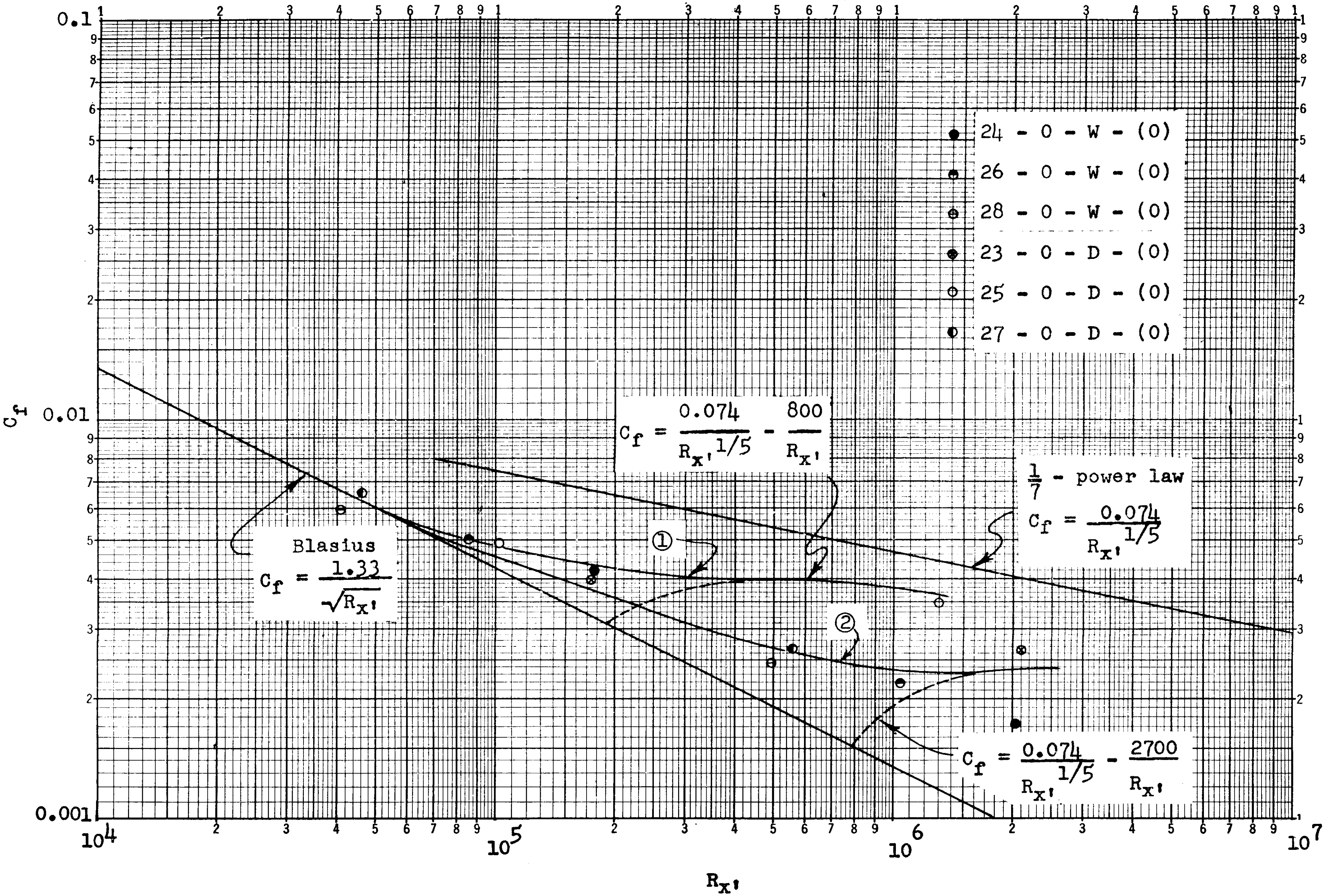

Fig. 22 Total drag coefficient for boundary layer in transition (boundary wet).

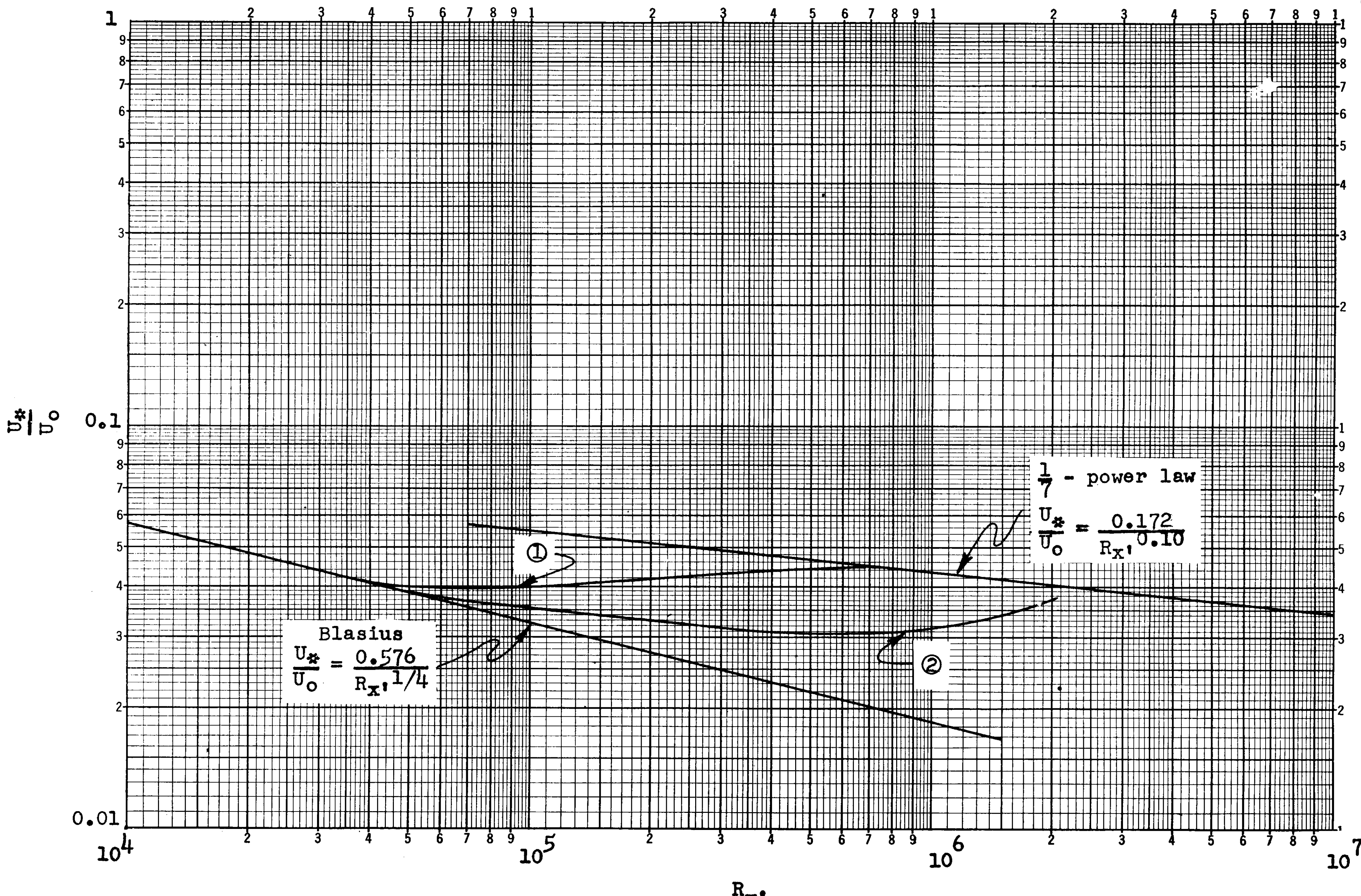

Fig. 23 Variation of U_*/U_o with $R_{x'}$ for boundary layer in transition (boundary wet).

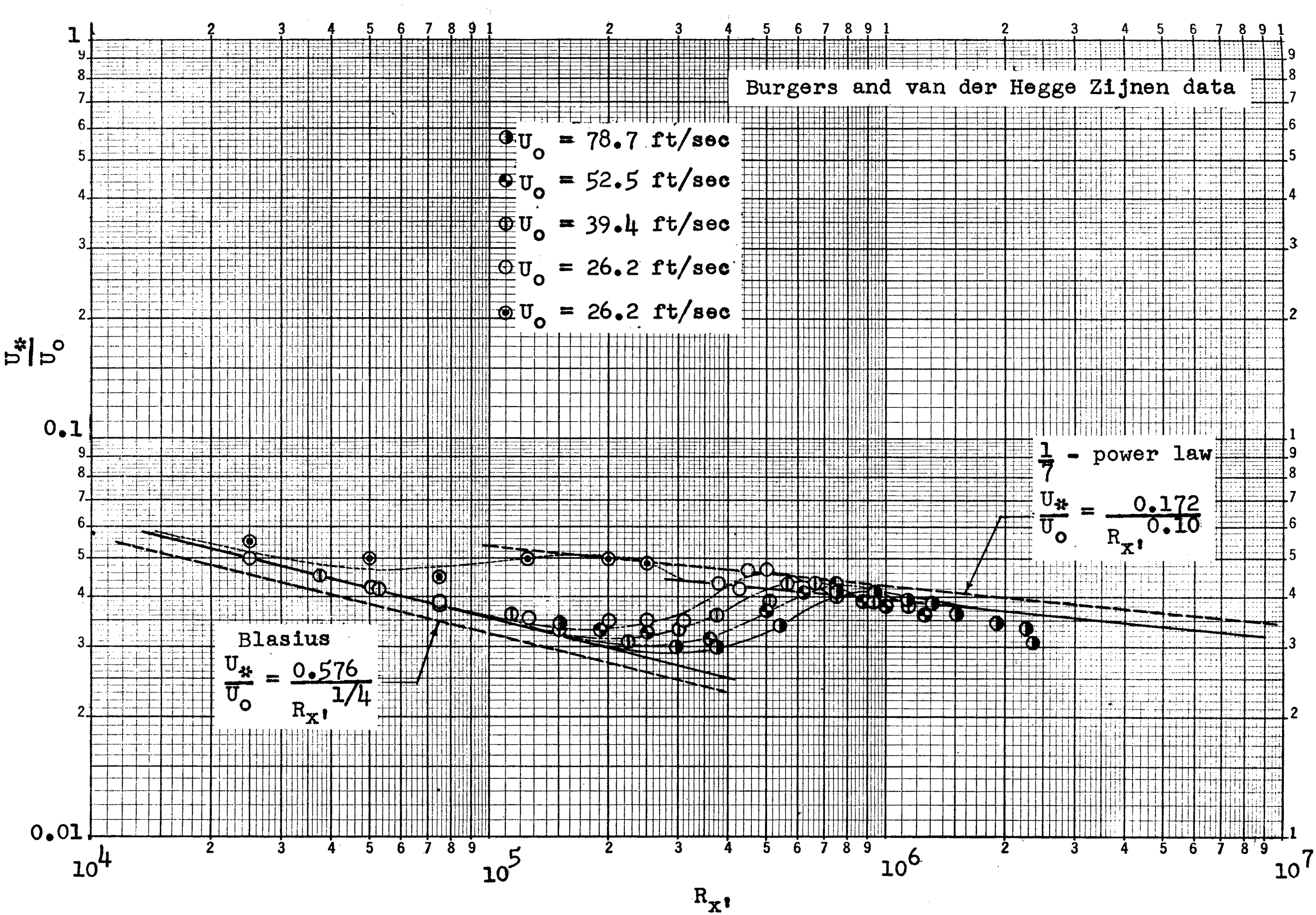

Fig. 24 Variation of U_*/U_o with $R_{x'}$ for boundary layer in transition (Delft data)

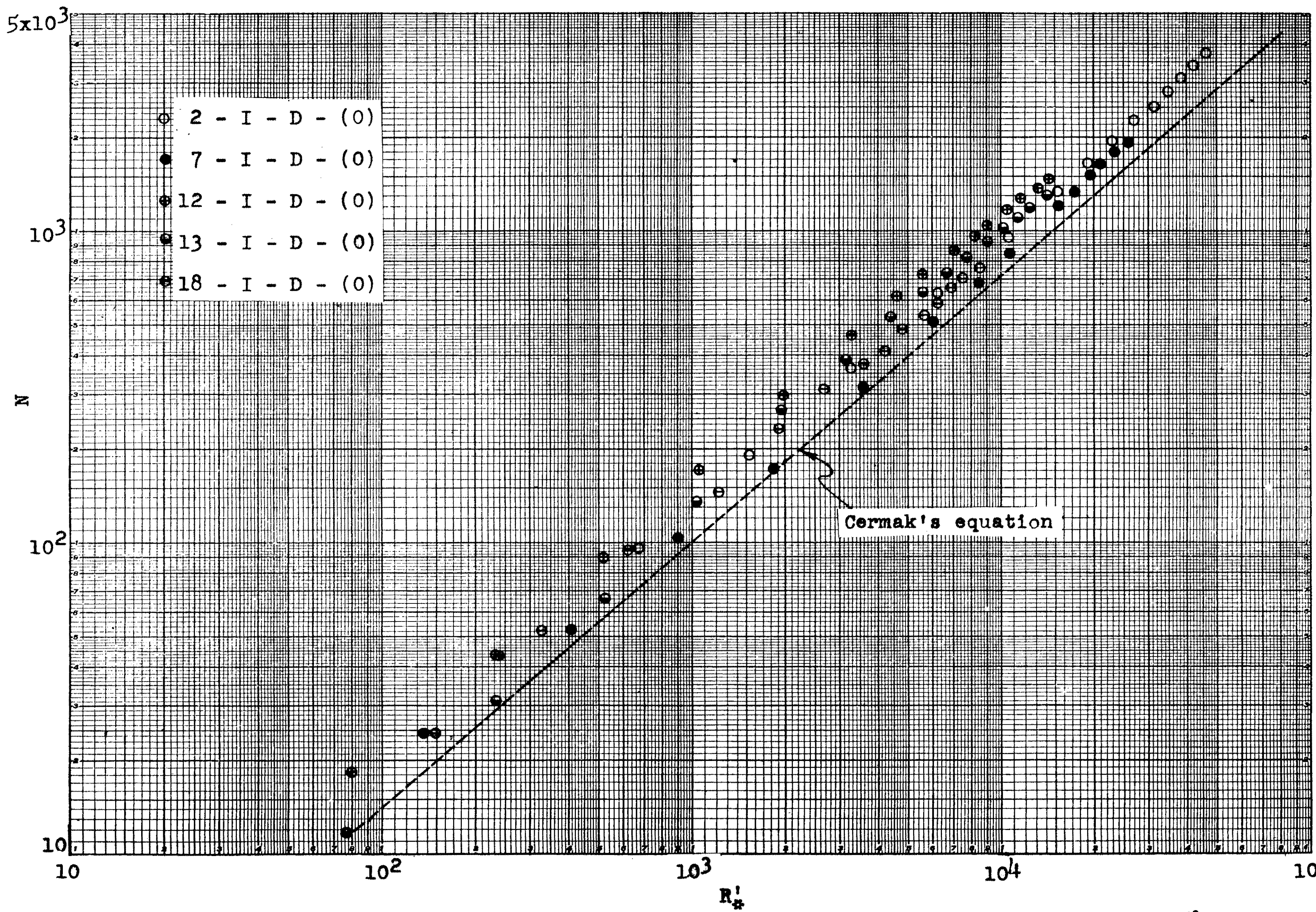

Fig. 25 Variation of N with R'_* for turbulent boundary layer (buffers dry, x = 135½ in.).

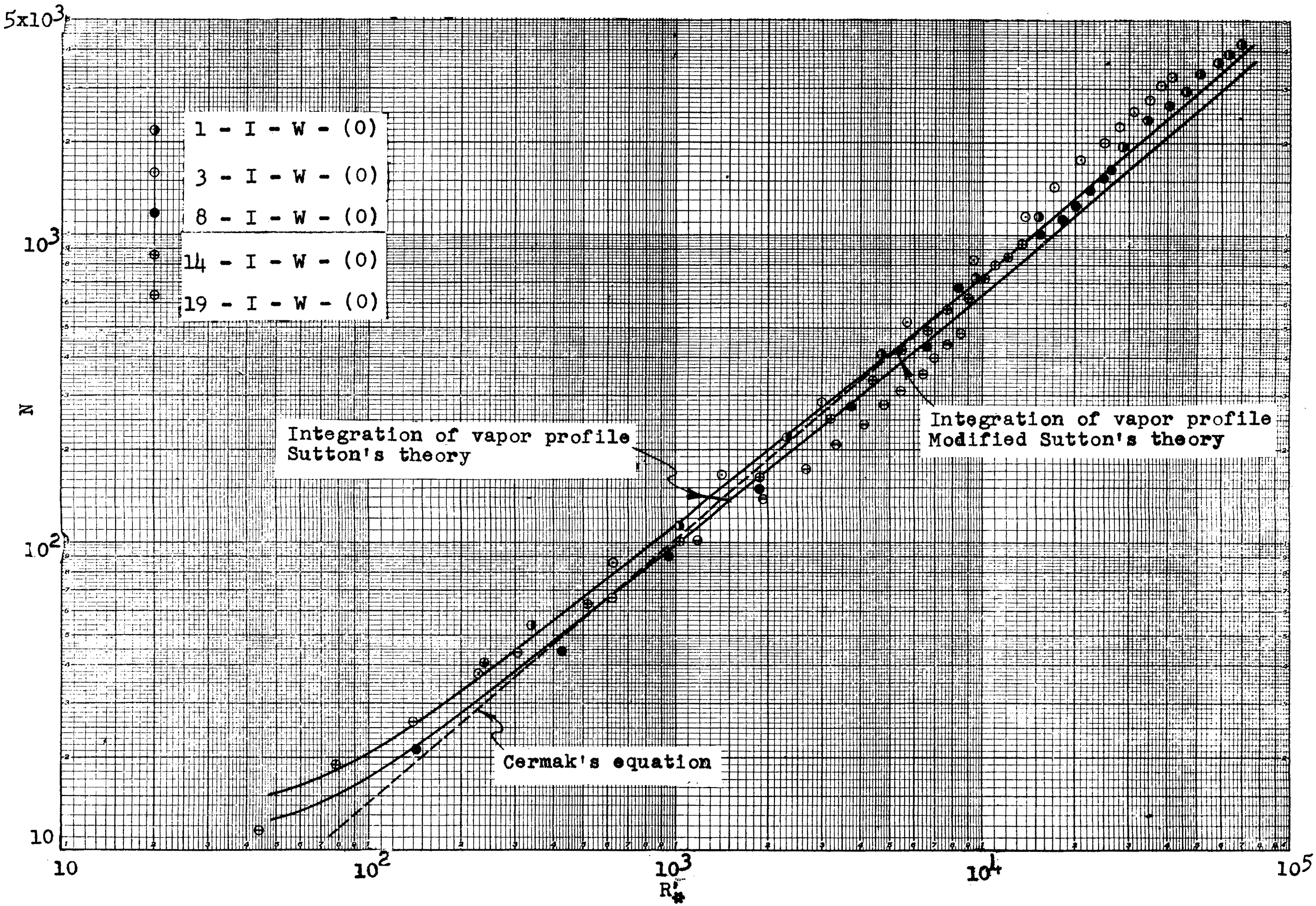

Fig. 26 Variation of N with R'_* for turbulent boundary layer (buffers wet, $x = 135\frac{1}{2}$ in.).

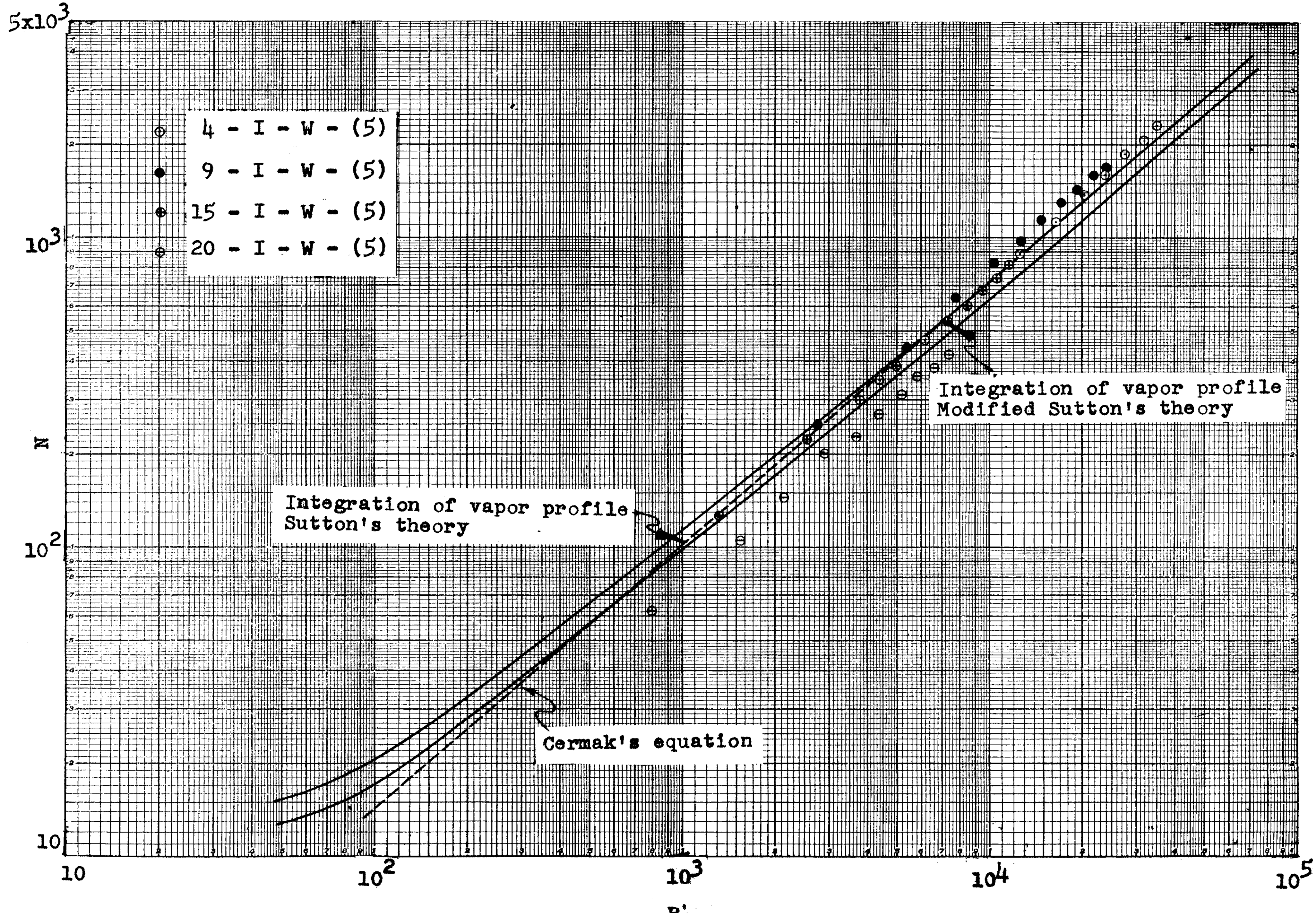

Fig. 27 Variation of N with R'_* for turbulent boundary layer (buffers wet, x = 120 in.).

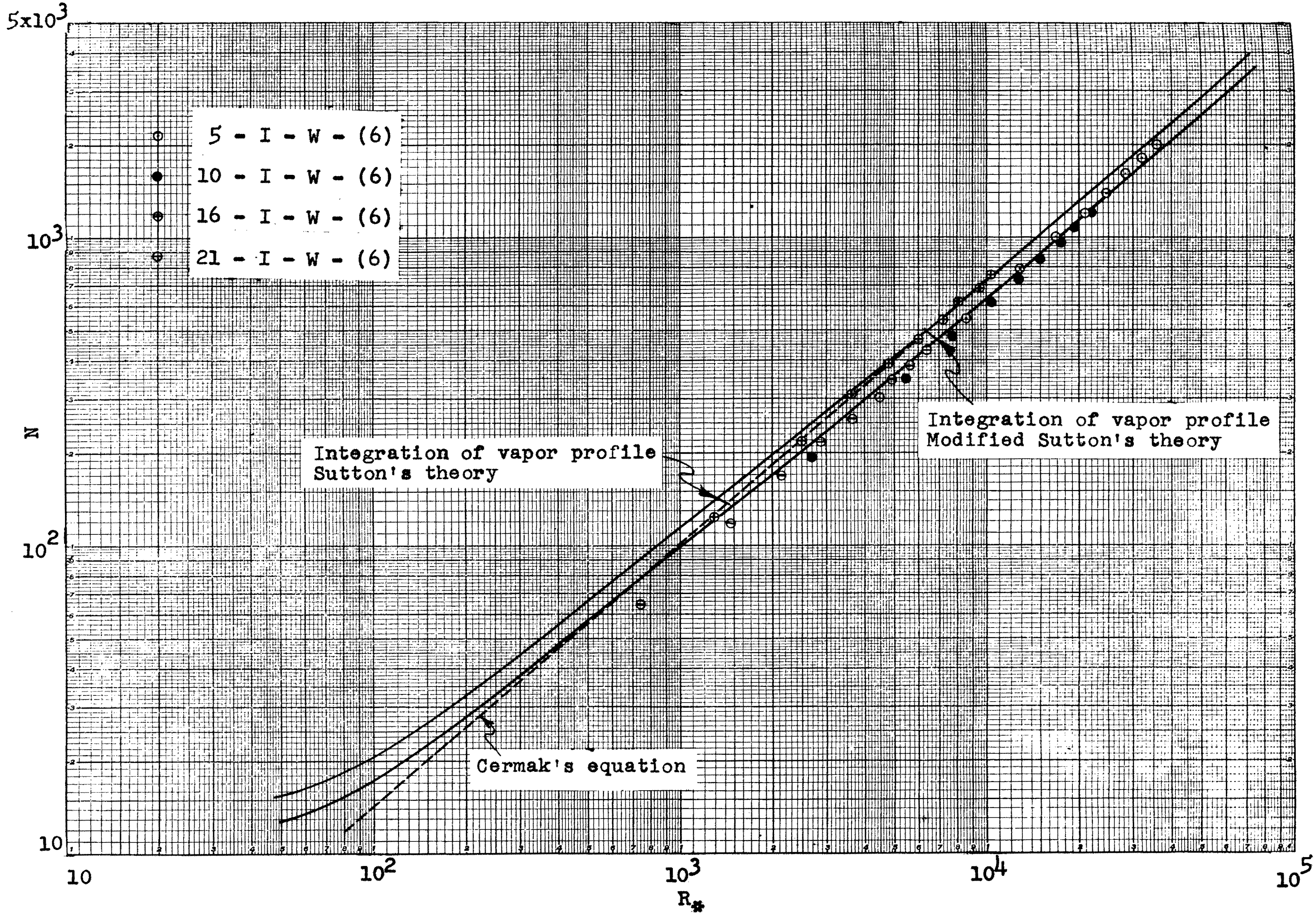

Fig. 28 Variation of N with R_* for turbulent boundary layer (buffers wet, x = 108 in.).

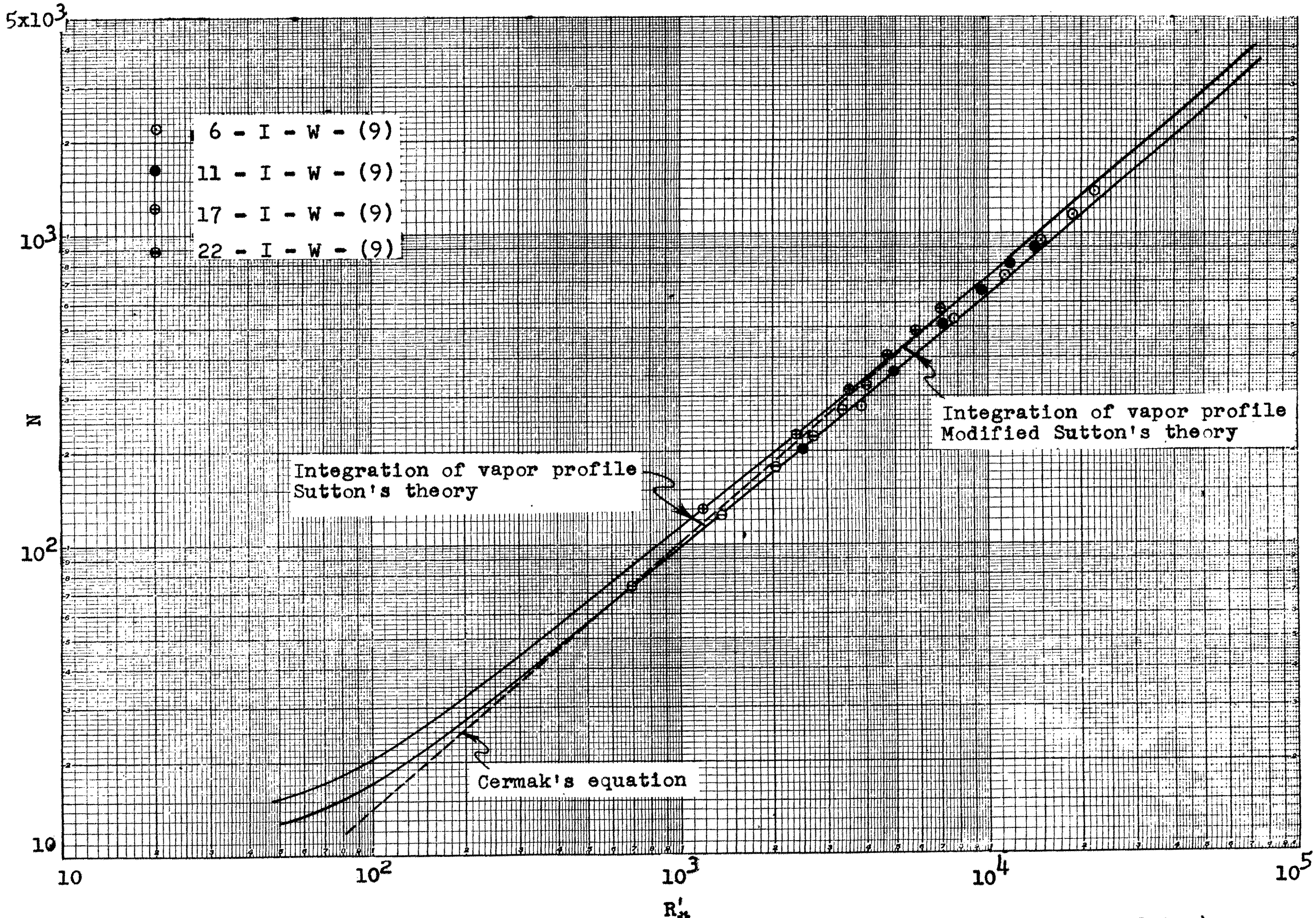

Fig. 29 Variation of N with R'_* for turbulent boundary layer (buffers wet, x = 72 in.).

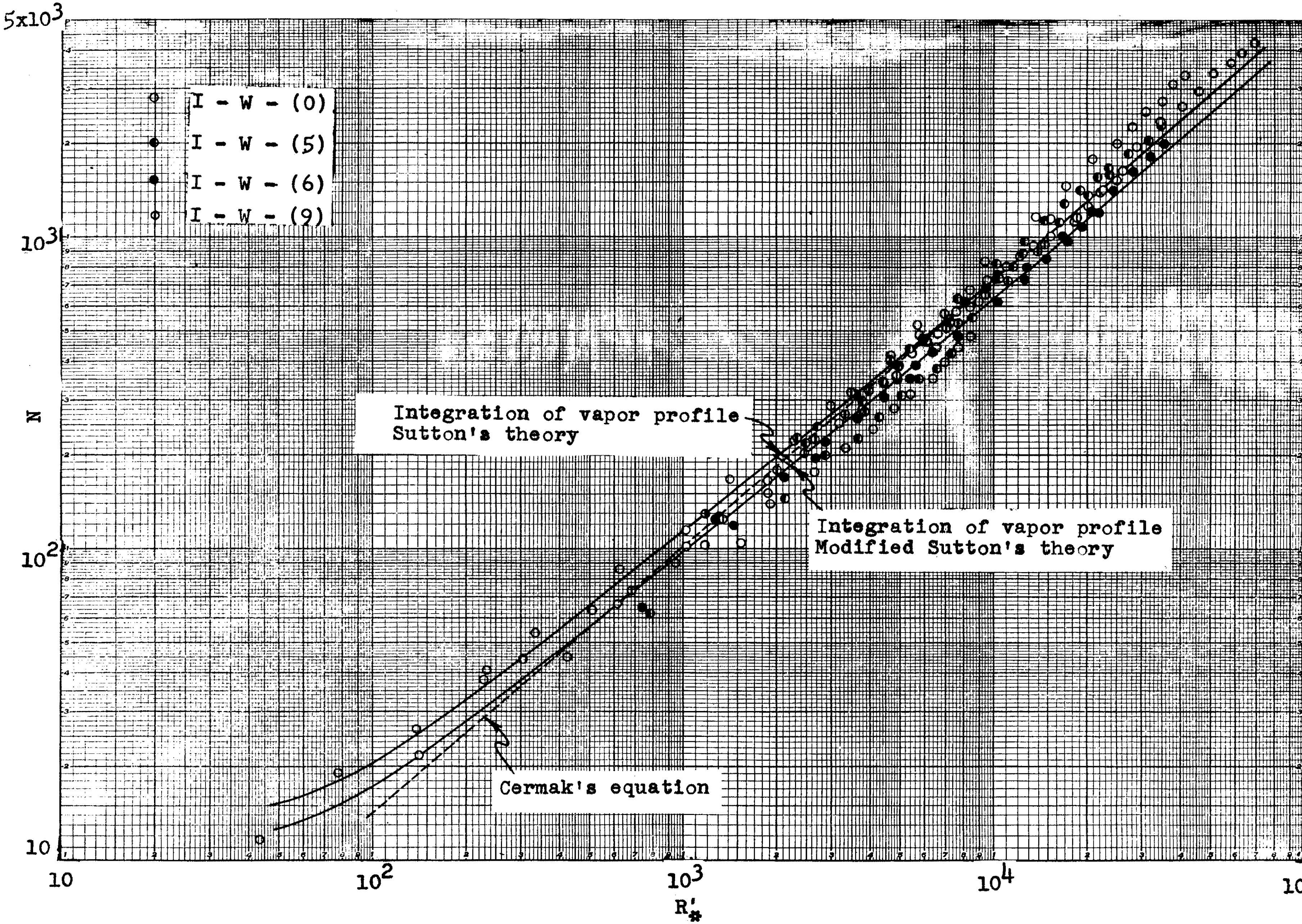

Fig. 30 Variation of N with R'_* for turbulent boundary layer (buffers wet, all data).

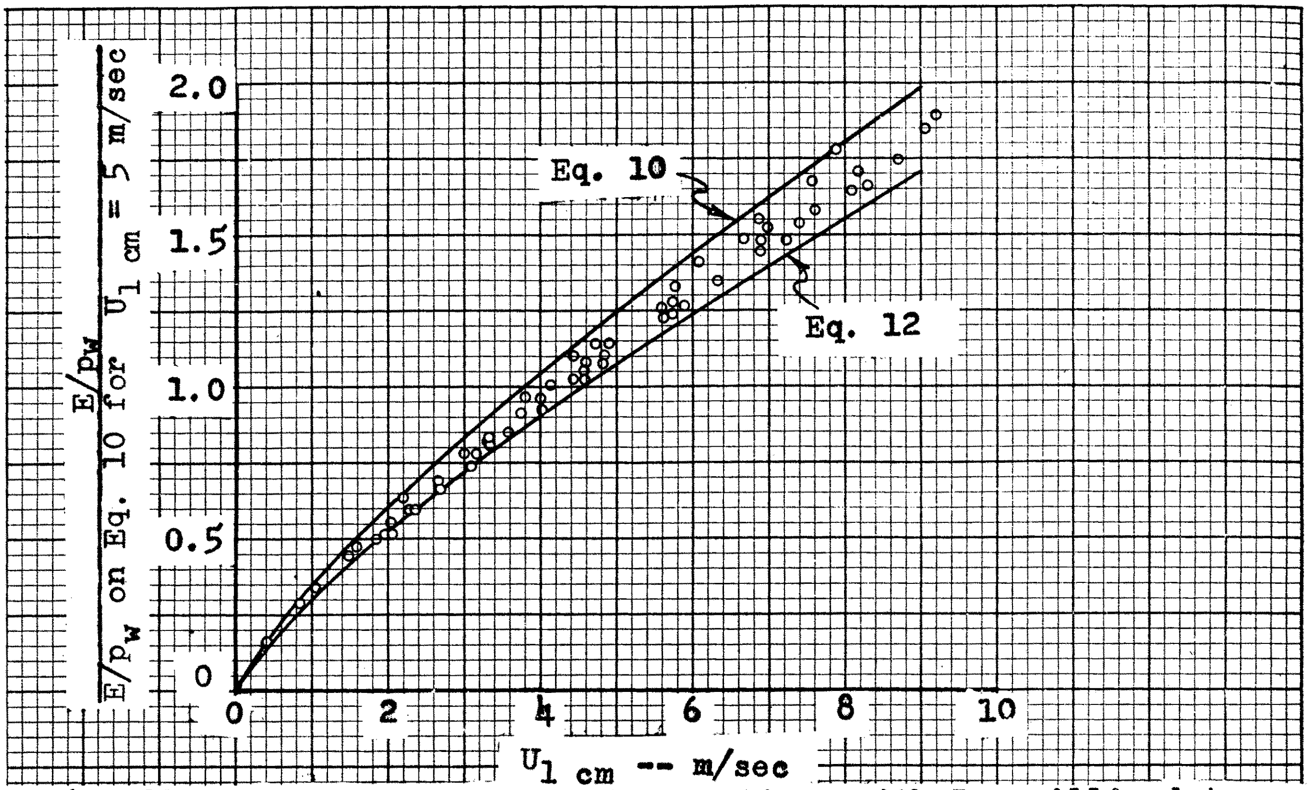

Fig. 31 Comparison of Sutton's equations with Pasquill's data.

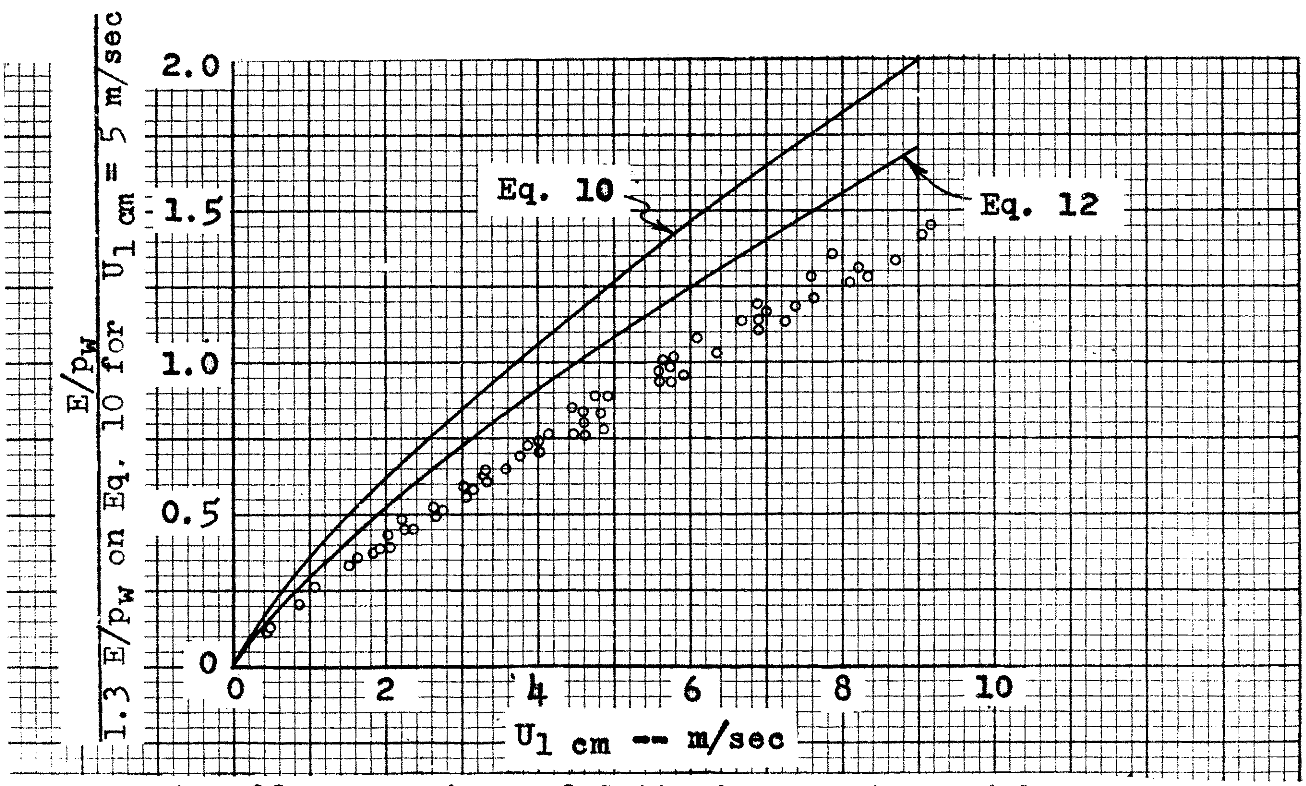

Fig. 32 Comparison of Sutton's equations with Pasquill's data (revised analysis).

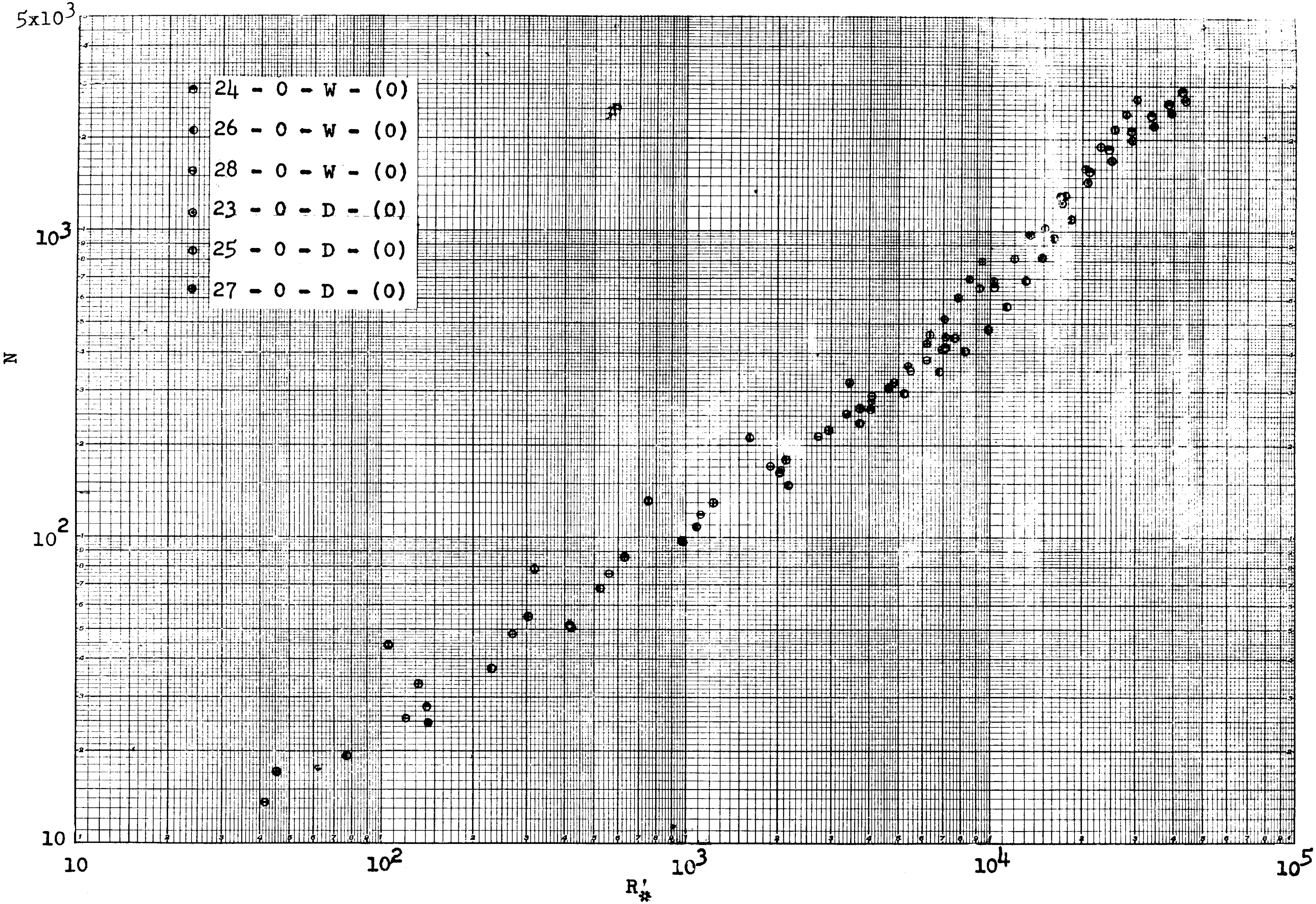

Fig. 33 Variation of N with R'_* for boundary layer in transition (all data).

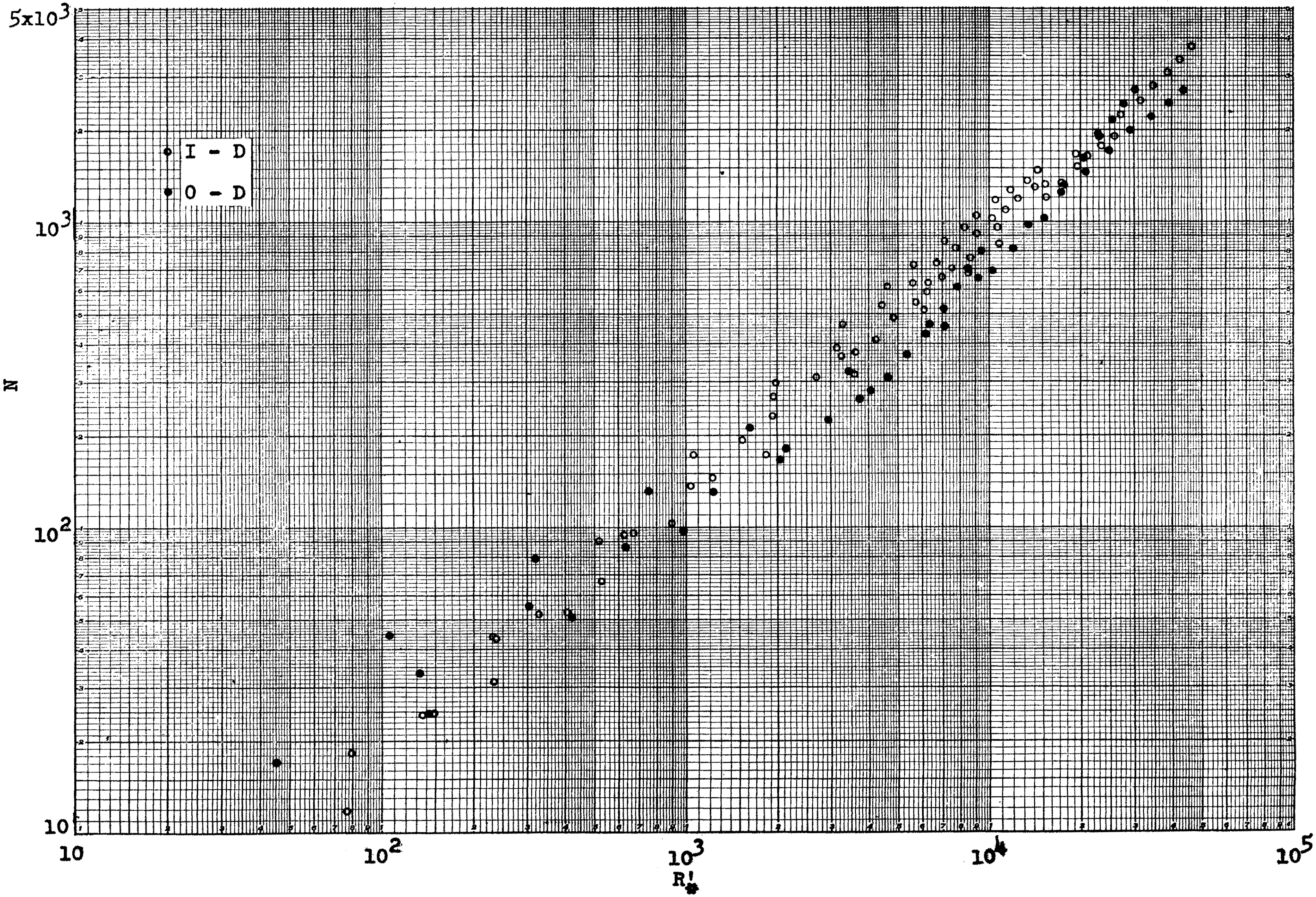

Fig. 34 Variation of N with R'_* for boundary layer in different regimes (buffers dry).

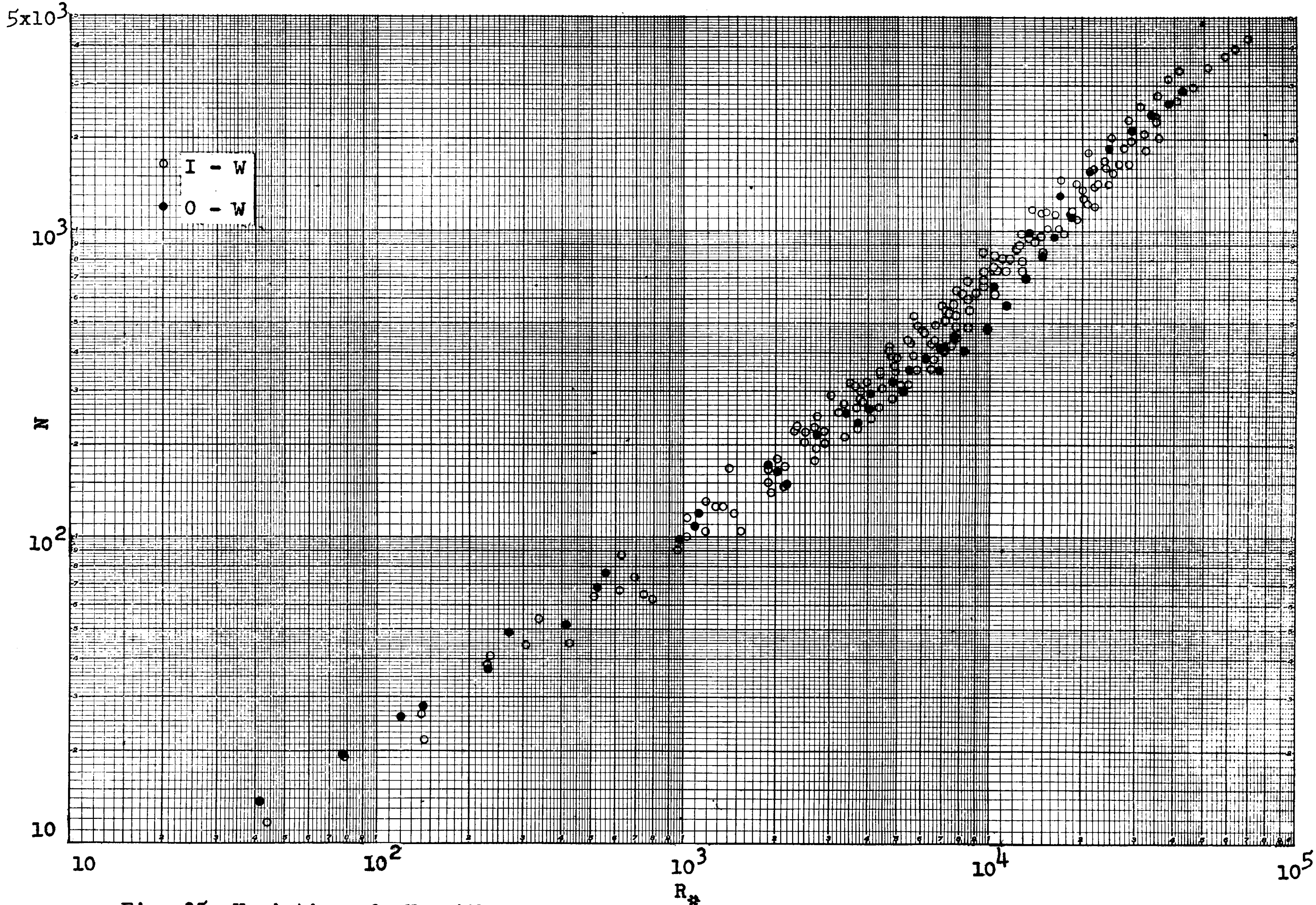

Fig. 35 Variation of N with R_* for boundary layer in different regimes (buffers wet).

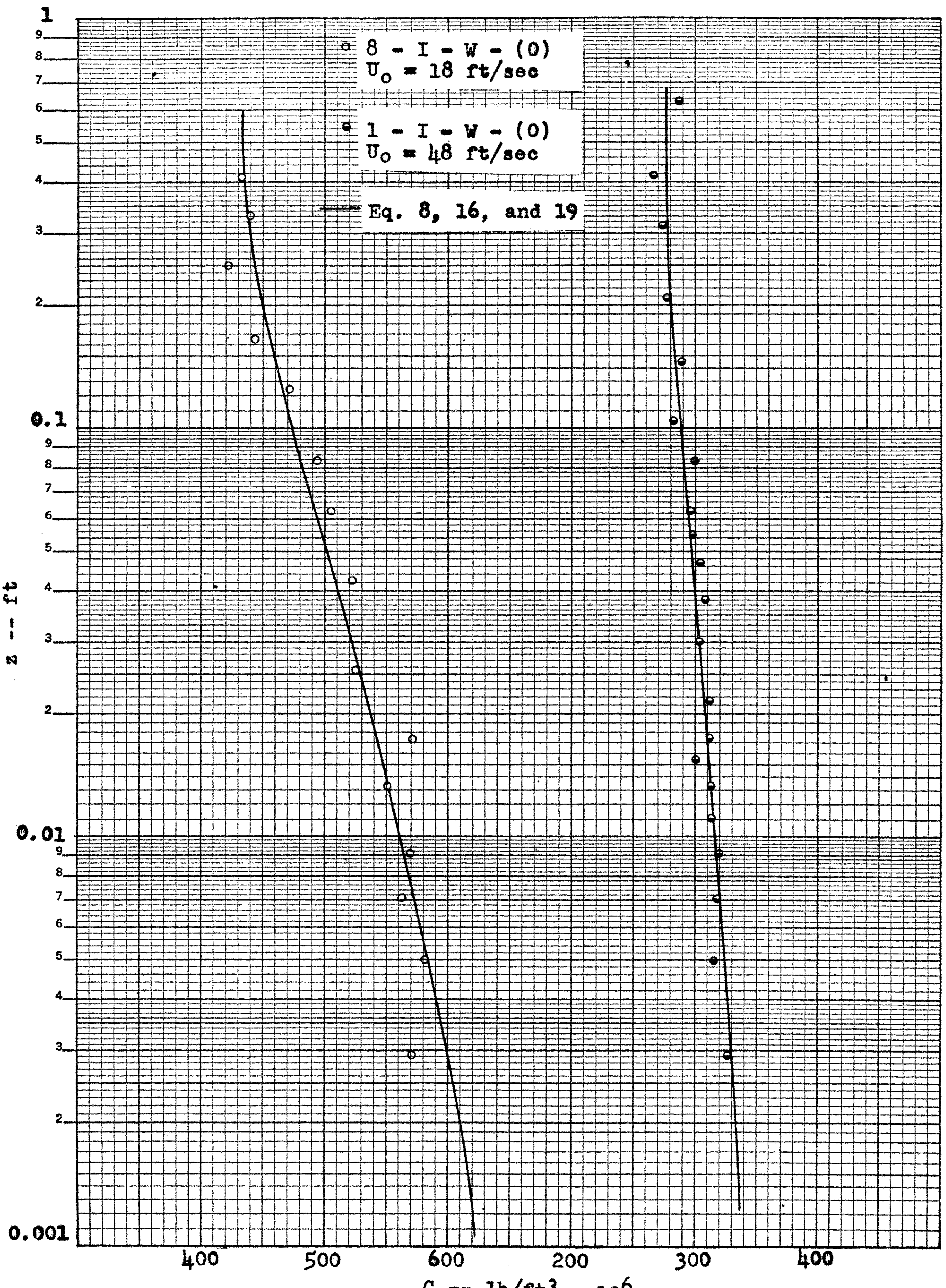

Fig. 36 Typical vapor concentration profiles.

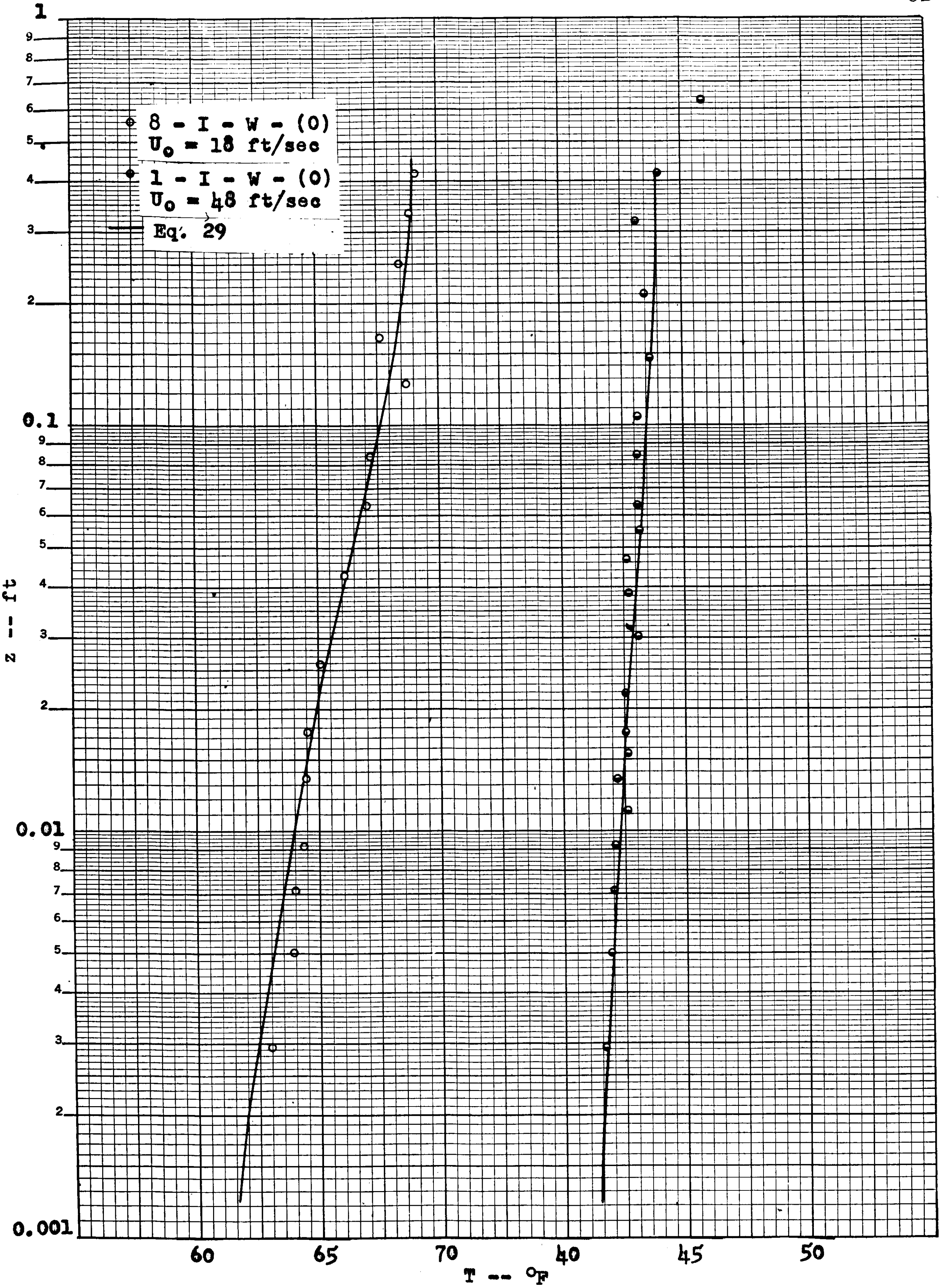

Fig. 37 Typical temperature profiles.

APPENDIX

Time MST	Psych(^oF) WB	DB
0840	34.5	43.0
0910	35.5	45.0
0941	36.5	46.5
1013	36.0	46.5
1043	36.5	47.5

Δt	7200	sec
T_o	45.8	^oF
f_o	39.3	%
P_o	25.1	in. Hg
$\nu_e x10^6$	297	ft^2/sec
$C_o x10^6$	197	lb/ft^3

Date of Run: May 2, 1953

From 0837 to 1037

U_o = 48 ft/sec

Tape: in

Buffers: wet

Mains dry: none

Plate No.	1	2	3	4	5	6	7	8	9	10	11	12	13	14	15
x (ft) x 10^2	4.17	12.5	29.2	62.5	129	229	329	429	529	629	729	829	929	1029	1129
T_p (^oF)	38.4	38.3	37.3	37.3	37.4	37.5	37.3	37.6	37.5	37.5	37.9	37.7	36.8	37.7	37.7
T_m (^oF)	38.4	38.3	37.7	37.5	37.5	37.5	37.4	37.5	37.5	37.5	37.5	37.5	37.5	37.5	37.5
C_i (lb/ft^3) x 10^6	384	382	374	371	371	371	370	371	371	371	371	371	371	371	371
ΔC (lb/ft^3) x 10^6	187	185	177	174	174	174	173	174	174	174	174	174	174	174	174
W (lb) x 10^4	72.5	80.4	135	223	386	518	478	486	507	404	414	405	402	392	187
ΣW (lb) x 10^4	72.5	159	288	511	897	1415	1893	2379	2886	3290	3704	4109	4511	4903	5090
E(lb/ft^2sec) x 10^7	724	570	411	341	290	257	240	231	228	219	212	207	203	199	188
N	54.6	116	229	413	725	1140	1540	1920	2340	2670	3000	3330	3660	3970	4120
U_* x 10^3	2450	2400	2380	2300	2210	2140	2060	2020	1990	1970	1920	1920	1920	1900	1880
R_* x 10^{-1}	34.4	101	234	484	960	1650	2280	2920	3540	4170	4710	5360	6000	6580	7150

Table 1 - Data for 1-I-W-(0)

Time MST	Psych(^oF) WB	DB
1117	48.7	62.7
1145	48.5	63.0
1235	50.0	66.5
1303	50.5	67.5

Δt	7200	sec
T_o	64.9	^oF
f_o	34.5	%
P_o	25.0	in. Hg
$\nu_e \times 10^6$	317	ft^2/sec
$C_o \times 10^6$	333	lb/ft^3

Date of Run: May 22, 1953

From 1049 to 1149

From 1216 to 1316

U_o = 32 ft/sec

Tape: in

Buffers: dry

Mains dry: none

Plate No.	1	2	3	4	5	6	7	8	9	10	11	12	13	14	15
x (ft) x 10^2	4.17	12.5	29.2	62.5	129	229	329	429	529	629	729	829	929	1029	1129
T_p (^oF)	54.4	54.3	52.9	52.8	53.8	54.2	52.1	54.2	53.5	55.0	54.5	54.2	55.1	54.3	--
T_m (^oF)	54.4	54.3	53.5	53.1	53.5	53.8	53.3	53.5	53.5	53.7	53.8	53.9	54.0	54.0	54.1
C_i (lb/ft^3) x 10^6	679	676	658	649	658	665	653	658	658	662	665	667	669	669	669
ΔC (lb/ft^3) x 10^6	346	343	325	316	325	332	320	325	325	329	332	334	336	336	336
W (lb) x 10^4	116	139	227	372	694	885	832	810	823	796	796	830	850	734	840
ΣW (lb) x 10^4	116	255	482	854	1548	2433	3265	4075	4898	5694	6490	7320	8170	8904	9744
E(lb/ft^2sec) x 10^7	1160	851	688	570	500	442	414	396	387	379	371	369	367	361	360
N	44.1	97.9	195	356	626	963	1340	1650	1990	2290	2570	2890	3200	3490	3820
U_* x 10^3	1760	1730	1700	1630	1550	1490	1460	1420	1390	1380	1360	1340	1330	1310	1310
R_* x 10^{-1}	23.1	68.1	157	321	630	1080	1520	1920	2320	2740	3120	3500	3890	4250	4660

Table 2 - Data for 2-I-D-0

Time MST	Psych(^oF) WB	DB
1639	62.5	90.0
1712	62.0	87.6

Δt	1500	sec
T_o	89.5	^oF
f_o	22.3	%
P_o	25.1	in. Hg
$\nu_e x10^6$	345	ft^2/sec
$C_o x10^6$	464	lb/ft^3

Date of Run: June 10, 1953

From 1636 to 1701

U_o = 32 ft/sec

Tape: in

Buffers: wet

Mains dry: none

Plate No.	1	2	3	4	5	6	7	8	9	10	11	12	13	14	15
x (ft) x 10^2	4.17	12.5	29.2	62.5	129	229	329	429	529	629	729	829	929	1029	1129
T_p (^oF)	69.4	69.3	68.1	71.1	67.9	68.0	67.2	68.0	68.2	68.2	68.7	69.4	69.4	69.4	68.8
T_m (^oF)	69.4	69.3	68.6	69.9	68.9	68.5	68.1	68.1	68.1	68.1	68.2	68.3	68.4	68.5	68.6
C_i (lb/ft^3) x 10^6	1118	1115	1090	1136	1100	1086	1072	1072	1072	1072	1076	1079	1083	1086	1090
ΔC (lb/ft^3) x 10^6	654	651	626	672	636	622	608	608	608	608	612	615	619	622	626
W (lb) x 10^4	43.1	52.9	84.3	137	253	331	300	303	298	278	296	312	291	286	259
ΣW (lb) x 10^4	43.1	96.0	180	317	570	901	1201	1504	1802	2080	2376	2688	2979	3265	3524
E(lb/ft^2sec) x 10^7	2070	1540	1240	1020	884	786	731	701	682	663	652	649	643	634	625
N	38.2	85.6	167	284	519	839	1150	1430	1720	1990	2250	2540	2800	3040	3270
U_* x 10^3	1790	1760	1730	1660	1570	1500	1470	1440	1410	1390	1370	1340	1340	1330	1310
R_* x 10^{-1}	21.7	63.7	146	301	586	995	1400	1790	2160	2530	2890	3220	3610	3960	4280

Table 3 - Data for 3-I-W-(0)

Time MST	Psych(^oF) WB	DB
1506	57.9	85.8
1532	57.7	85.7

Δt	1440	sec
T_o	85.8	^oF
f_o	17.7	%
P_o	24.9	in. Hg
$\nu_e x10^6$	343	ft^2/sec
$C_o x10^6$	330	lb/ft^3

Date of Run: June 15, 1953

From 1458 to 1522

U_o = 32 ft/sec

Tape: in

Buffers: wet

Mains dry: 5

Plate No.	1	2	3	4	5	6	7	8	9	10	11	12	13	14	15
x (ft) x 10^2						100	200	300	400	500	600	700	800	900	1000
T_p (^oF)						65.2	64.6	64.8	65.2	65.4	65.2	64.9	65.0	65.0	65.8
T_m (^oF)						65.2	64.9	64.9	64.9	65.0	65.1	65.0	65.0	65.0	65.1
C_i (lb/ft^3) x 10^6						975	966	966	966	970	972	970	970	970	972
ΔC (lb/ft^3) x 10^6						645	636	636	636	640	642	640	640	640	642
W (lb) x 10^4						376	294	280	266	263	255	247	241	225	243
ΣW (lb) x 10^4						376	670	950	1216	1489	1734	1981	2222	2447	2690
E(lb/ft^2sec) x 10^7						785	688	660	632	616	603	591	580	566	560
N						354	630	907	1160	1400	1640	1880	2110	2320	2540
U_* x 10^3						1500	1470	1420	1410	1380	1360	1340	1340	1330	1310
R_* x 10^{-1}						437	856	1240	1640	2010	2380	2730	3120	3490	3820

Table 4 - Data for 4-I-W-(5)

Time MST	Psych(°F) WB	DB
1330	51.2	69.4
1400	53.5	72.0

Δt	1800	sec
T_o	69.6	°F
f_o	29.0	%
P_o	25.0	in. Hg
$\nu_e x10^6$	325	ft^2/sec
$C_o x10^6$	326	lb/ft^3

Date of Run: June 25, 1953

From 1317 to 1347

U_o = 32 ft/sec

Tape: in

Buffers: wet

Mains dry: 6

Plate No.	1	2	3	4	5	6	7	8	9	10	11	12	13	14	15
x (ft) x 10^2							100	200	300	400	500	600	700	800	900
T_p (°F)							58.0	57.6	56.9	57.6	57.7	57.6	57.8	57.7	59.3
T_m (°F)							58.0	57.8	57.5	57.5	57.6	57.6	57.6	57.6	57.8
C_i (lb/ft^3) x 10^6							767	762	754	754	757	757	757	757	762
ΔC (lb/ft^3) x 10^6							441	436	428	428	431	431	431	431	436
W (lb) x 10^4							263	209	191	183	175	171	179	169	175
ΣW (lb) x 10^4							263	472	663	846	1021	1192	1371	1540	1715
E($lb/ft^2 sec$) x 10^7							439	393	368	353	340	331	326	321	318
N							306	555	794	1010	1210	1420	1630	1830	2020
U_* x 10^3							1460	1420	1410	1380	1360	1340	1330	1310	1310
R_* x 10^{-1}							449	873	1300	1700	2090	2480	2870	3230	3630

Table 5 - Data for 5-I-W-(6)

Time MST	Psych(^{o}F) WB	DB
1445	59.8	95.2
1508	60.3	96.6

Δt	1620	sec
T_o	95.4	^{o}F
f_o	10.9	%
P_o	25.0	in. Hg
$\nu_o x10^6$	354	ft^2/sec
$C_o x10^6$	270	lb/ft^3

Date of Run: June 29, 1953

From 1433 to 1500

U_o = 32 ft/sec

Tape: in

Buffers: wet

Mains dry: 9

Plate No.	1	2	3	4	5	6	7	8	9	10	11	12	13	14	15
x (ft) x 10^2										100	200	300	400	500	600
T_p (^{o}F)										71.3	70.4	70.6	69.4	70.6	71.7
T_m (^{o}F)										71.3	70.8	70.8	70.5	70.5	70.7
C_i (lb/ft^3) x 10^6										1189	1170	1170	1159	1159	1166
ΔC (lb/ft^3) x 10^6										919	900	900	889	889	896
W (lb) x 10^4										490	396	378	362	352	364
ΣW (lb) x 10^4										490	886	1264	1626	1978	2342
E($lb/ft^2 sec$) x 10^7										908	820	780	753	733	723
N										279	515	735	958	1170	1370
U_* x 10^3										1390	1380	1360	1340	1330	1310
R_* x 10^{-1}										393	780	1150	1520	1880	2220

Table 6 - Data for 6-I-W-(9)

Time MST	Psych(^oF) WB	DB
1246	62.9	87.5
1316	63.7	88.0

Δt	2760	sec
T_o	87.8	^oF
f_o	27.1	%
P_o	25.2	in. Hg
$\nu_e x10^6$	344	ft^2/sec
$C_o x10^6$	536	lb/ft^3

Date of Run: June 11, 1953

From 1238 to 1324

U_o = 18 ft/sec

Tape: in

Buffers: dry

Mains dry: none

Plate No.	1	2	3	4	5	6	7	8	9	10	11	12	13	14	15
x (ft) x 10^2	4.17	12.5	29.2	62.5	129	229	329	429	529	629	729	829	929	1029	1129
T_p (^oF)	74.0	73.9	72.6	75.6	73.2	72.5	70.6	71.8	70.5	71.8	72.5	72.6	72.7	72.3	73.9
T_m (^oF)	74.0	73.9	73.2	74.5	73.8	73.2	72.4	72.3	72.0	71.9	72.0	72.1	72.1	72.2	72.3
C_i (lb/ft^3) x 10^6	1295	1291	1263	1316	1287	1263	1231	1227	1215	1202	1215	1219	1219	1223	1227
ΔC (lb/ft^3) x 10^6	759	755	727	780	751	727	695	691	679	666	679	683	683	687	691
W (lb) x 10^4	58.8	69.6	114	185	335	412	356	362	336	334	362	364	336	310	296
ΣW (lb) x 10^4	58.8	128	242	427	762	1174	1530	1892	2228	2562	2924	3288	3624	3934	4230
E(lb/ft^2sec) x 10^7	1530	1120	901	744	642	557	506	479	458	444	436	431	425	415	407
N	24.5	53.3	105	173	321	510	696	864	1040	1220	1360	1520	1680	1810	1930
U_* x 10^3	1130	1110	1080	1030	960	910	880	860	840	830	820	810	790	790	790
R_* x 10^{-1}	13.7	40.4	91.8	187	360	605	841	1070	1290	1520	1740	1950	2130	2360	2590

Table 7 - Data for 7-I-D-(0)

Time MST	Psych(^oF) WB	Psych(^oF) DB
1025	49.0	63.8
1045	50.0	65.1
1114	51.2	67.6
1141	50.9	68.0

Δt	5400	sec
T_o	66.7	^oF
f_o	33.4	%
P_o	24.9	in. Hg
$\nu_e x 10^6$	323	ft^2/sec
$C_o x 10^6$	342	lb/ft^3

Date of Run: June 4, 1953

From 1026 to 1156

U_o = 18 ft/sec

Tape: in

Buffers: wet

Mains dry: none

Plate No.	1	2	3	4	5	6	7	8	9	10	11	12	13	14	15
x (ft) x 10^2	4.17	12.5	29.2	62.5	129	229	329	429	529	629	729	829	929	1029	1129
T_p (^oF)	56.4	56.4	55.0	55.4	55.5	54.5	55.4	54.8	55.2	55.7	55.0	55.7	54.8	53.8	56.1
T_m (^oF)	56.4	56.4	55.6	55.5	55.5	55.1	55.2	55.1	55.1	55.2	55.2	55.2	55.2	55.1	55.1
C_i (lb/ft^3) x 10^6	727	727	707	705	705	695	698	695	695	698	698	698	698	695	695
ΔC (lb/ft^3) x 10^6	385	385	365	363	363	353	356	353	353	356	356	356	356	353	353
W (lb) x 10^4	50.0	52.9	95.0	135	262	320	322	298	284	273	277	273	263	245	275
ΣW (lb) x 10^4	50.0	103	198	333	595	914	1236	1533	1817	2091	2368	2641	2904	3149	3424
E(lb/ft^2sec) x 10^7	670	458	377	297	256	222	241	199	191	185	180	177	174	170	169
N	22.5	46.0	93.3	150	281	445	689	748	885	1010	1140	1280	1400	1530	1670
U_* x 10^3	1110	1100	1060	1010	950	900	860	850	830	820	810	800	790	790	770
R_* x 10^{-1}	14.3	42.5	95.7	195	379	637	875	1130	1360	1590	1830	2050	2270	2510	2690

Table 8 - Data for 8-I-W-(0)

Time MST	Psych(^oF) WB	DB
1113	60.3	74.2
1140	59.8	74.6
1212	61.4	77.3

Δt	3600	sec
T_o	74.7	^oF
f_o	44.9	%
P_o	25.0	in. Hg
$\nu_e x 10^6$	330	ft^2/sec
$C_o x 10^6$	595	lb/ft^3

Date of Run: June 16, 1953

From 1102 to 1202

U_o = 18 ft/sec

Tape: in

Buffers: wet

Mains dry: 5

Plate No.	1	2	3	4	5	6	7	8	9	10	11	12	13	14	15
x (ft) x 10^2						100	200	300	400	500	600	700	800	900	1000
T_p (^oF)						64.3	63.9	64.2	63.1	64.3	64.2	64.8	64.4	63.7	64.6
T_m (^oF)						64.3	64.1	64.1	63.9	64.0	64.0	64.1	64.2	64.1	64.2
C_i (lb/ft^3) x 10^6						947	941	941	934	938	938	941	944	941	944
ΔC (lb/ft^3) x 10^6						352	346	346	339	343	343	346	349	346	349
W (lb) x 10^4						350	265	259	245	225	225	216	219	206	220
ΣW (lb) x 10^4						350	615	874	1119	1344	1569	1785	2004	2210	2430
E($lb/ft^2 sec$) x 10^7						292	256	243	233	224	218	213	209	205	202
N						252	448	640	833	989	1160	1310	1450	1620	1750
U_* x 10^3						900	870	850	840	830	810	800	790	790	780
R_* x 10^{-1}						273	527	772	1020	1260	1470	1700	1910	2150	2360

Table 9 Data for 9-I-W-(5)

Time MST	Psych(^oF) WB	DB
0920	47.0	59.0
0940	47.5	59.4
1010	49.3	61.3
1040	49.2	62.5
1110	50.2	64.5

Δt	7200	sec
T_o	61.9	^oF
f_o	41.3	%
P_o	25.2	in. Hg
$\nu_e x 10^6$	315	ft^2/sec
$C_o x 10^6$	361	lb/ft^3

Date of Run: June 25, 1953

From 0925 to 1125

U_o = 18 ft/sec

Tape: in

Buffers: wet

Mains dry: 6

Plate No.	1	2	3	4	5	6	7	8	9	10	11	12	13	14	15
x (ft) x 10^2							100	200	300	400	500	600	700	800	900
T_p (^oF)							53.6	53.6	53.1	53.7	53.6	53.8	53.7	53.4	54.1
T_m (^oF)							53.6	53.6	53.4	53.5	53.5	53.6	53.6	53.6	53.6
C_i (lb/ft^3) x 10^6							660	660	656	658	658	660	660	660	660
ΔC (lb/ft^3) x 10^6							299	299	295	297	297	299	299	299	299
W (lb) x 10^4							444	344	310	295	270	279	279	260	286
ΣW (lb) x 10^4							444	788	1098	1393	1663	1942	2221	2481	2767
E($lb/ft^2 sec$) x 10^7							185	164	152	145	139	135	132	129	128
N							196	348	492	622	743	860	982	1100	1220
U_* x 10^3							860	850	830	820	810	800	790	780	770
R_* x 10^{-1}							273	540	790	1040	1290	1520	1760	1980	2200

Table 10 - Data for 10-I-W-(6)

Time MST	Psych($^{\circ}$F) WB	DB
0930	58.1	70.5
1000	57.8	73.8
1030	59.5	76.0

Δt	7200	sec
T_o	74.1	$^{\circ}$F
f_o	42.1	%
P_o	25.1	in. Hg
$\nu_e \times 10^6$	328	ft^2/sec
$C_o \times 10^6$	549	lb/ft^3

Date of Run: June 29, 1953

From 0915 to 1115

U_o = 18 ft/sec

Tape: in

Buffers: wet

Mains dry: 9

Plate No.	1	2	3	4	5	6	7	8	9	10	11	12	13	14	15
x (ft) x 10^2										100	200	300	400	500	600
T_p ($^{\circ}$F)										63.9	63.4	63.6	63.6	63.6	64.0
T_m ($^{\circ}$F)										63.9	63.7	63.7	63.6	63.6	63.7
C_i (lb/ft^3) x 10^6										935	928	928	925	925	928
ΔC (lb/ft^3) x 10^6										386	379	379	376	376	379
W (lb) x 10^4										618	476	446	422	402	368
ΣW (lb) x 10^4										618	1094	1540	1962	2364	2732
E(lb/ft^{2}sec) x 10^7										257	228	214	204	197	190
N										203	366	516	662	798	915
U_* x 10^3										830	810	800	790	780	770
R_* x 10^{-1}										253	495	731	964	1190	1410

Table 11 — Data for 11-I-W-(9)

Time MST	Psych(^oF) WB	DB
1015	43.0	55.4
1043	43.3	57.0
1110	43.3	57.7
1141	44.0	58.0
1212	45.0	60.0
1325	46.5	62.8
1405	48.6	66.2
1418	47.5	63.5

Δt	12600	sec
T_o	60.6	^oF
f_o	30.8	%
P_o	25.0	in. Hg
$\nu_e x10^6$	315	ft^2/sec
$C_o x10^6$	258	lb/ft^3

Date of Run: May 15, 1953

From 1025 to 1225

From 1310 to 1440

U_o = 8 ft/sec

Tape: in

Buffers: dry

Mains dry: none

Plate No.	1	2	3	4	5	6	7	8	9	10	11	12	13	14	15
x (ft) x 10^2	4.17	12.5	29.2	62.5	129	229	329	429	529	629	729	829	929	1029	1129
T_p (^oF)	52.7	52.2	50.3	50.2	51.1	51.9	50.9	52.2	52.0	52.8	53.3	53.6	51.8	53.6	--
T_m (^oF)	52.7	52.3	51.2	50.7	50.9	51.3	51.2	51.4	51.5	51.7	52.0	52.2	52.1	52.3	52.4
C_i (lb/ft^3) x 10^6	640	631	607	597	601	610	607	612	614	618	625	629	627	631	633
ΔC (lb/ft^3) x 10^6	382	373	349	339	343	352	349	354	356	360	367	371	369	373	375
W (lb) x 10^4	92.1	126	198	354	641	759	634	627	626	545	583	573	556	519	559
ΣW (lb) x 10^4	92.1	218	416	770	1411	2170	2804	3431	4057	4602	5185	5758	6314	6833	7392
E($lb/ft^2 sec$) x 10^7	526	417	340	294	261	226	203	190	183	175	169	166	162	158	156
N	18.2	44.4	90.3	172	301	466	608	732	863	969	1060	1180	1300	1380	1490
U_* x 10^3	610	590	570	540	490	460	440	420	420	410	400	400	400	400	400
R_* x 10^{-1}	8.08	23.4	52.8	107	200	334	460	570	705	817	925	1050	1180	1310	1430

Table 12 – Data for 12-I-D-(0)

Time MST	Psych(^oF) WB	DB
1030	50.2	66.0
1058	50.0	66.0
1130	51.0	68.0
1210	53.5	70.8
1242	54.5	73.5

Δt	9000	sec
T_o	68.8	^oF
f_o	33.1	%
P_o	24.7	in. Hg
$\nu_e x10^6$	328	ft^2/sec
$C_o x10^6$	363	lb/ft^3

Date of Run: May 21, 1953

From 1013 to 1143

From 1154 to 1254

U_o = 8 ft/sec

Tape: in

Buffers: dry

Mains dry: none

Plate No.	1	2	3	4	5	6	7	8	9	10	11	12	13	14	15
x (ft) x 10^2	4.17	12.5	29.2	62.5	129	229	329	429	529	629	729	829	929	1029	1129
T_p (^oF)	61.1	60.6	58.8	58.9	59.5	59.7	58.1	60.6	60.7	61.4	61.3	61.4	59.8	61.1	--
T_m (^oF)	61.1	60.8	59.7	59.2	59.4	59.5	59.1	59.4	59.7	60.0	60.1	60.3	60.2	60.3	60.3
C_i (lb/ft^3) x 10^6	852	843	813	799	804	807	796	804	813	821	824	829	826	829	829
ΔC (lb/ft^3) x 10^6	489	480	450	436	441	444	433	441	450	458	461	466	463	466	466
W (lb) x 10^4	56.8	86.2	154	288	531	629	513	523	504	476	466	458	448	380	464
ΣW (lb) x 10^4	56.8	143	297	585	1116	1745	2258	2781	3285	3761	4227	4685	5133	5513	5977
E(lb/ft^2sec) x 10^7	454	382	339	312	288	254	229	216	207	200	193	189	185	179	177
N	11.8	30.3	67.0	136	257	399	530	640	742	836	931	1020	1130	1200	1300
U_* x 10^3	620	610	580	540	500	460	440	430	420	410	410	400	400	400	400
R_* x 10^{-1}	7.89	23.3	51.6	103	197	321	441	561	676	785	910	1010	1130	1250	1380

Table 13 - Data for 13-I-D-(0)

Time MST	Psych(^oF) WB	DB
1055	58.8	66.5
1118	58.7	66.5
1145	61.1	70.5
1215	61.6	70.9
1245	61.8	71.0
1316	61.9	70.7
1346	60.7	69.5
1415	60.8	70.2

Δt	12600	sec
T_o	69.9	^oF
f_o	62.0	%
P_o	25.1	in. Hg
$\nu_e \times 10^6$	325	ft^2/sec
$C_o \times 10^6$	705	lb/ft^3

Date of Run: June 1, 1953

From 1100 to 1430

U_o = 8 ft/sec

Tape: in

Buffers: wet

Mains dry: none

Plate No.	1	2	3	4	5	6	7	8	9	10	11	12	13	14	15
x (ft) x 10^2	4.17	12.5	29.2	62.5	129	229	329	429	529	629	729	829	929	1029	1129
T_p (^oF)	64.2	64.1	63.5	63.7	63.9	63.9	63.5	64.2	64.2	64.2	64.2	64.4	64.3	64.3	64.5
T_m (^oF)	64.2	64.1	63.8	63.7	63.8	63.8	63.8	63.9	64.0	64.0	64.0	64.0	64.0	64.1	64.1
C_i (lb/ft^3) x 10^6	944	941	932	928	932	932	932	934	938	938	938	938	938	941	941
ΔC (lb/ft^3) x 10^6	239	236	227	223	227	227	227	229	233	233	233	233	233	236	236
W (lb) x 10^4	62.7	68.6	72.5	120	190	288	249	249	237	265	243	233	225	221	233
ΣW (lb) x 10^4	62.7	131	204	324	514	802	1051	1300	1537	1802	2045	2278	2503	2724	2957
E(lb/ft^2sec) x 10^7	358	250	166	123	94.7	83.3	76.1	72.1	69.2	68.4	66.8	65.5	64.3	63.0	62.4
N	19.2	40.7	65.7	106	166	259	339	416	483	568	643	717	789	845	918
U_* x 10^3	620	600	580	540	500	460	440	420	410	400	400	400	390	390	390
R_* x 10^{-1}	7.95	23.1	52.1	104	198	324	445	554	666	772	895	1020	1110	1230	1350

Table 14 - Data for 14-I-W-(0)

Time MST	Psych(°F) WB	Psych(°F) DB
1050	64.5	87.4
1122	62.9	90.0
1200	62.4	91.5
1230	62.9	90.8
1430	61.3	80.4

Δt	4200	sec
T_o	89.3	°F
f_o	24.8	%
P_o	248	in. Hg
$\nu_e \times 10^6$	348	ft^2/sec
$C_o \times 10^6$	513	lb/ft^3

Date of Run: June 18, 1953

From 1042 to 1152

$U_o =$ 8 ft/sec

Tape: in

Buffers: wet

Mains dry: 5

Plate No.	1	2	3	4	5	6	7	8	9	10	11	12	13	14	15
x (ft) $\times 10^2$						100	200	300	400	500	600	700	800	900	1000
T_p (°F)						72.2	71.6	71.6	70.5	71.4	71.5	71.5	71.8	71.1	72.2
T_m (°F)						72.2	71.9	71.8	71.5	71.5	71.5	71.5	71.5	71.5	71.5
C_i (lb/ft^3) $\times 10^6$						1223	1202	1208	1196	1196	1196	1196	1196	1196	1196
ΔC (lb/ft^3) $\times 10^6$						710	689	695	683	683	683	683	683	683	683
W (lb) $\times 10^4$						441	310	283	269	251	249	242	239	225	247
ΣW (lb) $\times 10^4$						441	751	1034	1303	1554	1803	2045	2284	2509	2756
E($lb/ft^2 sec$) $\times 10^7$						315	268	246	233	222	215	209	204	199	197
N						128	223	305	392	466	542	615	686	753	828
$U_* \times 10^3$						460	440	440	430	420	420	410	410	410	400
$R_* \times 10^{-1}$						132	253	379	494	603	724	825	942	1060	1150

Table 15 – Data for 15-I-W-(5)

Time MST	Psych(^oF) WB	Psych(^oF) DB
0912	57.8	75.5
0935	58.8	76.4
1005	58.7	78.7
1035	59.5	81.7
1105	58.0	84.0
1135	57.3	83.0

Δt	9000	sec
T_o	80.7	^oF
f_o	27.4	%
P_o	24.8	in. Hg
$\nu_e x10^6$	340	ft^2/sec
$C_o x10^6$	437	lb/ft^3

Date of Run: June 24, 1953

From 0920 to 1150

U_o = 8 ft/sec

Tape: in

Buffers: wet

Mains dry: 6

Plate No.	1	2	3	4	5	6	7	8	9	10	11	12	13	14	15
x (ft) x 10^2							100	200	300	400	500	600	700	800	900
T_p (^oF)							66.0	66.1	65.2	66.0	66.1	65.9	66.2	65.5	66.6
T_m (^oF)							66.0	66.0	65.8	65.8	65.9	65.9	65.9	65.9	66.0
C_i (lb/ft^3) x 10^6							1001	1001	995	995	998	998	998	998	1001
ΔC (lb/ft^3) x 10^6							564	564	558	558	561	561	561	561	564
W (lb) x 10^4							722	553	498	470	454	438	442	406	454
ΣW (lb) x 10^4							722	1275	1773	2243	2697	3135	3577	3983	4437
E(lb/ft^2sec) x 10^7							241	212	197	187	180	174	170	166	164
N							126	221	312	394	471	548	625	696	771
U_* x 10^3							440	430	420	410	410	410	400	410	400
R_* x 10^{-1}							129	253	371	482	603	724	825	965	1060

Table 16 - Data for 16-I-W→(6)

Time MST	Psych(°F) WB	DB
0755	61.0	71.7
0820	59.6	75.5
0855	60.1	77.2
0925	60.1	79.4

Δt	5400	sec
T_o	76.9	°F
f_o	39.2	%
P_o	25.1	in. Hg
$\nu_e \times 10^6$	332	ft^2/sec
$C_o \times 10^6$	556	lb/ft^3

Date of Run: June 30, 1953

From 0803 to 0933

U_o = 8 ft/sec

Tape: in

Buffers: wet

Mains dry: 9

Plate No.	1	2	3	4	5	6	7	8	9	10	11	12	13	14	15
x (ft) x 10^2										100	200	300	400	500	600
T_p (°F)										65.3	64.9	65.0	65.2	65.3	65.4
T_m (°F)										65.3	65.1	65.1	65.1	65.1	65.2
C_i (lb/ft^3) x 10^6										979	972	972	972	972	975
ΔC (lb/ft^3) x 10^6										423	416	416	416	416	419
W (lb) x 10^4										330	235	221	215	213	211
ΣW (lb) x 10^4										330	565	786	1001	1214	1425
E(lb/ft^{2}sec) x 10^7										184	157	146	139	135	132
N										131	228	317	403	489	570
U_* x 10^3										400	400	390	390	390	390
R_* x 10^{-1}										120	241	352	470	587	705

Table 17 - Data for 17-I-W-(9)

Time MST	Psych(^{o}F) WB	DB
1046	43.0	58.5
1120	44.8	62.0
1145	45.0	63.0
1217	43.7	62.5
1248	43.9	62.3
1323	44.5	63.0
1357	45.1	64.0
1425	44.5	63.7
1456	43.7	61.5
1510	44.1	59.1

Δt	16200	sec
T_o	62.2	^{o}F
f_o	22.3	%
P_o	24.9	in. Hg
$\nu_e x 10^6$	318	ft^2/sec
$C_o x 10^6$	197	lb/ft^3

Date of Run: May 14, 1953

From 1031 to 1301

From 1312 to 1512

U_o = 4 ft/sec

Tape: in

Buffers: dry

Mains dry: none

Plate No.	1	2	3	4	5	6	7	8	9	10	11	12	13	14	15
x (ft) x 10^2	4.17	12.5	29.2	62.5	129	229	329	429	529	629	729	829	929	1029	1129
T_p (^{o}F)	55.2	54.8	52.9	53.0	53.5	54.1	53.6	54.4	54.9	54.2	55.0	55.2	53.9	55.0	--
T_m (^{o}F)	55.2	54.9	53.8	53.4	52.9	53.4	53.5	53.7	53.9	54.0	54.1	54.2	54.2	54.3	54.3
C_i (lb/ft^3) x 10^6	698	690	665	656	644	656	658	662	667	669	672	674	674	676	676
ΔC (lb/ft^3) x 10^6	501	493	468	459	447	459	461	465	470	472	475	477	477	479	479
W (lb) x 10^4	76.5	130	221	331	380	742	621	565	516	456	495	485	450	490	520
ΣW (lb) x 10^4	76.5	206	427	758	1138	1880	2501	3066	3582	4032	4533	5018	5468	5958	6478
E(lb/ft^{2}sec) x 10^7	340	306	271	225	163	152	141	132	121	119	115	112	109	107	106
N	8.90	24.4	53.2	96.3	148	238	317	384	445	499	556	614	669	725	788
U_* x 10^3	376	368	352	328	302	276	266	262	255	249	246	244	242	239	239
R_* x 10^{-1}	4.94	14.5	32.3	64.5	123	199	275	354	424	491	564	636	706	774	850

Table 18 - Data for 18-I-D-(0)

Time MST	Psych(^oF) WB	DB
1005	58.7	67.6
1025	59.8	69.3
1057	58.8	71.0
1125	60.1	74.0
1157	59.5	76.5
1225	59.0	78.7
1257	60.0	80.3
1325	58.3	82.0
1355	54.5	83.0
1425	54.2	83.7

Δt	16200	sec
T_o	77.5	^oF
f_o	34.6	%
P_o	24.8	in. Hg
$\nu_e x10^6$	335	ft^2/sec
$C_o x10^6$	500	lb/ft^3

Date of Run: June 2, 1953

From 1009 to 1439

U_o = 4 ft/sec

Tape: in

Buffers: wet

Mains dry: none

Plate No.	1	2	3	4	5	6	7	8	9	10	11	12	13	14	15
x (ft) x 10^2	4.17	12.5	29.2	62.5	129	229	329	429	529	629	729	829	929	1029	1129
T_p (^oF)	63.2	63.2	62.5	63.0	63.6	63.8	63.5	64.5	64.2	64.0	63.9	63.9	63.5	63.6	64.1
T_m (^oF)	63.2	63.2	62.8	62.9	63.3	63.5	63.5	63.7	63.8	63.8	63.8	63.9	63.8	63.8	63.8
C_i (lb/ft^3) x 10^6	913	913	901	904	916	922	922	928	932	932	932	934	932	932	932
ΔC (lb/ft^3) x 10^6	413	413	401	404	416	422	422	428	432	432	432	434	432	432	432
W (lb) x 10^4	96.0	108	116	182	265	316	285	259	285	283	308	304	322	352	350
ΣW (lb) x 10^4	96.0	204	320	502	767	1083	1368	1627	1912	2195	2503	2807	3129	3481	3831
E(lb/ft^2sec) x 10^7	426	302	203	149	110	87.4	77.0	70.2	67.0	64.6	63.6	62.8	62.4	62.6	62.9
N	12.8	27.2	44.0	68.7	102	145	179	210	245	281	320	359	400	445	490
U_* x 10^3	384	376	356	332	309	284	274	264	260	258	255	252	254	254	255
R_* x 10^{-1}	4.78	14.0	31.0	62.0	119	194	269	338	410	484	554	622	705	780	860

Table 19 - Data for 19-I-W-(0)

Time MST	Psych(^oF) WB	DB
1335	62.9	94.9
1347	64.5	95.8
1419	63.0	94.7
1453	64.1	95.1

Δt	5400	sec
T_o	95.1	^oF
f_o	17.4	%
P_o	249	in. Hg
$\nu_e x10^6$	355	ft^2/sec
$C_o x10^6$	427	lb/ft^3

Date of Run: June 17, 1953

From 1313 to 1443

U_o = 4 ft/sec

Tape in

Buffers: wet

Mains dry: 5

Plate No.	1	2	3	4	5	6	7	8	9	10	11	12	13	14	15
x (ft) x 10^2						100	200	300	400	500	600	700	800	900	1000
T_p (^oF)						76.5	76.0	76.0	75.2	75.8	75.6	75.3	75.6	75.2	76.0
T_m (^oF)						76.5	76.2	76.2	75.9	75.9	75.8	75.8	75.8	75.7	75.7
C_i (lb/ft^3) x 10^6						1401	1388	1388	1375	1375	1371	1371	1371	1366	1366
ΔC (lb/ft^3) x 10^6						974	961	961	948	948	944	944	944	939	939
W (lb) x 10^4						388	257	243	253	245	249	237	235	227	243
ΣW (lb) x 10^4						388	645	888	1141	1386	1635	1872	2107	2334	2577
E($lb/ft^2 sec$) x 10^7						216	179	165	159	154	151	149	146	144	143
N						62.5	105	145	189	229	270	311	348	389	429
U_* x 10^3						280	271	263	262	258	258	258	257	257	258
R_* x 10^{-1}						78.9	153	222	295	364	436	510	580	652	724

Table 20 - Data for 20-I-W-(5)

Time MST	Psych(^oF) WB	DB
1015	58.9	74.5
1045	57.5	75.3
1115	60.5	76.3
1145	60.8	79.2
1215	60.8	82.9
1255	62.9	85.6
1317	62.8	87.3

Δt	12600	sec
T_o	80.1	^oF
f_o	35.0	%
P_o	25.0	in. Hg
$\nu_e x 10^6$	337	ft^2/sec
$C_o x 10^6$	548	lb/ft^3

Date of Run: June 23, 1953

From 1000 to 1330

U_o = 4 ft/sec

Tape in

Buffers: wet

Mains dry: 6

Plate No.	1	2	3	4	5	6	7	8	9	10	11	12	13	14	15
x (ft) x 10^2							100	200	300	400	500	600	700	800	900
T_p (^oF)							67.2	67.3	66.5	67.4	67.2	67.2	67.4	67.1	67.5
T_m (^oF)							67.2	67.2	67.0	67.1	67.1	67.1	67.2	67.2	67.2
C_i (lb/ft^3) x 10^6							1041	1042	1034	1038	1038	1038	1041	1041	1041
ΔC (lb/ft^3) x 10^6							493	493	486	490	490	490	493	493	493
W (lb) x 10^4							448	372	342	338	314	304	306	269	324
ΣW (lb) x 10^4							448	820	1162	1500	1814	2118	2424	2693	3017
E($lb/ft^2 sec$) x 10^7							107	97.6	92.2	89.3	86.3	84.0	82.4	80.1	79.8
N							65.1	119	171	219	265	309	351	390	437
U_* x 10^3							254	252	244	246	246	244	242	242	243
R_* x 10^{-1}							75.4	150	217	292	365	435	502	575	649

Table 21 - Data for 21-I-W-(6)

Time MST	Psych(°F) WB	DB
0505	53.0	60.6
0515	53.9	60.8
0545	53.9	61.9
0610	55.5	64.4
0638	57.0	67.0
0714	59.1	68.0
0750	61.0	71.7

Δt	10800	sec
T_o	65.4	°F
f_o	60.1	%
P_o	25.1	in. Hg
$\nu_e x10^6$	320	ft^2/sec
$C_o x10^6$	590	lb/ft^3

Date of Run: June 30, 1953

From 0455 to 0755

U_o = 4 ft/sec

Tape: in

Buffers: wet

Mains dry: 9

Plate No.	1	2	3	4	5	6	7	8	9	10	11	12	13	14	15
x (ft) x 10^2										100	200	300	400	500	600
T_p (°F)										61.7	61.6	61.6	61.6	61.8	61.9
T_m (°F)										61.7	61.6	61.6	61.6	61.7	61.7
C_i (lb/ft^3) x 10^6										869	866	866	866	869	869
ΔC (lb/ft^3) x 10^6										279	276	276	276	279	279
W (lb) x 10^4										241	165	161	151	155	157
ΣW (lb) x 10^4										241	406	567	718	873	1030
E(lb/ft^2sec) x 10^7										67.0	56.4	52.5	49.9	48.5	47.7
N										75.1	128	178	226	272	321
U_* x 10^3										224	220	220	218	216	216
R_* x 10^{-1}										70.0	138	206	272	338	405

Table 22— Data for 22-I-W-(9)

Time MST	Psych(^oF) WB	DB
1405	46.6	72.0
1435	46.0	71.5

Δt	1800	sec
T_o	71.9	^oF
f_o	10.1	%
P_o	24.7	in. Hg
$\nu_e x10^6$	332	ft^2/sec
$C_o x10^6$	121	lb/ft^3

Date of Run: May 29, 1953

From 1357 to 1427

U_o = 32 ft/sec

Tape: out

Buffers: dry

Mains dry: none

Plate No.	1	2	3	4	5	6	7	8	9	10	11	12	13	14	15
x (ft) x 10^2	4.17	12.5	29.2	62.5	129	229	329	429	529	629	729	829	929	1029	1129
T_p (^oF)	62.0	62.2	61.2	61.6	62.8	62.2	56.2	59.6	57.4	59.6	57.7	58.8	60.0	59.3	59.8
T_m (^oF)	62.0	62.1	61.6	61.6	62.2	62.2	60.4	60.2	59.7	59.7	59.4	59.3	59.4	59.4	59.4
C_i (lb/ft^3) x 10^6	877	880	866	866	883	883	832	826	813	813	804	802	804	804	804
ΔC (lb/ft^3) x 10^6	756	759	745	745	762	762	711	705	692	692	683	681	683	683	683
W (lb) x 10^4	37.2	39.2	66.6	102	180	263	295	372	358	285	348	340	342	318	338
ΣW (lb) x 10^4	37.2	76.4	143	245	425	688	983	1355	1713	1998	2346	2686	3028	3346	3684
E(lb/ft^2sec) x 10^7	1490	1020	819	654	549	501	497	526	541	529	536	541	542	541	544
N	24.7	50.5	96.8	166	280	454	694	965	1250	1450	1720	1990	2220	2460	2710
U_* x 10^3	1140	1120	1110	1090	1050	1040	1040	1050	1080	1100	1140	1170	1220	1260	1270
R_* x 10^{-1}	14.3	42.2	97.6	205	409	719	1030	1360	1720	2080	2500	2920	3420	3910	4310

Table 23 — Date for 23-0-D-(0)

Time MST	Psych(^{o}F) WB	DB
1226	62.9	88.3
1300	59.8	90.6

Δt	1980	sec
T_o	88.8	^{o}F
f_o	23.1	%
P_o	25.2	in. Hg
$\nu_e \times 10^6$	345	ft^2/sec
$C_o \times 10^6$	471	lb/ft^3

Date of Run: June 10, 1953

From 1217 to 1250

U_o = 32 ft/sec

Tape: out

Buffers: wet

Mains dry: none

Plate No.	1	2	3	4	5	6	7	8	9	10	11	12	13	14	15
x (ft) x 10^2	4.17	12.5	29.2	62.5	129	229	329	429	529	629	729	829	929	1029	1129
T_p (^{o}F)	71.8	72.1	70.9	71.6	72.4	71.7	69.7	69.4	69.0	69.7	68.4	69.4	69.6	69.6	70.0
T_m (^{o}F)	71.8	72.0	71.4	71.5	72.0	71.8	71.2	70.8	70.4	70.3	70.1	70.0	69.9	69.9	69.9
C_i (lb/ft^3) x 10^6	1207	1215	1192	1196	1215	1208	1185	1170	1155	1151	1144	1140	1136	1136	1136
ΔC (lb/ft^3) x 10^6	736	744	721	725	744	737	714	699	684	680	673	669	665	665	665
W (lb) x 10^4	47.0	41.2	72.5	106	182	254	362	480	498	402	386	392	388	376	378
ΣW (lb) x 10^4	47.0	88.2	161	267	449	703	1065	1545	2043	2445	2831	3223	3611	3987	4365
E(lb/ft^{2}sec) x 10^7	1710	1070	834	647	527	464	491	546	586	591	588	590	590	587	586
N	28.1	52.1	97.9	162	265	418	656	971	1310	1580	1850	2120	2390	2630	2880
U_* x 10^3	1170	1160	1150	1120	1090	1070	1070	1090	1110	1130	1160	1200	1240	1290	1310
R_* x 10^{-1}	14.2	42.0	97.4	203	407	710	1020	1350	1700	2060	2450	2880	3340	3850	4290

Table 24 - Data for 24-0-W-(0)

Time MST	Psych(°F) WB	DB
1255	60.5	70.0
1330	60.6	69.0
1403	59.8	68.3
1432	60.0	66.5
1458	59.8	66.0
1530	59.8	64.3

Δt	10800	sec
T_o	67.3	°F
f_o	68.0	%
P_o	25.1	in. Hg
$\nu_e \times 10^6$	322	ft^2/sec
$C_o \times 10^6$	711	lb/ft^3

Date of Run: May 27, 1953

From 1246 to 1546

U_o = 18 ft/sec

Tape: out

Buffers: dry

Mains dry: none

Plate No.	1	2	3	4	5	6	7	8	9	10	11	12	13	14	15
x (ft) x 10^2	4.17	12.5	29.2	62.5	129	229	329	429	529	629	729	829	929	1029	1129
T_p (°F)	61.8	61.9	61.6	61.7	62.0	62.2	60.7	62.2	61.6	61.1	61.0	60.9	60.9	61.2	61.2
T_m (°F)	61.8	61.9	61.7	61.7	61.8	62.0	61.6	61.7	61.7	61.6	61.5	61.4	61.4	61.4	61.4
C_i (lb/ft^3) x 10^6	872	875	869	869	872	877	866	869	869	866	863	860	860	860	860
ΔC (lb/ft^3) x 10^6	161	164	158	158	161	166	155	158	158	155	152	149	149	149	149
W (lb) x 10^4	83.3	66.6	94.0	141	216	286	290	317	398	464	460	458	464	444	523
ΣW (lb) x 10^4	83.3	150	244	385	601	887	1177	1494	1892	2356	2816	3274	3738	4182	4705
E(lb/ft^{2}sec) x 10^7	555	333	232	171	129	108	99.5	96.7	99.4	104	108	110	112	113	116
N	44.6	78.8	132	210	322	461	656	815	1030	1310	1600	1900	2160	2420	2720
U_* x 10^3	820	820	830	840	861	892	902	902	923	902	902	892	882	871	861
R_* x 10^{-1}	10.6	31.8	75.3	163	345	635	921	1200	1520	1760	2040	2300	2550	2790	3020

Table 25 - Data for 25-0-D-(0)

Time MST	Psych(^oF) WB	DB
1308	52.3	72.5
1317	52.5	72.8
1348	53.4	74.4
1417	53.5	75.0
1445	54.0	75.5

Δt	7200	sec
T_o	74.4	^oF
f_o	24.9	%
P_o	24.9	in. Hg
$\nu_e x 10^6$	332	ft^2/sec
$C_o x 10^6$	327	lb/ft^3

Date of Run: June 4, 1953

From 1300 to 1500

U_o = 18 ft/sec

Tape: out

Buffers: wet

Mains dry: none

Plate No.	1	2	3	4	5	6	7	8	9	10	11	12	13	14	15
x (ft) x 10^2	4.17	12.5	29.2	62.5	129	229	329	429	529	629	729	829	929	1029	1129
T_p (^oF)	60.3	60.6	59.6	60.3	60.9	60.4	61.8	62.7	61.8	61.3	59.6	59.5	59.2	57.9	29.0
T_m (^oF)	60.3	60.5	60.0	60.2	60.6	60.5	60.9	61.3	61.4	61.4	61.2	60.9	60.7	60.5	60.3
C_i (lb/ft^3) x 10^6	829	835	821	826	838	835	846	857	860	860	854	846	840	835	829
ΔC (lb/ft^3) x 10^6	502	508	494	499	511	508	519	530	533	333	527	519	513	508	502
W (lb) x 10^4	77.4	72.5	119	161	255	272	265	249	255	296	384	456	498	505	533
ΣW (lb) x 10^4	77.4	150	268	430	685	957	1222	1471	1726	2022	2406	2862	3360	3865	4398
E($lb/ft^2 sec$) x 10^7	774	500	383	287	193	174	155	143	136	135	137	144	151	156	162
N	19.4	37.1	68.2	108	147	236	296	348	406	480	570	693	823	952	1100
U_* x 10^3	612	612	595	578	561	544	527	527	520	519	519	524	527	527	540
R_* x 10^{-1}	7.70	23.1	52.3	109	218	375	523	680	828	984	1140	1310	1480	1630	1840

Table 26 - Data for 26-0-W-(0)

Time MST	Psych(°F) WB	DB
1117	51.2	66.5
1147	50.5	63.0
1217	52.0	65.0
1250	52.0	64.5
1317	53.6	67.7
1348	56.5	70.7

Δt	9000	sec
T_o	64.7	°F
f_o	43.3	%
P_o	25.2	in. Hg
$\nu_e \times 10^6$	318	ft^2/sec
$C_o \times 10^6$	416	lb/ft^3

Date of Run: May 26, 1953

From 1101 to 1331

U_o = 8 ft/sec

Tape: out

Buffers: dry

Mains dry: none

Plate No.	1	2	3	4	5	6	7	8	9	10	11	12	13	14	15
x (ft) x 10^2	4.17	12.5	29.2	62.5	129	229	329	429	529	629	729	829	929	1029	1129
T_p (°F)	60.0	61.1	59.7	59.8	60.3	60.9	61.0	62.2	62.3	62.0	61.4	60.9	61.0	60.6	61.0
T_m (°F)	60.0	60.1	59.9	59.8	60.1	60.4	60.6	61.0	61.2	61.3	61.4	61.3	61.3	61.2	61.2
C_i (lb/ft^3) x 10^6	821	824	818	815	824	832	838	849	854	856	860	857	858	854	854
ΔC (lb/ft^3) x 10^6	405	408	402	399	408	416	422	433	438	440	444	441	442	438	438
W (lb) x 10^4	65.6	62.7	8.23	116	178	214	191	185	189	247	304	342	366	372	410
ΣW (lb) x 10^4	65.6	128	210	326	504	718	909	1094	1283	1530	1834	2176	2542	2914	3324
E($lb/ft^2 sec$) x 10^7	524	343	240	174	130	104	92.2	85.0	81.0	81.3	83.8	87.6	91.4	94.3	98.2
N	17.1	33.1	55.0	86.0	130	181	226	265	308	365	433	519	606	698	797
U_* x 10^3	344	339	331	320	305	296	287	278	278	272	270	270	268	265	265
R_* x 10^{-1}	4.51	13.3	30.4	62.9	124	213	297	375	462	538	618	703	783	857	940

Table 27 - Data for 27-O-D-(0)

Time MST	Psych(°F) WB	Psych(°F) DB
1411	63.1	85.3
1439	63.5	87.0
1507	63.3	86.0

Δt	5400	sec
T_o	86.1	°F
f_o	29.7	%
P_o	25.0	in. Hg
$\nu_e \times 10^6$	343	ft²/sec
$C_o \times 10^6$	559	lb/ft³

Date of Run: June 9, 1953

From 1355 to 1525

U_o = 8 ft/sec

Tape: out

Buffers: wet

Mains dry: none

Plate No.	1	2	3	4	5	6	7	8	9	10	11	12	13	14	15
x (ft) $\times 10^2$	4.17	12.5	29.2	62.5	129	229	329	429	529	629	729	829	929	1029	--
T_p (°F)	71.3	71.4	70.4	70.6	72.0	73.0	73.0	74.2	74.2	74.8	74.4	74.6	73.8	74.1	--
T_m (°F)	71.3	71.4	70.8	70.7	71.4	72.1	72.4	72.8	73.1	73.3	73.5	73.6	73.6	73.7	--
C_i (lb/ft³) $\times 10^6$	1189	1192	1166	1166	1192	1219	1231	1247	1259	1267	1275	1279	1279	1283	--
ΔC (lb/ft³) $\times 10^6$	630	633	607	607	633	660	672	688	700	708	716	720	720	724	--
W (lb) $\times 10^4$	52.9	47.0	82.3	116	188	231	185	195	173	155	141	137	157	153	--
ΣW (lb) $\times 10^4$	52.9	99.9	182	298	486	717	902	1097	1270	1425	1566	1703	1860	2013	--
E(lb/ft²sec) $\times 10^7$	705	445	347	265	209	174	153	142	134	126	119	114	111	109	--
N	13.6	25.6	48.6	76.2	119	172	213	254	291	323	352	383	414	450	--
$U_* \times 10^3$	341	332	318	308	299	284	278	271	266	264	259	257	257	256	--
$R_* \times 10^{-1}$	4.15	12.1	27.1	56.1	113	190	266	339	410	484	550	620	695	769	--

Table 28 - Data for 28-0-W-(0)

	2-I-D-(0)		3-I-W-(0)		4-I-W-(5)		5-I-W-(6)		6-I-W-(9)	7-I-D-(0)		8-I-W-(0)	
x'	0.96	12.25	0.96	12.25	12.25	2.25	12.25	3.25	6.25	0.96	12.25	0.96	12.25
Vert. Dist.													
0.010	6.8	7.9	10.7	30.3	14.8	--	--	10.6	10.7	10.7	7.1	3.7	3.4
0.035	11.6	14.0	18.7	31.4	18.6	13.7	17.7	16.8	10.5	18.7	10.0	3.4	6.2
0.060	14.8	18.5	22.4	32.4	20.3	19.0	19.5	18.9	12.6	22.4	11.2	7.0	8.3
0.085	15.2	19.0	23.5	34.9	21.0	--	21.0	19.9	16.4	23.5	--	9.0	8.8
0.110	16.7	20.3	26.3	36.0	22.2	21.2	21.5	21.0	18.0	26.3	12.5	10.0	9.5
0.160	17.8	21.5	26.4	36.3	23.4	--	22.3	21.7	19.9	26.4	--	11.3	10.6
0.210	18.0	22.0	30.4	27.9	24.1	26.1	22.3	23.2	21.0	--	13.7	13.3	10.6
0.310	19.0	23.5	32.0	37.5	24.5	--	23.3	25.5	22.8	30.4	14.5	14.0	11.7
0.510	21.4	24.0	34.3	39.0	26.3	28.2	25.3	27.0	25.0	32.0	15.6	14.8	11.8
0.760	21.5	25.8	34.7	39.7	28.0	31.2	26.8	28.6	27.7	34.3	16.5	15.2	12.2
1.01	23.5	26.5	37.3	39.7	29.0	31.6	28.3	29.2	29.1	34.7	17.0	16.0	13.4
1.51	26.0	28.2	37.5	39.7	30.0	34.0	30.0	31.2	30.6	37.3	17.8	16.3	13.4
2.01	26.5	30.1	37.5	29.7	30.8	35.5	30.2	32.8	32.2	37.5	18.6	16.7	14.6
3.01	28.5	31.8	37.5	39.7	30.8	35.5	30.6	33.6	33.3	37.5	19.8	16.7	15.5
4.01	29.0	32.8	--	--	30.8	35.7	32.0	34.3	--	37.5	--	--	15.2
4.51	--	--	--	--	--	--	--	--	--	--	20.6	--	15.0
5.01	29.0	33.5	--	--	--	--	32.0	34.3	--	--	--	--	--
6.01	--	--	--	--	--	--	--	--	--	--	20.6	--	--

Note. x' in feet
Vertical distance in inches
Velocity in feet per second

Table 29-Mean Velocity Profiles

	9-I-V-(5)		10-I-V-(6)		11-I-V-(9)		12-I-D-(0)	13-I-D-(6)		15-I-V-(5)		16-I-V-(6)	
x'	12.25	2.25	3.25	12.25	6.25	12.25	12.25	12.25	0.96	12.25	2.25	12.25	3.25
Vert. Dist.													
0.010	13.4	8.5	4.4	3.6	14.8	5.9	1.8	1.6	1.52	1.70	1.1	2.15	1.55
0.035	18.1	10.3	7.3	8.4	16.8	6.7	2.8	2.74	1.80	3.24	1.8	3.50	3.00
0.060	21.0	11.7	9.1	10.0	18.3	8.3	4.0	3.80	2.17	4.00	2.8	4.40	3.73
0.085	22.2	11.8	9.8	11.2	18.5	9.9	4.0	4.60	2.32	4.40	3.71	5.00	4.45
0.110	22.5	12.8	10.4	11.6	19.0	9.7	4.3	4.80	2.52	4.48	4.32	5.20	4.60
0.160	--	--	11.7	12.4	19.4	10.5	5.0	5.30	2.52	--	5.05	5.70	5.10
0.210	23.3	14.0	11.7	13.2	19.7	10.5	--	5.70	3.32	5.50	5.5	6.00	5.60
0.250	--	--	--	--	--	--	5.5	--	--	--	--	--	--
0.310	24.1	15.3	12.1	13.8	20.6	11.5	--	5.95	--	5.85	5.9	6.30	6.10
0.410	--	--	--	--	--	--	6.0	--	--	--	--	--	--
0.510	25.0	16.8	14.3	14.4	21.2	12.2	--	6.35	2.32	5.85	6.7	6.60	6.70
0.610	--	--	--	--	--	--	6.1	--	--	--	--	--	--
0.760	25.8	17.5	14.8	15.3	21.3	12.7	--	7.70	--	6.40	7.5	7.10	7.20
0.810	--	--	--	--	--	--	6.8	--	--	--	--	--	--
1.01	26.1	18.3	16.0	14.1	22.3	13.2	6.8	8.10	1.95	6.50	7.8	7.30	7.80
1.51	26.5	19.2	16.6	16.1	23.4	13.8	6.8	8.30	--	6.8	8.3	7.90	8.20
2.01	27.1	19.7	17.7	17.5	23.8	14.3	6.9	8.30	1.95	7.4	8.5	8.20	8.40
3.01	27.6	20.0	18.2	18.3	24.3	15.0	6.9	8.60	2.17	7.9	8.7	8.7	8.90
4.01	28.1	19.8	18.2	18.8	24.3	15.0	7.3	8.90	3.95	8.4	8.7	8.9	8.90
4.51	--	--	--	--	--	--	--	--	--	--	--	--	--
5.01	--	19.8	--	18.8	--	15.5	7.6	9.0	6.00	8.6	--	8.9	--
6.01	28.1	--	--	--	--	--	7.7	9.0	6.30	--	--	--	--
7.51	--	--	--	--	--	--	--	--	6.50	--	--	--	--

Table 29-Mean Velocity Profiles (continued)

	17-I-V-(9)	19-I-V-(0)		20-I-V-(5)		21-I-V-(6)		22-I-V-(9)	23-U-D-(0)		24-U-[illegible]-(0)	
x'	6.25	0.96	12.25	2.25	12.25	3.25	12.25	6.25	0.96	12.25	0.96	12.25
Vert. Dist.												
0.010	1.40	0.41	0.94	0.66	0.72	0.58	0.68	0.58	4.8	10.1	4.75	20.2
0.035	2.05	0.43	0.84	0.66	1.07	0.62	1.22	0.71	10.5	18.8	10.60	23.3
0.060	3.15	0.59	0.94	0.72	1.46	0.75	1.42	1.17	20.2	21.0	19.50	24.3
0.085	3.65	1.02	1.48	0.99	1.90	1.52	1.93	1.52	27.7	22.5	28.00	25.0
0.110	4.50	1.16	1.73	1.32	2.16	1.75	2.22	1.72	32.0	23.5	32.50	25.5
0.160	4.90	2.10	2.01	--	--	1.92	2.53	2.02	34.5	24.5	37.00	26.5
0.210	5.10	2.13	2.57	2.27	2.95	2.00	2.70	2.50	--	25.5	--	--
0.260	--	--	--	--	--	--	--	--	--	--	38.00	28.0
0.310	5.70	3.07	2.57	2.70	3.04	2.55	3.00	2.74	--	26.0	--	--
0.360	--	--	--	--	--	--	--	--	--	--	37.00	30.0
0.510	6.00	3.40	3.09	3.30	3.08	2.85	3.10	2.96	--	26.2	37.50	29.5
0.760	6.60	3.40	3.08	3.8	3.30	3.10	3.10	3.43	--	28.5	38.0	30.5
1.01	7.10	3.40	3.08	3.82	3.62	3.52	3.37	3.90	--	30.2	37.5	31.0
1.51	7.70	3.40	3.08	4.00	3.62	3.60	3.55	3.93	--	32.0	38.0	32.5
2.01	7.80	3.40	3.75	4.45	3.90	3.60	3.70	4.00	--	33.4	--	34.0
3.01	8.60	3.85	3.75	4.45	3.95	3.70	3.60	4.30	--	33.4	--	33.0
4.01	8.40	3.78	3.75	--	3.95	3.70	3.60	4.30	--	--	--	33.0
4.51	8.40	--	--	--	--	--	--	--	--	--	--	--
5.01	--	--	3.75	--	3.95	--	3.60	4.30	--	--	--	33.5

Table 29-Mean Velocity Profiles (continued)

	25-0-D-(0)		26-0-W-(0)		27-0-D-(0)	28-0-W-(0)		I_a-I-D-(15)			
x'	0.96	12.25	0.96	12.25	.96	0.96	12.25	1.02	3.89	6.89	12.0
Vert. Dist.											
0.010	1.77	3.42	1.06	4.7	0.60	0.84	1.4	11.0	12.5	15.0	11.0
0.020	--	--	--	--	0.84	--	--	--	--	--	--
0.030	--	--	--	--	1.16	--	--	--	--	--	--
0.035	4.75	7.45	2.38	8.5	--	1.65	1.95	18.0	18.0	18.0	15.5
0.040	--	--	--	--	1.80	--	--	--	--	--	--
0.050	--	--	--	--	1.98	--	--	--	--	--	--
0.060	9.10	10.10	5.63	10.5	2.63	2.50	2.65	19.5	19.5	19.0	18.0
0.085	12.80	11.20	9.30	11.5	3.90	3.87	2.80	22.0	21.0	--	--
0.110	15.50	12.50	12.70	12.2	5.0	5.10	3.10	22.5	22.0	19.5	19.0
0.135	--	--	--	--	5.9	--	--	--	--	--	--
0.160	18.60	13.20	15.10	12.6	6.9	7.0	4.35	23.5	--	--	--
0.210	19.50	13.70	16.30	13.2	8.3	--	--	--	22.0	21.0	22.0
0.260	--	--	--	--	9.0	8.35	4.70	25.5	--	--	--
0.310	19.90	14.50	17.00	14.5	--	--	--	--	23.5	22.0	22.0
0.360	--	--	--	--	--	8.35	6.00	27.0	--	--	--
0.510	19.90	15.50	17.00	14.7	--	8.35	6.8	27.0	25.5	25.0	23.5
0.710	--	--	--	--	--	8.35	7.2	--	--	--	--
0.760	19.90	16.30	17.00	16.2	--	--	--	30.0	29.0	--	--
1.01	19.7	17.70	17.00	16.7	--	8.35	8.2	31.0	30.0	29.0	27.0
1.51	--	19.10	--	16.7	--	8.35	8.2	31.0	31.0	31.0	29.0
2.01	--	19.70	--	17.0	--	--	8.2	32.0	31.0	31.0	30.0
2.51	--	--	--	--	--	--	--	31.0	31.0	31.0	31.0
3.01	--	20.10	--	16.9	--	--	8.2	--	--	31.0	--
3.51	--	--	--	--	--	--	--	--	31.0	--	31.0
4.01	--	20.30	--	--	--	--	8.2	--	--	--	31.0
5.01	--	20.50	--	--	--	--	8.2	--	--	--	--

Table 29-Mean Velocity Profiles (continued)

	2_a-I-D-(15)				3_a-I-D-(15)				4_a-I-D-(15)			
x'	1.02	3.89	6.89	12.0	1.02	3.89	6.89	12.0	1.02	3.89	6.89	12.0
Vert. Dist.												
0.010	2.96	4.5	5.6	2.95	0.94	0.94	0.76	0.76	0.55	0.64	0.74	0.64
0.035	5.18	7.9	7.4	6.00	1.68	2.05	0.94	1.37	0.85	1.11	1.27	0.74
0.060	7.90	9.7	8.4	7.40	2.25	2.70	1.23	2.45	1.27	1.27	1.72	1.57
0.085	10.8	9.7	--	--	--	--	--	--	--	--	--	--
0.110	11.5	10.2	9.0	8.40	3.24	3.25	2.70	2.95	2.12	1.72	2.12	1.57
0.160	12.3	--	--	--	--	--	--	--	2.52	2.53	2.53	--
0.210	--	10.8	10.2	10.2	4.80	4.20	3.80	3.50	2.78	2.78	2.78	1.92
0.260	12.9	--	--	--	--	--	--	--	3.33	--	--	--
0.310	--	11.5	10.8	10.8	5.60	--	4.20	--	--	3.04	3.04	2.78
0.360	--	--	--	--	--	--	--	--	3.60	--	--	--
0.410	--	--	--	--	--	--	--	--	--	--	--	2.78
0.460	--	--	--	--	--	--	--	--	3.60	--	--	--
0.510	14.5	12.3	12.2	11.5	6.00	4.50	4.80	4.80	--	3.33	3.60	--
0.610	--	--	--	--	--	--	--	--	3.60	--	--	2.78
0.760	--	--	--	--	--	--	--	--	--	3.60	3.33	3.04
0.810	--	--	--	--	--	--	--	--	3.60	--	--	3.33
1.01	15.3	14.5	13.0	12.2	6.90	5.50	5.50	5.20	3.90	3.90	3.60	--
1.51	15.3	15.3	--	--	6.90	6.00	--	--	4.23	4.23	3.90	3.33
2.01	16.2	--	15.4	15.2	6.90	--	6.00	6.00	4.23	3.90	3.90	3.60
2.51	--	16.2	--	--	6.90	7.00	--	--	4.55	4.23	3.90	3.90
3.01	17.0	--	16.2	16.2	--	--	7.00	6.40	--	4.23	--	--
3.51	--	16.2	--	--	--	7.4	--	--	4.23	4.23	3.90	3.90
4.01	--	--	16.2	17.0	--	--	7.40	7.00	4.23	--	--	--
4.51	--	16.2	--	--	--	7.4	--	--	--	--	3.90	3.90
5.01	--	--	--	--	--	--	7.4	7.00	--	--	--	--
6.01	--	--	--	17.0	--	--	--	--	--	--	--	--

Table 29-Mean Velocity Profiles (continued)

	5a-O-D-(15)								6a-O-D-(15)			
x'	0.83	0.96	1.17		2.0	3.92	7.83	11.92		.95		0.96
Vert. Dist.				Vert. Dist.					Vert. Dist.		Vert. Dist.	
0.010	3.36	4.6	9.10	0.010	9.9	11.8	10.0	5.00	0.0115	1.14	0.010	2.03
0.020	5.10	6.8	12.30	0.035	18.2	14.7	15.0	11.30	0.0165	1.65	0.015	2.71
0.030	9.10	10.1	15.50	0.060	20.4	19.5	16.60	15.00	0.0215	2.47	0.020	3.49
0.040	13.00	13.5	18.0	0.085	22.0	20.5	18.5	16.70	0.0265	3.22	0.025	4.37
0.050	17.20	17.0	21.2	0.110	22.0	20.5	18.5	17.5	0.0315	3.77	0.030	5.04
0.060	21.20	19.8	23.5	0.160	25.0	--	--	--	0.0365	4.72	0.035	5.80
0.070	23.50	24.8	--	0.210	26.2	24.0	20.5	20.7	0.0415	5.40	0.040	6.58
0.080	--	26.7	--	0.310	28.7	25.0	22.6	22.0	0.0465	6.22	0.045	7.52
0.085	--	--	27.2	0.410	30.0	27.6	24.0	--	0.0515	7.10	0.050	8.0
0.090	25.80	28.3	--	0.510	32.0	29.4	24.0	23.0	0.0565	8.00	0.055	9.07
0.100	30.0	--	--	0.760	32.0	31.0	26.5	--	0.0615	8.54	0.060	10.30
0.110	31.2	--	30.0	1.01	--	32.0	28.5	26.7	0.0665	9.70	0.065	10.80
0.115	--	31.7	--	1.26	--	32.0	--	--	0.0715	10.8	0.070	11.60
0.135	31.7	--	30.0	1.51	--	32.0	30.5	29.7	0.0765	10.8	0.075	12.20
0.140	--	32.0	--	2.01	--	--	31.7	31.7	0.0865	12.9	0.080	12.9
0.160	32.0	--	30.0	2.51	--	--	31.7	32.0	0.0965	13.8	0.090	14.5
0.165	--	32.0	--	3.01	--	--	--	32.0	0.1065	15.5	0.100	15.5
0.185	--	--	30.0	3.51	--	--	--	32.0	0.1165	16.3	0.110	16.3
0.210	32.0	--	31.7	--	--	--	--	--	0.1265	17.4	0.120	17.4
0.235	--	--	31.7	--	--	--	--	--	0.1365	17.4	0.130	17.4
0.260	32.0	--	31.7	--	--	--	--	--	0.1465	18.5	0.140	18.5
0.265	--	32.0	--	--	--	--	--	--	0.1565	18.5	0.150	18.5
0.360	--	--	32.0	--	--	--	--	--	0.1665	19.6	0.160	19.6
0.390	--	32.0	--	--	--	--	--	--	0.1765	19.6	0.170	19.6
0.460	--	--	32.0	--	--	--	--	--	0.1865	19.9	0.180	19.6
0.510	32.0	--	32.0	--	--	--	--	--	0.1965	19.9	0.205	19.6
--	--	--	--	--	--	--	--	--	0.2215	19.9	0.230	19.6

Table 29-Mean Velocity Profiles (continued)

6a-O-D-(15)

x'	0.98	1.04	1.17	1.42	1.92	2.75		3.75		4.75
Vert. Dist.							Vert. Dist.		Vert. Dist.	
0.015	2.03	2.24	1.65	1.14	1.14	0.74	0.015	0.74	0.015	0.64
0.025	3.22	4.04	2.71	1.47	2.24	0.86	0.025	0.74	0.025	0.55
0.035	5.40	5.04	4.37	2.71	2.95	1.91	0.035	1.40	0.035	0.98
0.045	7.10	7.10	5.80	4.37	4.37	2.75	0.045	2.09	0.045	1.74
0.055	8.00	8.54	7.52	5.40	5.40	2.98	0.055	3.23	0.055	2.27
0.065	10.30	10.30	8.54	6.58	6.58	4.40	0.065	3.80	0.065	2.98
0.075	11.60	11.60	10.3	8.00	8.00	4.74	0.075	4.40	0.075	3.50
0.085	13.80	12.2	10.8	9.70	9.07	5.90	0.085	5.50	0.085	4.10
0.095	14.5	13.8	12.2	10.30	10.30	6.30	0.095	5.90	0.095	5.13
0.105	15.5	14.5	13.8	11.60	10.80	7.18	0.105	6.66	0.105	5.13
0.115	16.3	15.5	14.5	12.20	12.20	8.06	0.115	7.18	0.115	5.90
0.125	17.4	16.3	15.5	12.9	12.90	8.06	0.125	8.06	0.125	6.30
0.135	18.5	16.3	16.3	14.5	13.80	9.06	0.135	8.06	0.135	7.18
0.145	18.5	17.4	16.3	15.5	14.50	9.06	0.145	8.56	0.145	7.54
0.155	19.6	17.4	17.4	15.5	15.50	9.06	0.155	9.06	0.170	7.54
0.165	--	18.5	17.4	16.3	16.30	--	0.165	10.2	0.195	9.06
0.175	--	18.5	17.4	16.3	16.30	--	0.175	--	0.220	9.64
0.180	19.6	--	--	17.4	17.40	10.2	0.180	--	0.245	10.2
0.195	--	18.5	18.5	17.4	17.40	--	0.195	--	0.270	10.8
0.205	19.6	18.5	18.5	18.5	17.40	11.4	0.205	10.8	0.295	11.4
0.230	19.6	18.5	18.5	18.5	18.50	12.2	0.230	12.2	0.320	11.4
0.255	--	18.5	--	18.5	18.50	12.2	0.255	12.2	0.345	12.2
0.280	--	--	--	18.5	18.50	12.8	0.280	12.8	0.370	12.2
0.305	--	--	--	--	--	12.8	0.305	12.8	0.395	12.2
0.330	--	--	--	--	--	12.8	0.330	12.8	0.420	12.8
0.355	--	--	--	--	--	12.8	0.355	--	0.445	12.8

Table 29--Mean Velocity Profiles (continued)

	6a-0-D-(15)								7a-0-D-(15)		
x'	5.75	6.75	7.75		8.75	9.75	10.75	11.75		0.95	0.96
Vert. Dist.				Vert. Dist.					Vert. Dist.		
0.015	0.74	0.64	2.20	0.005	2.60	2.62	2.15	3.96	0.005	1.17	2.97
0.025	0.74	0.98	3.35	0.015	5.90	3.66	2.87	5.41	0.030	3.50	6.50
0.035	1.11	1.74	4.35	0.025	8.05	7.16	5.47	7.63	0.055	7.50	10.50
0.045	1.91	2.09	5.80	0.035	9.70	8.63	7.64	9.88	0.080	11.80	14.10
0.055	2.52	2.98	6.70	0.045	11.00	10.30	9.18	10.40	0.105	14.2	16.8
0.065	3.23	3.50	8.20	0.055	11.50	10.90	10.30	11.70	0.130	16.8	17.7
0.075	3.80	3.80	8.60	0.065	12.20	--	--	12.50	0.155	17.7	17.7
0.085	4.40	4.40	9.20	0.075	13.0	--	--	12.50	0.180	18.7	18.7
0.095	6.13	4.74	9.20	0.080	--	12.2	11.5	--	0.205	18.7	18.7
0.105	5.13	5.13	11.00	0.085	13.0	--	--	12.5	0.305	18.7	18.7
0.130	6.66	6.66	11.50	0.095	13.7	--	--	--	0.405	18.7	18.7
0.155	7.54	7.54	13.00	0.105	13.7	13.7	12.2	13.2	0.505	18.7	--
0.180	8.56	8.56	14.50	0.130	14.5	--	--	--	0.755	18.7	18.7
0.205	9.06	9.64	15.2	0.155	14.5	14.5	13.0	14.2	1.005	--	--
0.230	10.2	10.2	15.2	0.180	14.5	--	--	--	--	--	--
0.255	10.8	10.8	17.0	0.205	15.2	15.3	13.7	14.9	--	--	--
0.280	11.4	10.8	18.0	0.255	16.2	15.3	14.5	15.7	--	--	--
0.305	12.2	11.4	18.0	0.305	17.0	--	--	--	--	--	--
0.330	12.2	12.2	18.0	0.380	17.6	16.2	15.3	16.7	--	--	--
0.355	12.8	12.2	18.0	0.505	19.0	17.1	17.1	17.9	--	--	--
0.380	12.8	12.8	18.0	0.755	20.5	19.2	18.1	20.3	--	--	--
0.405	12.8	12.8	--	1.005	21.5	20.5	19.2	21.8	--	--	--
0.430	13.3	12.8	19.2	1.505	21.5	21.6	21.6	23.8	--	--	--
0.455	13.3	12.8	--	2.005	21.5	21.6	21.6	25.1	--	--	--
0.480	13.3	13.3	19.2	2.505	--	21.6	21.6	25.1	--	--	--
0.505	--	13.3	--	--	--	--	--	--	--	--	--
0.530	--	13.3	20.5	--	--	--	--	--	--	--	--
0.550	--	13.3	--	--	--	--	--	--	--	--	--
0.580	--	--	20.5	--	--	--	--	--	--	--	--
0.630	--	--	20.5	--	--	--	--	--	--	--	--

Table 29- ean Velocity Profiles (continued)

7_a-0-D-(15)

x'	1.42		1.92	2.75	3.75	4.75	5.75	6.75	7.75	8.75	9.75	10.75	11.75
Vert. Dist.		Vert. Dist.											
0.005	4.5	0.005	4.82	5.6	5.6	4.5	6.0	4.1	4.8	3.51	2.30	2.5	2.75
0.030	8.6	0.030	8.00	9.8	9.2	8.0	9.2	8.0	9.2	7.50	6.00	6.9	6.50
0.055	10.5	0.055	11.10	11.2	11.1	10.5	11.1	9.8	10.4	9.20	9.20	9.2	8.0
0.080	12.7	0.080	11.80	12.6	11.7	11.1	11.8	11.1	11.1	10.80	9.80	9.8	9.8
0.105	13.4	0.105	12.7	13.4	12.6	11.8	12.5	11.8	11.8	11.20	10.40	10.4	11.1
0.130	15.0	0.130	13.4	13.4	13.4	12.5	13.3	12.5	--	--	--	--	--
0.155	16.8	0.155	14.2	13.4	13.4	13.4	14.2	13.3	12.5	11.90	11.8	11.8	11.8
0.180	16.8	0.180	14.2	14.2	--	--	--	--	--	--	--	--	--
0.230	16.8	0.205	14.2	15.0	14.2	13.4	15.0	13.3	13.3	12.5	12.5	--	--
0.280	17.7	0.255	16.0	15.0	--	--	--	--	--	--	--	12.5	12.5
0.380	18.7	0.305	16.8	16.0	16.0	15.0	16.0	14.2	14.2	14.3	13.3	--	--
0.480	18.7	0.405	17.8	15.8	16.8	16.0	16.8	16.0	14.2	14.3	13.3	--	--
0.980	18.7	0.505	17.8	17.7	16.8	16.8	17.7	16.0	15.0	15.0	14.2	15.0	15.0
--	--	0.755	17.8	18.7	17.7	17.7	18.7	16.8	16.8	16.9	16.0	--	--
--	--	0.1005	17.8	18.7	17.7	17.7	19.7	18.1	17.7	17.7	16.8	16.8	16.8
--	--	1.505	--	18.7	17.7	17.7	20.7	19.7	18.7	19.7	18.7	18.7	18.7
--	--	2.005	--	--	--	--	--	19.7	18.7	19.7	18.7	19.7	19.7
--	--	2.505	--	--	--	--	--	19.7	18.7	19.7	19.7	19.7	19.7
--	--	3.005	--	--	--	--	--	--	18.7	19.7	--	19.7	19.7
--	--	3.505	--	--	--	--	--	--	--	--	19.7	19.7	--

Table 29- Mean Velocity Profiles (continued)

8_a-0-D-(15)

x'	0.07	0.98	1.04	1.17	1.42
Vert. Dist.					
0.010	--	--	--	--	1.85
0.015	2.24	--	--	--	--
0.020	--	2.55	2.70	2.75	2.55
0.025	3.65	--	--	--	--
0.030	--	4.20	3.55	4.5	4.15
0.035	4.9	--	--	--	--
0.040	--	5.5	5.70	5.5	6.20
0.045	6.6	--	--	--	--
0.050	--	7.1	7.20	6.6	6.60
0.055	8.9	--	--	--	--
0.060	--	8.9	8.70	8.1	7.60
0.085	--	12.8	11.50	--	9.80
0.110	15.0	15.0	15.00	11.6	11.50
0.135	17.5	16.5	16.5	13.5	13.50
0.161	17.5	17.5	17.5	14.5	14.00
0.185	18.5	17.5	17.5	14.5	14.00
0.210	18.5	17.5	18.5	14.5	15.00
0.230	18.5	--	--	--	--
0.251	18.5	17.5	--	--	--
0.310	--	--	18.5	15.0	16.5
0.351	18.5	18.5	--	--	--
0.451	18.5	18.5	--	--	16.5
0.510	--	--	18.5	16.5	--
0.610	18.5	18.5	--	--	--
0.760	--	--	--	--	--
1.01	--	--	--	16.5	16.5

x'	1.92	2.75	3.75	10.75
Vert. Dist.				
0.010	2.3	3.2	3.5	2.5
0.035	5.5	7.5	9.5	6.5
0.060	7.5	9.0	11.5	9.0
0.085	11.1	11.0	13.5	10.5
0.110	11.1	11.0	14.0	11.0
0.135	11.5	11.5	--	--
0.160	12.0	11.5	14.8	11.5
0.210	13.2	12.5	15.8	--
0.310	14.1	13.5	16.5	--
0.510	15.1	15.0	19.0	--
0.760	16.5	16.5	20.0	15.8
1.01	16.5	16.5	20.0	16.5
1.51	16.5	16.5	20.0	17.5
2.01	--	--	--	17.5
2.51	--	--	--	16.0
3.01	--	--	--	16.0
--	--	--	--	--
--	--	--	--	--
--	--	--	--	--
--	--	--	--	--
--	--	--	--	--
--	--	--	--	--
--	--	--	--	--
--	--	--	--	--
--	--	--	--	--
--	--	--	--	--

Table 29-Mean Velocity Profiles (continued)

9a-0-D-(15)

x'	0.54	1.02	1.88	2.89		3.89	6.89	12.0
Vert. Dist.					Vert. Dist.			
0.010	1.22	1.07	0.95	0.84	0.010	1.22	1.38	0.95
0.020	1.55	1.22	1.22	--	0.035	2.85	2.10	2.00
0.030	2.6	1.92	1.72	1.54	0.060	3.70	3.10	3.10
0.040	3.7	2.60	2.6	--	0.085	4.60	4.0	--
0.050	4.4	3.10	2.85	--	0.110	4.70	5.10	4.40
0.060	5.6	3.40	3.10	2.35	0.160	5.10	--	--
0.085	6.0	5.10	4.10	3.10	0.210	5.60	5.6	4.70
0.110	7.4	6.0	4.80	3.70	0.310	6.40	--	5.10
0.135	9.0	--	--	--	0.510	6.90	6.0	5.60
0.160	9.3	7.4	6.4	4.75	0.760	7.40	--	--
0.185	9.3	--	--	--	1.01	8.00	7.6	6.80
0.210	9.3	8.4	7.4	--	1.51	8.00	7.6	6.80
0.260	--	--	--	6.0	2.51	--	--	7.80
0.310	9.3	9.3	8.7	--	3.51	--	--	7.80
0.410	--	--	9.0	--	--	--	--	--
0.510	--	9.3	9.0	7.4	--	--	--	--
0.760	--	--	9.0	--	--	--	--	--
1.01	--	--	--	7.4	--	--	--	--
1.51	--	--	--	7.4	--	--	--	--

Table 29--Mean Velocity Profiles (continued)

1-I-W-(0)		2-I-D-(0)		3-I-W-(0)		4-I-W-(5)		5-I-W-(6)		6-I-W-(9)	
x'	12.25		12.25		12.25		12.25		12.25		12.25
Vert. Dist.		Vert. Dist.		Vert. Dist.		Vert. Dist.		Vert. Dist.		Vert. Dist.	
0.010	40.6	0.010	56.9	0.010	79.8	0.010	77.2	0.010	68.0	0.010	86.7
0.035	41.5	0.035	57.2	0.035	80.15	0.035	77.75	0.035	68.55	0.060	88.5
0.060	41.8	0.060	57.3	0.060	79.90	0.060	77.20	0.060	68.10	0.085	88.6
0.085	41.9	0.085	57.3	0.110	80.20	0.110	78.40	0.085	69.20	0.110	88.4
0.110	42.1	0.110	57.3	0.210	81.00	0.210	79.4	0.110	69.75	0.160	89.6
0.135	42.5	0.160	57.7	0.310	81.05	0.310	79.9	0.160	70.20	0.210	90.3
0.160	42.2	0.210	57.7	0.510	82.10	0.510	80.1	0.210	70.20	0.310	91.0
0.185	42.6	0.310	56.5	0.760	83.50	0.760	81.35	0.310	70.05	0.510	92.6
0.210	42.5	0.510	59.3	1.01	83.65	1.01	82.30	0.510	70.95	0.760	93.8
0.260	42.5	0.760	59.2	1.51	83.70	1.51	82.5	0.760	72.05	1.01	94.0
0.360	43.0	1.01	59.5	2.01	85.2	2.01	82.9	1.01	71.80	1.51	94.9
0.460	42.7	1.51	59.1	3.01	86.0	3.01	83.4	1.51	72.3	2.01	95.5
0.560	42.6	2.01	59.1	5.01	84.75	4.01	84.25	2.01	73.55	3.01	97.2
0.660	43.2	3.01	59.6	--	--	5.01	84.20	3.01	74.0	4.01	95.5
0.760	43.1	4.01	60.8	--	--	6.01	84.2	4.01	73.4	5.01	95.9
1.01	43.1	5.01	60.1	--	--	--	--	5.01	74.05	--	--
1.26	43.1	6.01	59.6	--	--	--	--	--	--	--	--
1.76	43.6	--	--	--	--	--	--	--	--	--	--
2.51	43.8	--	--	--	--	--	--	--	--	--	--
3.76	43.2	--	--	--	--	--	--	--	--	--	--
5.01	44.0	--	--	--	--	--	--	--	--	--	--
7.51	45.8	--	--	--	--	--	--	--	--	--	--

Note: x' in feet
Vertical distance in inches
Temperature in degrees Fahrenheit

Table 30-Mean Temperature Profiles

7-I-D-(0)		8-I-W-(0)		9-I-W-(5)		10-I-W-(6)		11-I-W-(9)		12-I-D-(0)	
x'	12.25		12.25		12.25		12.25		12.25		12.25
Vert. Dist.		Vert. Dist.		Vert. Dist.		Vert. Dist.		Vert. Dist.		Vert. Dist.	
0.010	79.2	0.010	62.7	0.010	74.9	0.010	60.8	0.010	75.2	0.010	58.2
0.035	80.0	0.035	63.0	0.035	75.1	0.035	60.9	0.035	75.8	0.035	58.2
0.060	80.7	0.060	63.9	0.060	75.3	0.060	62.25	0.060	75.55	0.060	58.2
0.110	81.1	0.085	64.0	0.085	75.15	0.085	61.30	0.085	75.80	0.085	58.1
0.210	82.2	0.110	64.3	0.110	76.0	0.110	61.80	0.110	76.45	0.110	58.1
0.310	83.4	0.160	64.4	0.210	75.6	0.160	62.30	0.160	76.05	0.160	58.3
0.510	82.8	0.210	64.5	0.310	75.95	0.210	62.30	0.210	76.35	0.260	58.7
0.760	84.6	0.310	65.1	0.510	76.55	0.310	62.85	0.310	76.60	0.410	58.4
1.01	84.7	0.510	66.1	0.76	76.60	0.510	62.85	0.510	77.35	0.610	58.7
1.51	87.4	0.760	66.9	1.01	76.70	0.760	64.0	0.760	78.00	0.810	58.7
2.01	88.6	1.01	67.2	1.51	77.75	1.01	64.4	1.01	78.40	1.01	58.8
3.01	88.2	1.51	68.7	2.01	77.6	1.51	64.55	1.51	79.90	1.26	58.8
4.51	87.3	2.01	67.6	3.01	78.25	2.01	65.55	2.01	80.60	1.51	59.0
6.01	87.6	3.01	68.4	4.01	77.95	3.01	65.4	3.01	81.05	2.01	59.4
--	--	4.01	68.8	6.01	78.33	4.01	65.2	4.01	81.30	3.01	59.0
--	--	5.01	69.4	--	--	5.01	66.3	5.01	80.5	4.01	59.3
--	--	--	--	--	--	--	--	--	--	5.01	59.8
--	--	--	--	--	--	--	--	--	--	6.01	59.8

Table 30-Mean Temperature Profiles (continued)

13-I-D-(0)		15-I-W-(5)		16-I-W-(6)		17-I-W-(9)		19-I-W-(0)		20-I-W-(5)		21-I-W-(6)	
x'	12.25		12.25		12.25		12.25		12.25		12.25		12.25
Vert. Dist.		Vert. Dist.		Vert. Dist.		Vert. Dist.		Vert. Dist.		ert. ist.		Vert. Dist.	
0.010	69.5	0.010	79.55	0.010	75.55	0.010	72.5	0.010	69.30	0.010	80.8	0.010	80.80
0.035	69.9	0.035	80.15	0.035	76.8	0.035	72.2	0.035	71.60	0.035	80.85	0.035	80.85
0.060	70.3	0.060	80.40	0.060	76.75	0.060	73.1	0.060	71.90	0.060	81.2	0.060	81.20
0.085	70.7	0.085	80.67	0.085	77.65	0.085	73.4	0.085	72.0	0.085	82.25	0.085	82.25
0.110	71.1	0.110	80.70	0.110	78.2	0.110	73.4	0.110	72.9	0.110	82.20	0.110	82.20
0.160	71.7	0.210	81.67	0.160	79.05	0.160	73.9	0.160	73.4	0.160	82.30	0.160	82.30
0.210	71.8	0.310	82.15	0.210	79.35	0.210	74.5	0.210	74.7	0.210	82.80	0.210	82.8
0.310	72.8	0.510	82.30	0.310	79.25	0.310	74.8	0.310	74.4	0.310	83.55	0.310	83.55
0.510	73.0	0.760	82.50	0.510	80.20	0.510	75.4	0.510	76.3	0.510	85.05	0.510	85.05
0.760	73.4	1.01	82.90	0.760	80.70	0.760	75.9	0.760	77.0	0.760	85.75	0.760	85.75
1.01	73.9	1.51	83.73	1.01	81.35	1.01	76.2	1.01	78.0	1.01	86.20	1.01	86.20
1.51	75.1	2.01	84.05	1.51	81.75	1.51	77.1	1.51	79.3	1.51	87.5	1.51	87.50
2.01	75.2	3.01	83.5	2.01	82.05	2.01	77.8	2.01	80.0	2.01	88.25	2.01	88.25
3.01	75.1	4.01	84.55	3.01	82.85	3.01	78.6	3.01	79.9	3.01	90.30	3.01	90.30
4.01	74.7	5.01	84.25	4.01	83.10	4.01	79.2	4.01	81.4	4.01	90.65	4.01	90.65
5.01	75.3	6.26	83.85	5.01	83.3	5.01	79.3	5.01	81.0	5.01	90.70	5.01	90.70
6.01	74.3	--	--	--	--	--	--	--	--	--	--	--	--

Table 30-Mean Temperature Profiles (continued)

22-I-W-(9)		23-0-D-(0)		24-0-W-(0)		25-0-D-(0)		26-0-W-(0)		27-0-D-(0)		28-0-W-(0)	
x'	12.25		12.25		12.25		12.25		12.25		12.25		12.25
Vert. Dist.		Vert. Dist.		Vert. Dist.		Vert. Dist.		Vert. Dist.		Vert. Dist.		Vert. Dist.	
0.010	61.2	0.010	65.0	0.010	80.7	0.010	58.85	0.010	65.0	0.010	65.3	0.010	78.7
0.035	61.7	0.035	65.6	0.035	82.3	0.035	59.00	0.035	65.4	0.035	66.7	0.035	80.5
0.060	61.7	0.060	66.8	0.060	82.2	0.060	59.1	0.060	66.0	0.060	66.3	0.060	79.7
0.085	61.7	0.085	66.7	0.085	82.4	0.085	59.05	0.085	65.9	0.085	66.2	0.085	80.4
0.110	61.8	0.110	67.3	0.110	83.1	0.110	59.05	0.110	66.7	0.110	66.9	0.110	81.4
0.160	61.8	0.160	67.3	0.160	83.1	0.150	59.15	0.160	66.8	0.160	67.1	0.160	82.5
0.210	61.9	0.210	68.0	0.260	84.6	0.210	59.7	0.210	66.7	0.210	67.3	0.210	82.9
0.310	61.9	0.310	69.4	0.360	84.2	0.310	60.0	0.310	67.1	0.310	67.6	0.310	83.8
0.510	61.6	0.510	69.8	0.510	85.7	0.510	60.45	0.510	67.6	0.510	67.4	0.510	85.5
0.760	61.7	0.760	69.9	0.760	87.0	0.760	60.60	0.760	68.3	0.760	67.7	0.760	85.6
1.01	61.5	1.01	69.8	1.01	88.1	1.01	60.80	1.01	68.8	1.01	67.8	1.01	85.8
1.51	61.5	1.51	69.9	1.51	88.3	1.51	60.80	1.51	69.6	1.51	67.2	1.51	86.3
2.01	61.6	2.01	71.1	2.01	89.7	2.01	60.85	2.01	69.9	2.01	68.3	2.01	87.6
3.01	61.8	3.01	71.0	3.01	90.8	3.01	60.90	3.01	70.0	3.01	66.8	3.01	86.7
4.01	61.9	--	--	4.01	90.8	4.01	60.10	4.01	70.1	4.01	68.9	4.01	85.2
5.01	61.7	--	--	5.01	89.9	5.01	60.15	--	--	5.01	68.1	5.01	86.3

Table 30-Mean Temperature Profiles (continued)